Extreme diversity of the human vascular mesenchymal cell landscape

Bruijn, L.E.; Akker, B.E.W.M. van den; Rhijn, C.M. van; Hamming, J.F.; Lindeman, J.H.N.

Journal of the American Heart Association

SYSTEMATIC REVIEW AND META-ANALYSIS

Extreme Diversity of the Human Vascular Mesenchymal Cell Landscape

Laura E. Bruijn, BSc; Brendy E. W. M. van den Akker, BSc; Connie M. van Rhijn, BSc; Jaap F. Hamming, MD, PhD; Jan H. N. Lindeman, MD, PhD

BACKGROUND: Human mesenchymal cells are culprit factors in vascular (patho)physiology and are hallmarked by phenotypic and functional heterogeneity. At present, they are subdivided by classic umbrella terms, such as "fibroblasts," "myofibroblasts," "smooth muscle cells," "fibrocytes," "mesangial cells," and "pericytes." However, a discriminative marker-based subclassification has to date not been established.

METHODS AND RESULTS: As a first effort toward a classification scheme, a systematic literature search was performed to identify the most commonly used phenotypical and functional protein markers for characterizing and classifying vascular mesenchymal cell subpopulation(s). We next applied immunohistochemistry and immunofluorescence to inventory the expression pattern of identified markers on human aorta specimens representing early, intermediate, and end stages of human atherosclerotic disease. Included markers comprise markers for mesenchymal lineage (vimentin, FSP-1 [fibroblast-specific protein-1]/S100A4, cluster of differentiation (CD) 90/thymocyte differentiation antigen 1, and FAP [fibroblast activation protein]), contractile/non-contractile phenotype (α-smooth muscle actin, smooth muscle myosin heavy chain, and nonmuscle myosin heavy chain), and auxiliary contractile markers (h1-Calponin, h-Caldesmon, Desmin, SM22α [smooth muscle protein 22α], non-muscle myosin heavy chain, smooth muscle myosin heavy chain, Smoothelin-B, α-Tropomyosin, and Telokin) or adhesion proteins (Paxillin and Vinculin). Vimentin classified as the most inclusive lineage marker. Subset markers did not separate along classic lines of smooth muscle cell, myofibroblast, or fibroblast, but showed clear temporal and spatial diversity. Strong indications were found for presence of stem cells/Endothelial-to-Mesenchymal cell Transition and fibrocytes in specific aspects of the human atherosclerotic process.

CONCLUSIONS: This systematic evaluation shows a highly diverse and dynamic landscape for the human vascular mesenchymal cell population that is not captured by the classic nomenclature. Our observations stress the need for a consensus multiparameter subclass designation along the lines of the cluster of differentiation classification for leucocytes.

Key Words: atherosclerosis ■ fibroblasts ■ myofibroblasts ■ vascular smooth muscle cells

Vascular mesenchymal cells are critically involved in blood vessel development and homeostasis and are progressively acknowledged as key effector cells in vascular pathological conditions, such as atherosclerosis, aneurysmal disease, and neointima formation.[1-3]

In the context of vascular pathology, mesenchymal cells are generally subclassified by classic umbrella terms, such as "fibroblasts," "myofibroblasts," "smooth muscle cells" (SMCs),[4] "fibrocytes,"[5] "mesangial cells,"[6] and "pericytes."[7] This generic nomenclature is based on the process under investigation, their presumed function or specific anatomical location, and/or their in vitro behavior.[8,9] At this point, a discriminative consensus (sub)classification for vascular mesenchymal cells, let alone classifying marker sets required for mechanistic understanding, is needingly missing. In this light, and in the context of the emerging key roles for mesenchymal cells in human vascular disease, we considered a systematic

Correspondence to: Jan H. N. Lindeman MD, PhD, Postbox 9600, 2300 RC Leiden, the Netherlands. E-mail: lindeman@lumc.nl

Supplementary Material for this article is available at https://www.ahajournals.org/doi/suppl/10.1161/JAHA.120.017094

For Sources of Funding and Disclosures, see page 22.

JAHA is available at: www.ahajournals.org/journal/jaha

CLINICAL PERSPECTIVE

What Is New?

- A classification scheme for the vascular mesenchymal cell population is missing.
- This study provides a first framework for a systematic marker-based classification of human vascular mesenchymal cells, and implies an underappreciated, extremely diverse spectrum of human mesenchymal cells within the aortic wall.

What Are the Clinical Implications?

- Mesenchymal cells play a central role in vascular pathological conditions, such as atherosclerosis and abdominal aortic aneurysms.
- This systematic evaluation indicates an extreme diverse and dynamic mesenchymal cell landscape, but also implies an unappreciated cellular flexibility with indications for both Endothelial-to-Mesenchymal cell Transition as well as Leucocyte-to-Mesenchymal cell Transition (fibrocytes) as common events.
- This study provides a first step in a better understanding of the role of vascular mesenchymal cells in human disease.

Nonstandard Abbreviations and Acronyms

AIT	adaptive intimal thickening
FAP	fibroblast activation protein
FCP	fibrocalcific plaque
FSP-1	fibroblast-specific protein-1
HR	healed rupture
LFA	late fibroatheroma
P4HB	prolyl 4-hydroxylase β
SM22α	smooth muscle protein 22α
SMC	smooth muscle cell
Smemb	nonmuscle myosin heavy chain
SM-MHC	smooth muscle myosin heavy chain
Thy-1	thymocyte differentiation antigen 1
αSMA	α-smooth muscle actin

exploration of potential relevant class-specific marker sets.

To address this point, we performed a systematic literature search to identify candidate mesenchymal cell-specific markers, and evaluated the expression pattern and the expression dynamics of the identified markers in different stages of the human atherosclerotic process.

METHODS

This study is based on a 2-step approach. First, we conducted a systematic literature search to map the reported markers for vascular mesenchymal cell subpopulation characterization and classification. Subsequently, we applied immunohistochemistry and immunofluorescence to evaluate the specificity and expression pattern of the identified markers in a representative sample of early, intermediate, and (stabilized) end stages of the human aortic atherosclerotic process (Virmani classification,[10] respectively: adaptive intimal thickening [AIT], late fibroatheroma [LFA], and fibrocalcific plaque [FCP]) (Figure 1).

The authors declare that all supporting data are available within the article (and its online supplementary files).

Systematic Literature Review of Phenotypical Immunohistochemical Markers

A systematic literature review was conducted according to the Preferred Reporting Items for Systematic Reviews and Meta-Analyses guidelines. Studies were identified by searching PubMed and Embase. The search strategy (outlined in Data S1 and S2 [Systematic Review Protocol]) was based on 3 search themes, combined in the search by AND. The first theme was created for vascular remodeling and phenotypic heterogeneity. The second theme included descriptions of fibroblasts, myofibroblasts, and SMCs. The final, third theme consisted of terms for atherosclerosis, aortic aneurysmal disease, and fibrosis. Because the focus of the study was on the classic supportive mesenchymal vascular cell type, we considered aspects of osteogenic, adipogenic, and pericyte differentiation beyond the scope of the literature review.

The search was most recently updated in December 2019. First, 2 authors (J.L. and L.B.) independently reviewed the titles and abstracts for eligibility. Thereafter, full-text articles were assessed.

In parallel to the above phenotypic markers, we mapped reported markers of a synthetic and proinflammatory phenotype for functional subclassification, as these functions are considered independent of the cell phenotype (ie, SMCs, myofibroblasts, and fibroblasts can be synthetic and/or inflammatory).

Human Atherosclerotic Tissue Sampling

Formalin-fixed, paraffin-embedded aortic wall samples were selected from the Vascular Tissue Repository at the Department of Vascular Surgery, Leiden, the Netherlands. These human perirenal aortic patches were obtained during clinical organ transplantation

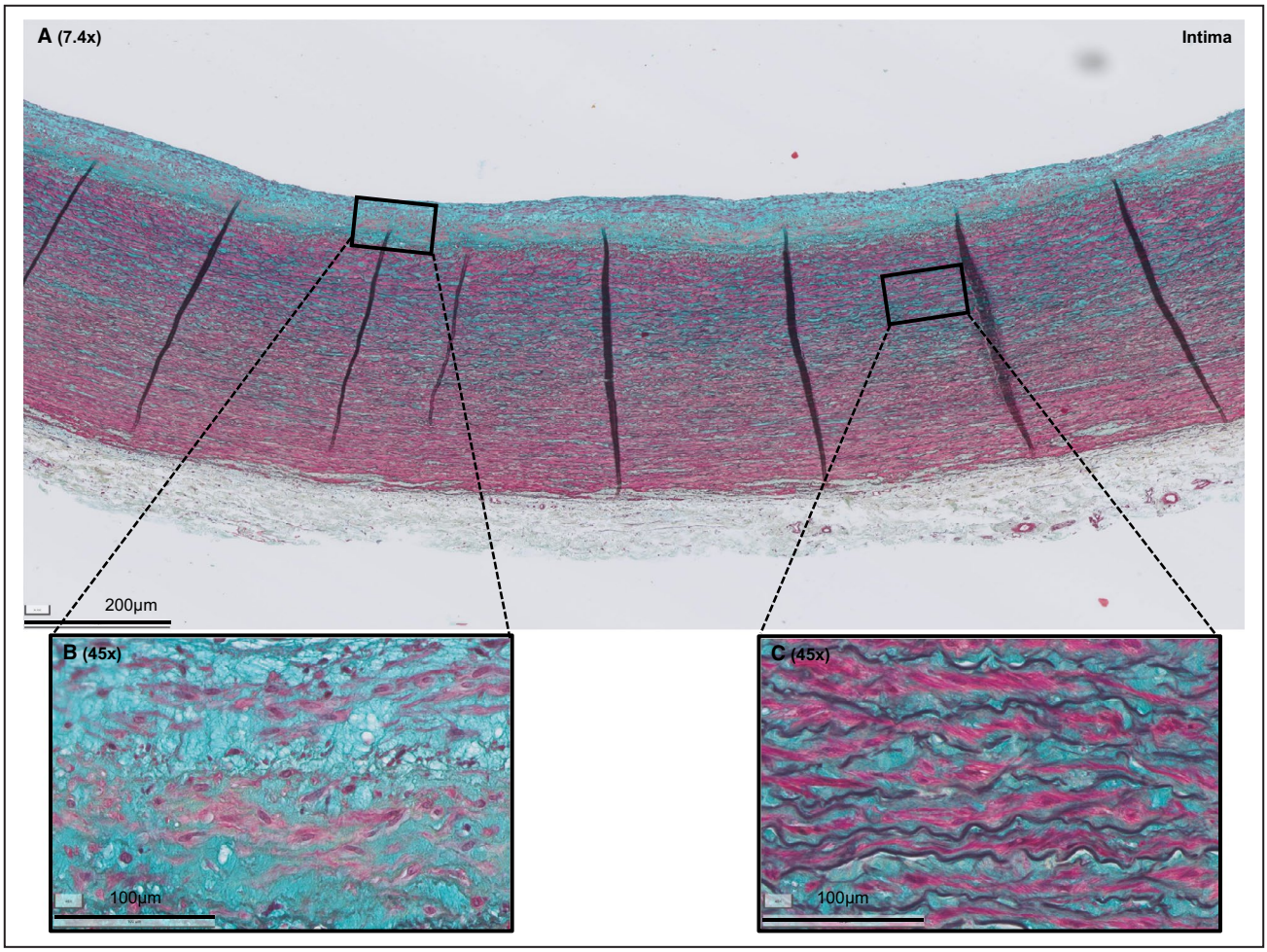

Figure 1. Histologic overview (Movat pentachrome staining) of selected representative sections of adaptive intimal thickening (AIT), late fibroatheroma (LFA), and fibrotic calcified plaque (FCP).
A, AIT is characterized by a thickening intima, consisting of smooth muscle cells (SMCs) in a proteoglycan-rich matrix (**B**) and a normal media and adventitia (**C**). **D**, LFA is characterized by a necrotic core of cellular debris and cholesterol crystals that is covered by a multilayered fibrous cap, consisting of SMCs in a collagenous proteoglycan-rich matrix with infiltration of inflammatory cells (**F**). **E**, Shoulder regions. **G**, FCP is characterized by extensive fibrosis, a condensated (former) necrotic core, and ample calcification (**H**) and neointimal formation (**I**). Legend to the Movat staining: *red*, SMCs/fibrin; *violet*, leukocytes; *black*, elastin; *blue*, proteoglycans/mucins; *yellow*, collagen. Various shades of *green* reflect colocalization of collagen (*yellow*) and proteoglycans (*blue*).

with grafts derived from cadaveric donors. Histologic sections were prepared for each tissue block, sections were Movat pentachrome stained (for protocol, see Data S3), and the extent of atherosclerosis was classified (modified American Heart Association classification, according to Virmani et al[10]) The tissue block showing the highest degree of atherosclerosis was used as the reference block. For this evaluation, we randomly selected preclassified tissue blocks representative for AIT, LFA, and FCP (Figure 1). All stainings were performed on sequential tissue sections from the selected tissue blocks.

To evaluate mesenchymal cell presence in respectively progressive and stabilizing atherosclerotic lesions, representative sections of the unstable lesion thin cap fibroatheroma[10] in addition to the stable lesion LFA and healed rupture (HR)[10] were selected. HR was selected as well because of a suspected enrichment of the mesenchymal cell subtype fibrocytes.[11]

Immunohistochemical Staining on Atherosclerotic Lesions

Single-Labeling Immunohistochemistry

Consecutive (4-µm) sections were immunostained for the 28 immunohistochemistry markers (Table 1) identified in the literature review. All single stainings were performed by immunohistochemistry, because immunohistochemistry allows for direct clear overview, provides superior contextual information, and is not interfered by background staining (mainly caused by elastin) when assessed by immunofluorescence.

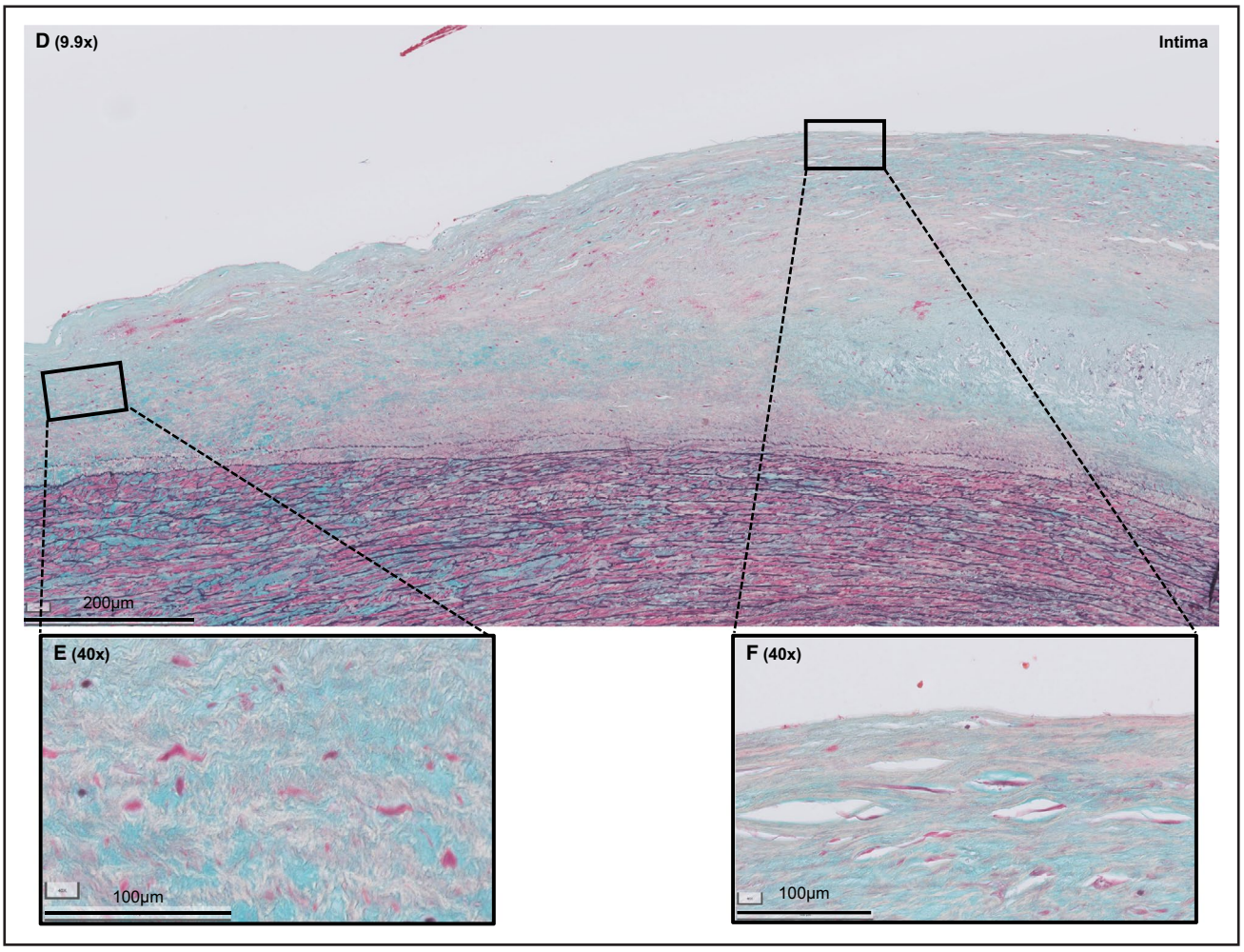

Figure 1. Continued

Heat-induced (Tris/EDTA, pH 9.2/citrate, pH 6) or enzyme-induced antigen retrieval was performed if required (Table 1).

All primary antibodies were diluted in 1% BSA/PBS and were incubated overnight at 4°C. Endogenous peroxidase activity was blocked with a 20-minute incubation of 0.3% hydrogen peroxide. The Envision/3,3'-diaminobenzidine (Dako, Glostrup, Denmark) system was used for visualization. Nuclei were counterstained by Mayer hematoxylin (Merck Millipore, Amsterdam, the Netherlands). Slides stained for phosphorylated nuclear factor-κB were washed with Triton X-100 (Abcam, Cambridge, UK) 0.1% in PBS for 10 minutes. All stainings for a given antibody were processed in a single batch.

Imaging of Immunohistochemistry Slides

Immunohistochemistry images were captured by means of a digital microscope (Philips IntelliSite Pathology Solution Ultra-Fast Scanner; Philips Eindhoven, the Netherlands).

Evaluation of Marker Expression on Atherosclerotic Tissue

For all markers, expression patterns were inventoried for 6 separate aspects of the aortic wall (see Figure S1 for an outline): intima, inner media, middle media, outer media, adventitia, as well as at the level of the arteriole-type (thick-walled) vasa vasorum and venule-type (thin-walled) vasa vasorum in the adventitia. In addition, we evaluated the mesenchymal populations in the areas adjacent to shoulders of and covering (multilayered fibrous cap) the necrotic core of the LFA-type lesion. For the FCP lesion type, the cells in the newly formed intima overlying the fibrous lesion, rather than the remnants of the former fibrous cap, were appreciated.

Scoring was performed by 2 observers using semi-quantitative scoring estimates (ie, 0%, <10%, 10%–50%, or >50% positivity) for each region.

Multilabeling Immunohistochemistry

Double-labeling stainings were primarily performed by immunohistochemistry, for the same reasons single

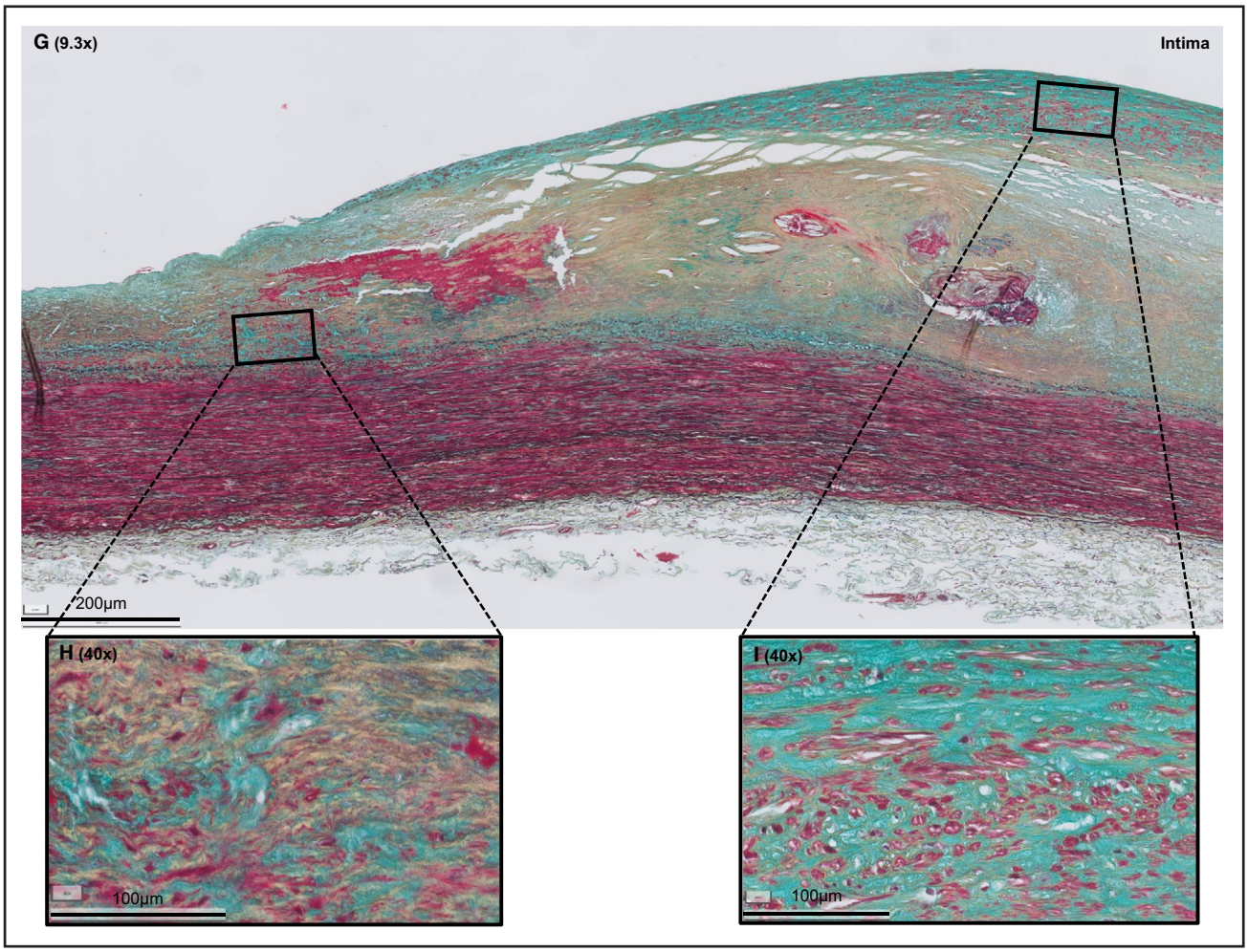

Figure 1. Continued

immunohistochemistry stainings were preferred over single immunofluorescence stainings.

Double-labeling immunohistochemistry stainings were performed by sequential single-labeling immunohistochemistry. A second heat-induced antigen retrieval after the first chromogen staining was used to inactivate the previous signal. All epitopes resisted the second heat retrieval. Vulcan red (10 minutes, dilution 1:50) and Ferangi blue (5 minutes, dilution 1:50; both from BioCare Medical, Pacheco, CA; both alkaline phosphatase enzymatic chromogens) were combined in the double staining because these chromogens provide optimal color separation and a clear colocalization signal (purple). Double-stained slides were not counterstained.

Immunofluorescence Staining

Multilabeling Immunofluorescence

Colocalization of >2 markers was visualized by immunofluorescence, as no triple chromogen panel could be established that provided adequate color differentiation.

All primary (Table 2) and Alexa Fluor secondary antibodies (dilution 1:200; Thermofisher, Waltham, MA) were diluted in 1% PBS/BSA and incubated overnight at 4°C and 60 minutes at room temperature, respectively. Negative controls were created by omitting the primary antibodies, and antigen stability was checked after the first heat retrieval.

In the triple-labeling immunofluorescence stainings, cluster of differentiation (CD) 45 staining was first performed as a single staining: the CD45 antibody was incubated overnight and visualized using goat anti-mouse (MACH2 AP-Polymer; Biocare Medical) as a secondary antibody (30 minutes incubation at room temperature) and visualized using Vulcan Fast Red (10 minutes, dilution 1:50; Biocare Medical) fluorescence. After a second heat retrieval, the other 2 antibodies of different isotypes were incubated overnight and corresponding fluorescent-labelled seondary antibodies were applied.

Slides were mounted using ProLong Gold with 4′,6-diamidino-2-phenylindole antifade reagent (Thermofisher) and stored at 4°C until analysis. Vulcan

Table 1. Antibodies Used for Immunohistochemistry

Antibody, Clone or Catalog No.	Abbreviation Used in Study	Host Isotype; Subclass	Purification	Cellular Localization	Pretreatment	Protein Block (Dako)	Dilution	Secondary Antibody	Source
Vimentin, 3B4	Vim	Mouse IgG2a	Purified from cell culture supernatant	Cytoskeleton (intermediate filament)	Tris-EDTA (pH 9.2)	No	1:2000	1. DAKO EnVision+ System, anti-mouse 2. MACH2 Biocare Medical, anti-mouse	Dako
Fibroblast-specific protein-1/S100A4, D9F9D	FSP-1	Rabbit IgG	Not specified	Nucleus, cytoplasm, and extracellular space	Tris-EDTA (pH 9.2)	No	1:6000	DAKO EnVision+ System, anti-rabbit	Cell Signaling Technology
CD90/thymocyte differentiation antigen 1, ERP3133	Thy-1	Rabbit IgG	Purified from tissue culture supernatant	Cell membrane	Tris-EDTA (pH 9.2)	No	1:200	DAKO EnVision+ System, anti-rabbit	Abcam
Fibroblast activation protein, AF3715	FAP	Sheep IgG	Antigen affinity purified	Cell membrane	Tris-EDTA (pH 9.2)	No	1:40	Donkey anti-sheep IgG-HRP, A16047 (ThermoFisher)	R&D Systems
α-Smooth muscle actin, 1A4	αSMA	Mouse IgG2a	Purified from cell culture supernatant	Cytoskeleton (actin filaments)	Tris-EDTA (pH 9.2)	No	1:4000	1. DAKO EnVision+ System, anti-mouse 2. MACH2 Biocare Medical, anti-mouse	Dako
Nonmuscle myosin heavy chain, NBP2-38566	Smemb	Rabbit IgG	Immunogen affinity purified	Cytoskeleton (myosin binding)	Tris-EDTA (pH 9.2)	No	1:600	DAKO EnVision+ System, anti-rabbit	Novusbio
Smooth muscle myosin heavy chain I (SM1), 3F8	SM-MHC (SM1)	Mouse IgG1	Ascites	Cytoskeleton (myosin)	Tris-EDTA (pH 9.2)	No	1:5000	DAKO EnVision+ System, anti-mouse	Abcam
Smooth muscle myosin heavy chain 11 (SM2), ab53219	SM-MHC (SM2)	Rabbit IgG	Ion exchange chromatography	Cytoskeleton (myosin)	Tris-EDTA (pH 9.2)	No	1:500	DAKO EnVision+ System, anti-rabbit	Abcam
Calponin, hCO	Calp	Mouse IgG1	Ascites	Cytoskeleton (thin filament-associated protein)	Tris-EDTA (pH 9.2)	Yes	1:3 000 000	1. DAKO EnVision+ System, anti-mouse 2. MACH2 Biocare Medical, anti-mouse	Merck
Caldesmon, h-CALD	h-Caldes	Mouse IgG1	Protein A or G	Cytoskeleton (microfilaments) and ECM	Citrate (pH 6)	No	1:2000	DAKO EnVision+ System, anti-mouse	Novusbio
Desmin, AF3844	Des	Goat IgG	Antigen affinity purified	Cytoskeleton (intermediate filament)	Tris-EDTA (pH 9.2)	No	1:50	Donkey anti-goat IgG-HRP, ab97120 (Abcam)	R&D Systems
Smooth muscle protein 22α/transgelin, 8C8	SM22α	Mouse IgG1	Antigen affinity purified	Cytoskeleton (actin binding)	No retrieval	No	1:25000	DAKO EnVision+ System, anti-mouse	Novusbio
Smoothelin, R4A	Smooth	Mouse IgG1	Not specified	Cytoskeleton (intermediate filament)	Tris-EDTA (pH 9.2)	No	1:300	DAKO EnVision+ System, anti-mouse	Thermo Fisher Scientific
Tropomyosin, F-6	Tropo	Mouse IgG2b	Not specified	Cytoskeleton (actin binding)	Tris-EDTA (pH 9.2)	No	1:8000	1. DAKO EnVision+ System, anti-mouse 2. MACH2 Biocare Medical, anti-mouse	Santa Cruz Biotechnology

(*Continued*)

Table 1. Continued

Antibody, Clone or Catalog No.	Abbreviation Used in Study	Host Isotype; Subclass	Purification	Cellular Localization	Pretreatment	Protein Block (Dako)	Dilution	Secondary Antibody	Source
Myosin light chain kinase/ Telokin A01697-2	Telokin	Rabbit IgG	Not specified	Cytoskeleton (myosin binding)	No retrieval	No	1:1000	DAKO EnVision+ System, anti-rabbit	Bosterbio
Paxillin, 5H11	Pax	Mouse IgG1	Protein G	Cytoplasm > cytoskeleton (focal adhesion protein)	Tris-EDTA (pH 9.2)	No	1:500	DAKO EnVision+ System, anti-mouse	Invitrogen
Vinculin, hVIN-1	Vinc	Mouse IgG1	Unpurified	Cytoskeleton (actin binding)	Citrate (pH 6)	No	1:200 000	DAKO EnVision+ System, anti-mouse	Novusbio
Collagen-I, MBS502155	Col-I	Rabbit IgG	Affinity chromatography	ECM	Citrate (pH 6), Tris-EDTA (pH 9.2), and pepsin	No	No specific signal	DAKO EnVision+ System, anti-rabbit	MyBioScource
Collagen-I, C7510-17K	Col-I	Goat IgG	Affinity chromatography	ECM	Citrate (pH 6), Tris-EDTA (pH 9.2), and pepsin	No	No specific signal	Donkey anti-goat IgG-HRP, AB97120 (Abcam)	USBIO
Procollagen-I, PC8-7	Procol-I	Mouse IgG1	Not specified	Secreted	Citrate (pH 6) and Tris/EDTA (pH 9.2)	No	No specific signal	DAKO EnVision+ System, anti-mouse	Abnova
Procollagen-I, M58	Procol-I	Rat IgG1	Affinity chromatography	Secreted	Citrate (pH 6) and Tris-EDTA (pH 9.2)	No	No specific signal	Goat anti-rat IgG-Biotine, BA-9401 (Vector)	Chemicon International
Prolyl 4-hydroxylase β, 3-2B12	P4HB	Mouse IgG1	Affinity chromatography	Endoplasmic reticulum lumen, cell membrane	Citrate (pH 6)	No	1:4000	DAKO EnVision+ System, anti-mouse	Acris Antibodies
Osteopontin, AF1433	OPN	Polyclonal goat IgG	Antigen affinity purified	ECM	Tris-EDTA (pH 9.2)	No	1:100	Donkey anti-goat IgG-HRP, AB97120 (Abcam)	R&D Systems
Fibronectin, FBN11	FBN	Mouse IgG1	Protein G	ECM	Tris-EDTA (pH 9.2)	No	1:900	DAKO EnVision+ System, anti-mouse	Thermofisher
Laminin, ab11575	Lam	Polyclonal rabbit IgG	Immunogen affinity purified	ECM	Tris-EDTA (pH 9.2)	No	1:200	DAKO EnVision+ System, anti-rabbit	Abcam
Cellular retinoid-binding protein-I, B8	CRBP-I	Mouse IgG1	Not specified	Cytoplasm	Citrate (pH 6) and Tris-EDTA (pH 9.2)	No	No signal	DAKO EnVision+ System, anti-mouse	Santa Cruz Biotechnology
Platelet-derived growth factor receptor α, ab61219	PDGF-α	Rabbit IgG	Immunogen affinity purified	Cell membrane	Citrate (pH 6) and Tris-EDTA (pH 9.2)	No	A specific signal (nuclear)	DAKO EnVision+ System, anti-rabbit	Abcam
Phosphorylated nuclear factor-κB p105, 178F3	NF-κB	Rabbit IgG	Not specified	Nucleus	Citrate (pH 6), Tris-EDTA (pH 9.2), and pepsin	No	No specific signal	DAKO EnVision+ System, anti-rabbit	Cell Signaling Technology
Phosphorylated nuclear factor-κB p65, MCFA30	NFκB	Mouse IgG1	Antigen affinity purified	Nucleus	Citrate (pH 6), Tris-EDTA (pH 9.2), and pepsin	No	No specific signal	DAKO EnVision+ System, anti-mouse	eBioscience
Interleukin 6, NYRhIL6	IL-6	Mouse IgG2a	Not specified	Secreted	Citrate (pH 6)	Yes	1:300	DAKO EnVision+ System, anti-mouse	Santa Cruz Biotechnology

(*Continued*)

Table 1. Continued

Antibody, Clone or Catalog No.	Abbreviation Used in Study	Host Isotype; Subclass	Purification	Cellular Localization	Pretreatment	Protein Block (Dako)	Dilution	Secondary Antibody	Source
Monocyte chemoattractant protein-I, 23002	MCP-I	Mouse IgG2b	Protein A or G	Secreted	Citrate (pH 6), Tris-EDTA (pH 9.2), and pepsin	No	No signal	DAKO EnVision+ System, anti-mouse	R&D Systems
Interleukin 8, bs0708R	IL-8	Rabbit IgG	Protein A	Secreted	Tris-EDTA (pH 9.2)	No	1:600	DAKO EnVision+ System, anti-rabbit	Bioss
CD31, JC70A	CD31	Mouse IgG1	Tissue culture supernatant	Cell membrane	Tris-EDTA (pH 9.2)	No	1:1000	MACH-2 Biocare Medical, anti-mouse	Dako
CD45, HI30	CD45	Mouse IgG1	Affinity chromatography	Cell membrane	Tris-EDTA (pH 9.2)	No	1:2000	MACH-2 Biocare Medical, anti-mouse	Biolegend
CD34, M1636	CD34	Mouse IgG1	Affinity chromatography	Cell membrane	Citrate (pH 6)	Yes	1:1 000 000	MACH-2 Biocare Medical, anti-mouse	Sanquin
CD4, H-370	CD4	Rabbit IgG	Not specified	Cell membrane	Tris-EDTA (pH 9.2)	No	1:800	MACH-2 Biocare Medical, anti-rabbit	Santa Cruz Biotechnology
CD8, C8/144B	CD8	Mouse IgG1	Not specified	Cell membrane	Tris-EDTA (pH 9.2)	No	1:200	MACH-2 Biocare Medical, anti-mouse	Dako
Rabbit IgG Ref x0903 Lot 20011861									Dako
Rabbit IgG Ref I5006 Lot SLBK1653V									Sigma-Aldrich
Mouse IgG Ref x0931 Lot 20023783									Dako
Rabbit serum Ref x0902									Dako
Mouse serum Ref x0910									Dako

CD indicates cluster of differentiation; and ECM, extracellular membrane.

Table 2. Antibodies Used for Immunofluorescence

Antibody, Clone	Host Isotype; Subclass	Purification	Cellular Localization	Pretreatment	Protein Block (Dako)	Dilution	Secondary Antibody (+Chromogen If Used)	Reference/Source
CD45, HI30	Mouse IgG1	Affinity chromatography	Cell membrane	Tris-EDTA (pH 9.2)	No	1:500	1. MACH-2 Biocare Medical, anti-mouse 2. Vulcan Red (Biocare Medical, LOT042418)	Biolegend
CD68, KP1	Mouse IgG1	Affinity chromatography	Lysosomes, endosomes, and cell surface	Tris-EDTA (pH 9.2)	No	1:6000	1. Alexa Fluor 488 goat–anti-mouse IgG1 (Life Technologies No. 21121) 2. Alexa Fluor 647 goat–anti-mouse IgG (Invitrogen, Thermo Fisher No. 21240)	Dako
CD31, JC70A	Mouse IgG1	Tissue culture supernatant	Cell membrane	Tris-EDTA (pH 9.2)	No	1:500	Alexa Fluor 546 goat–anti-mouse IgG1 (ThermoFisher No. 21123)	Dako
Vimentin, 3B4	Mouse IgG2a	Purified from cell culture supernatant	Cytoskeleton (intermediate filament)	Tris-EDTA (pH 9.2)	No	1:2000	1. Alexa Fluor 647 goat–anti-mouse IgG2a (Life Technologies No. 21241) 2. Alexa Fluor 488 goat-anti-mouse IgG1 (Life Technologies No. 21121)	Dako
Vimentin, VI-10	Mouse IgM	Precipitation and chromatography	Cytoplasm	Tris-EDTA (pH 9.2)	No	1:6000	Alexa Fluor 488 goat–anti-mouse IgG (Life Technologies No. 21042)	Abcam
α-Smooth muscle actin, 1A4	αSMA	Mouse IgG2a	Purified from cell culture supernatant	Cytoskeleton (actin filaments)	Tris/EDTA (pH 9.2)	No	Alexa Fluor 647 goat–anti-mouse IgG2a (Life Technologies No. 21241)	Dako
FSP-1/S100A4, D9F9D	Rabbit IgG	Unknown	Nucleus, cytoplasm, and extracellular space	Tris-EDTA (pH 9.2)	No	1:4000	Alexa Fluor 647 goat–anti-rabbit IgG (Invitrogen, Thermo Fisher No. 31573)	Cell Signaling Technology
CD90/Thy-1, ERP3133	Rabbit IgG	Tissue culture supernatant	Cell membrane	Tris-EDTA (pH 9.2)	No	1:200	Alexa Fluor 647 goat–anti-rabbit (Invitrogen, Thermo Fisher No. 31573)	Abcam
FAP, AF3715	Sheep IgG	Antigen affinity purified	Cell membrane	Tris-EDTA (pH 9.2)	No	1:40	Alexa Fluor 546 donkey–anti-sheep IgG (ThermoFisher No. 16047)	R&D Systems
Paxillin, 5H11	Mouse IgG1	Protein G	Cytoplasm > cytoskeleton (focal adhesion protein)	Tris-EDTA (pH 9.2)	No	1:500	Alexa Fluor 647 goat–anti-mouse IgG1 (Life Technologies No. 21240)	Invitrogen
Nonmuscle myosin heavy chain, NBP2-38566	Rabbit IgG	Immunogen affinity purified	Cytoskeleton (myosin)	Tris-EDTA (pH 9.2)	No	1:600	Alexa Fluor 647 donkey–anti-rabbit IgG (Life Technologies No. 31573)	Novusbio

CD indicates cluster of differentiation; FAP, fibroblast activation protein; FSP-1, fibroblast-specific protein-1; and Thy-1, thymocyte differentiation antigen 1.

Red fluorescence was visualized using a Texas Red Filter (542–582 nm).

Imaging of Immunofluorescence Slides

Digital images were acquired using the Panoramic MIDI Digital Slide Scanner (3D HISTECH Ltd, Budapest, Hungary) and analyzed with CaseViewer software (3D HISTECH Ltd). Minor linear adjustments (brightness and contrast) were performed. Nonlinear adjustments were not performed.

Because (partial) overlapping cells may result in pseudocolocalization in widefield optical microscopy, the anticipated pseudocolocalization of CD31 and respectively FSP-1 (fibroblast-specific protein-1)/thymocyte differentiation antigen 1 (Thy-1)/FAP (fibroblast activation protein), as well as the anticipated genuine colocalization of CD45 and vimentin, was validated by confocal microscopy (Zeiss LSM 800 CLSM, Oberkochen, Germany). Image analysis was performed with ZEN Lite (Zeiss).

RESULTS

Literature Review

Identification of Phenotypical Immunohistochemistry Markers

The search strategy identified 3246 articles after removal of duplicates, 655 of which were considered of potential relevance (Figure 2 [Preferred Reporting Items for Systematic Reviews and Meta-Analyses diagram]). Potentially relevant articles mainly addressed SMC differentiation (n=559 articles), and to a lesser extent aspects of (myo)fibroblastic or mesenchymal differentiation (96 articles). The abstracts of these latter 96 articles were all assessed for potential relevance. Given the large number of publications on SMC

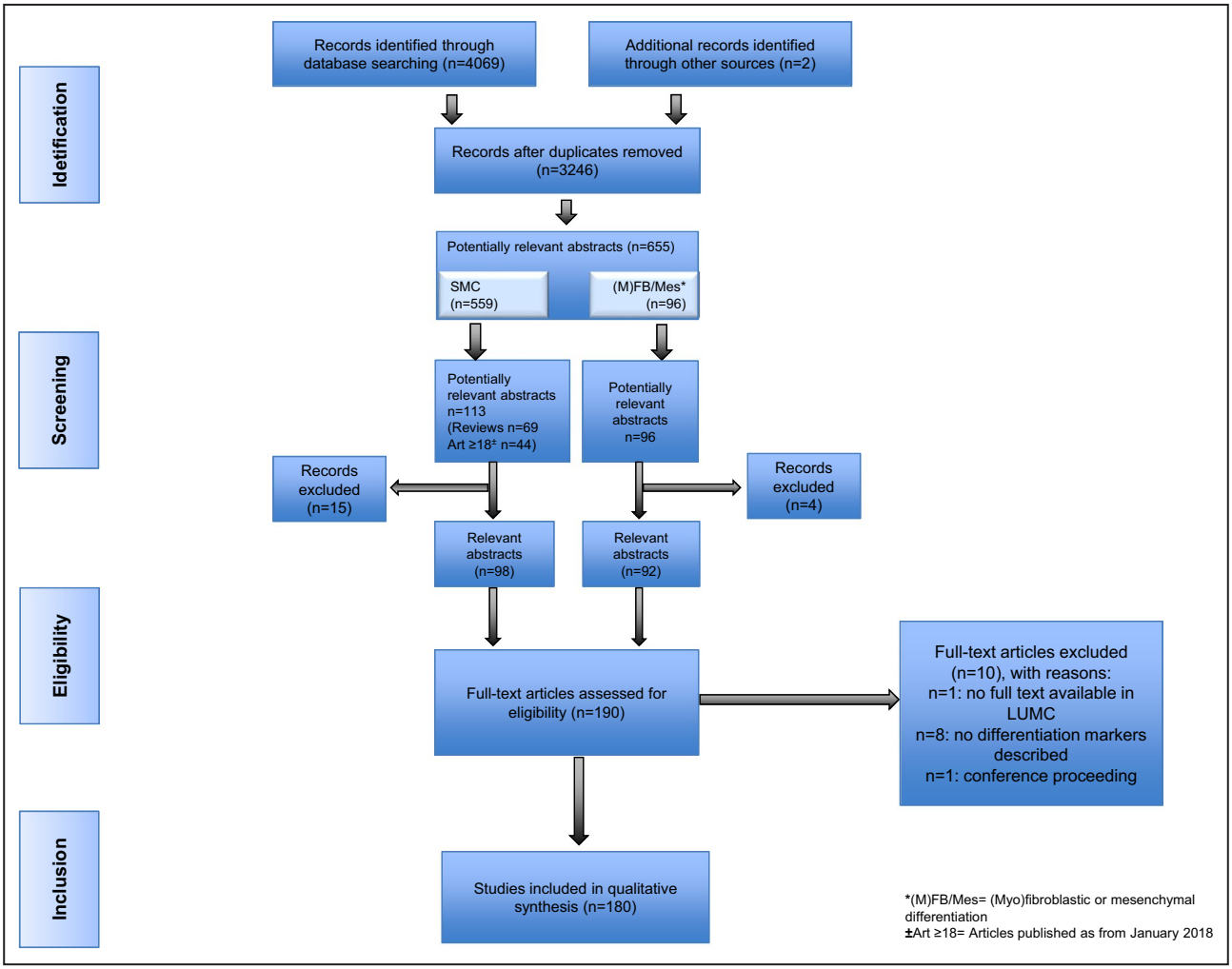

Figure 2. Preferred Reporting Items for Systematic Reviews and Meta-Analyses diagram for selection of articles on phenotypical mesenchymal markers.
SMC indicates smooth muscle cell.

differentiation (n=559), it was decided for an alternative approach by focusing on all review articles for assessment of the abstracts (n=69). Because the most recent review was published in March 2018, we additionally screened abstracts of articles published after January 2018 (n=44). On exclusion of articles deemed not relevant for this study, the abstract screening resulted in 190 potentially relevant articles, of which 180 full-text articles were included for the qualitative synthesis. Motivation for noneligibility of full-text articles is provided in Table S1.

The identified markers were included for further evaluation (Table 3)[12-89] if at least 3 independent studies referenced them. Markers excluded in this evaluation are summarized in Table S2. All in all, this strategy yielded 16 candidate markers (either lineage or differentiation specific), which are summarized in Table 3.

Cell Identity Markers

On the basis of the literature, identified markers were classified as (mesenchymal) lineage or (sub)class specific (ie, potentially discriminating between fibroblasts, myofibroblasts, or SMCs). The literature synopsis did not indicate a discriminatory marker(set) for myofibroblasts versus SMCs (Table 3), nor a single fibroblast-specific marker.

In this context, it was decided to categorize the identified markers along the following lines: we first defined a group of 4 markers that are reported as lineage specific (eg, vimentin) and a second group consisting of 3 markers associated with the principal force generating machinery (α-smooth muscle actin [αSMA], the 2 smooth muscle myosin heavy chain [SM-MHC] isoforms [SM1 and SM2], and nonmuscle myosin heavy chain [Smemb]). This cluster may allow differentiation between contractile (expressed in both SMC-like and myofibroblastic classes) and noncontractile mesenchymal cells.

A third group constituted of 7 molecules that are accessory to the contractile machinery (eg, tropomyosin). The final 2 markers (final fourth subset) are associated with cell-cell and/or cell-matrix interactions (eg, vinculin).

Markers of Functional Status

The literature review for candidate functional markers (ie, proinflammatory and synthetic markers) in the context of vascular biology research identified 222 full-text articles (Figure 3). Motivation for noneligibility of the reviewed full-text articles is provided in Table S3. Again, a threshold of at least 3 independent references for each functional marker was adopted to include the marker for immunohistochemistry evaluation (Tables S4 and S5).

On the basis of this search strategy, 8 synthetic and 4 proinflammatory markers were selected for further evaluation (Table 4).[90-128]

Histological Validation

Interference by Rabbit Polyclonal Antibodies

A particular point of concern that emerged from the histological evaluation was an apparent interference when using rabbit polyclonal antibodies on formalin-fixed, paraffin-embedded vessel wall samples. Interference was consistent for different sources and batches of isotype controls, and found for rabbit serum (Figure S2). In fact, all rabbit immunoglobulins in concentrations beyond 1 μg/mL produced a characteristic staining pattern on the arterial wall samples. This phenomenon was rabbit IgG/serum specific. Consequently, we avoided the use of rabbit polyclonal antibodies requiring working dilutions of ≥1 μg/mL in this evaluation.

Vascular Distribution and Specificity

We validated the expression patterns and staining specificity of the phenotypical and functional cell markers identified in the literature review on the vessel wall samples from the biobank. All markers selected in the review process were stained (single staining) on consecutive slides of the reference tissue block. Results from the evaluation (summarized as semiquantitative scores for the different aspects of the arterial wall) are summarized in Figure 4.

Lineage (mesenchymal) markers

Vimentin, FSP-1/S100A4, Thy-1/CD90, and FAP were identified as mesenchymal lineage-specific markers (Figure 5A).

All 4 markers were diffusely expressed throughout the vessel wall and vasa vasorum in the early atherosclerotic (AIT) reference sample. However, a notable inconsistent expression was found for these markers in the media, with subsets of spindle-shaped cells being vimentin$^+$ and FAP$^+$, but negative for both FSP-1 and Thy-1, challenging Thy-1 and FSP-1 as generic mesenchymal lineage markers. Indeed, validation of this observation in triple immunofluorescence stainings of (Thy-1/FSP-1/FAP)/vimentin/αSMA showed that up to 10% of the spindle-shaped αSMA$^+$/vimentin$^+$ or αSMA$^+$/FAP$^+$ cells in the media were negative for both Thy-1 and FSP-1 (Figure S3).

This dissociation between vimentin and Thy-1 expression became even more pronounced in the more advanced atherosclerotic stages by an apparent inverse association between Thy-1 expression and disease progression, with a particularly low expression of

Table 3. Overview of Selected Potential Phenotypic Markers

	Antibody*	Function†	Specificity in Vasculature†	Fibroblastic Cells	Myofibroblastic Cells	C-SMCs
Mesenchymal lineage	1. Vimentin[12-14]	Stabilization of cytoskeletal interactions and maintenance of cell shape and integrity of the cytoplasm[48,49]	Expressed in leukocytes and endothelial cells as well[50,51]			
	2. S100A4/FSP-1[15-17]	Involved in proteolytic activity during ECM remodeling and cell migration, proliferation, differentiation, and contractility[52-54]	Expressed in leukocytes as well[52,54,55]			
	3. CD90/Thy-1[15,18,19]	Involved in cell adhesion and cell communication[56]	Expressed in endothelial cells as well[57]			
	4. FAP[20-22]	Thought to promote cellular invasion through the ECM[58]	Expressed in leukocytes as well[59]			
Contractile apparatus	5. αSMA[23-25]	Force generation[60-62]	Expressed in macrophage-like phenotype (foam cells) as well[63,64]			
	6. Smemb[25-27]	Thought to be involved in diverse processes, including cytokinesis, cell shape, and secretion[65]	Restricted to mesenchymal cells[66]			
	7. SM-MHC[28-30]	Force generation[17,67]	Restricted to mesenchymal cells[68]			
Accessory contractile	8. h1-Calponin[28,31,32]	Regulation and modulation of smooth muscle contraction[69]	Restricted to mesenchymal cells[70]			
	9. h-Caldesmon[13,33,34]	Regulation of smooth muscle contraction[71]	Restricted to mesenchymal cells[72]			
	10. Desmin[13,34,35]	Maintenance of myofibril, myofiber, and whole muscle tissue structural and functional integrity[73,74]	Restricted to mesenchymal cells (in vasculature)[75]			
	11. SM22α [22,28,29]	Involved in the reorganization of the actin cytoskeleton and cell contractility[76,77]	Restricted to mesenchymal cells[78]			
	12. Smoothelin-B[28,36,37]	Associates with stress fibers and constitutes part of the cytoskeleton[79]	Restricted to mesenchymal cells[80]			
	13. a-Tropomyosin[27,38,39]	Regulation of smooth muscle contraction[81]	Restricted to mesenchymal cells[82]			
	14. Telokin[40-42]	Involved in initiation or maintenance of smooth muscle relaxation as well as in contraction[83,84]	Restricted to mesenchymal cells[85]			
Focal adhesion	15. Paxillin[43-45]	Focal adhesion protein involved in cell-matrix adhesion and presumably coordination of transmission of downstream signals in cell movement and migration[86]	Expressed in leukocytes, endothelial cells, and epithelial cells as well[87]			
	16. Vinculin[38,46,47]	F-actin binding protein involved in cell-matrix adhesion and cell-cell interactions[88]	Expressed in leukocytes, endothelial cells, and epithelial cells as well[89]			

The selected phenotypical markers are divided in 3 main groups, of which the contractile markers are subdivided on the basis of whether they are part of the contractile apparatus or they are accessory proteins that regulate actin-myosin interaction. Fibroblastic cells, myofibroblastic cells, and C-SMCs were evaluated on their reported discriminative power: dark gray represents controversy over discriminating ability of the marker, and light gray represents consensus that the marker is nondiscriminative. CD indicates cluster of differentiation; C-SMC, contractile smooth muscle cell; ECM, extracellular membrane; FAP, fibroblast activation protein; FSP-1, fibroblast-specific protein-1; αSMA, α-smooth muscle actin; SM22α, smooth muscle protein 22α; Smemb, nonmuscle myosin heavy chain; SM-MHC, smooth muscle myosin heavy chain; and Thy-1, thymocyte differentiation antigen 1.

*References from systematic review.

†Supplementary references (not from systematic review).

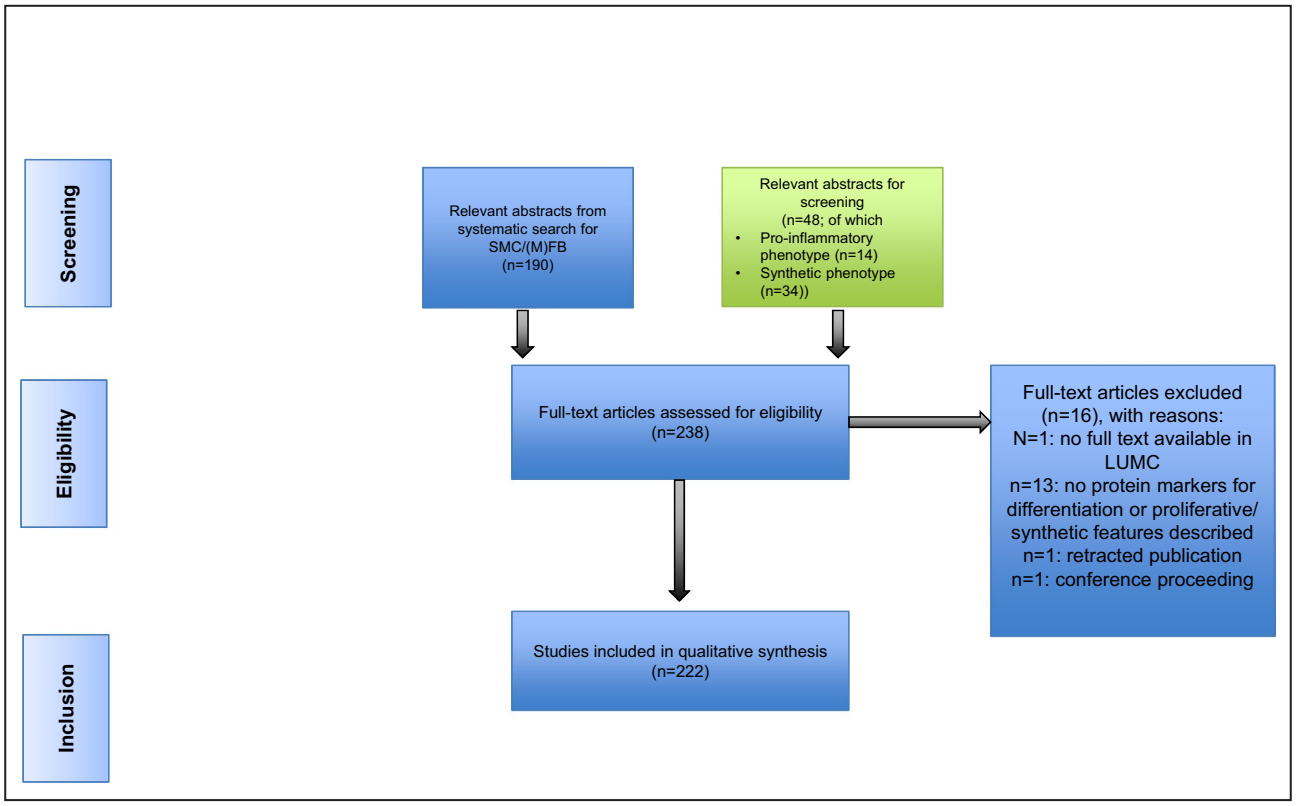

Figure 3. Diagram for selection of articles on synthetic/proinflammatory markers.
SMC indicates smooth muscle cell; and LUMC, Leiden University Medical Center.

Thy-1 in the neointima. Further discrepancies were observed for vimentin and FAP. Although medial vimentin expression remained stable in advanced-stage (LFA) atherosclerotic disease samples, FAP expression varied (Figure S4).

For explorative purposes, we also evaluated vimentin and αSMA coexpression in the cap of progressive lesions (ie, LFA and the unstable progressive atherosclerotic lesion [thin cap fibroatheroma]), as well as a stabilized lesion type (HR) (Figure S5). The cap in LFA was rich in mesenchymal cells (elongated vimentin$^+$ cells). Transition to a thin cap fibroatheroma was associated with a clear decrease in cap cell density. In both LFA and thin cap fibroatheroma, ≈80% of the vimentin$^+$ cells were double vimentin$^+$/αSMA$^+$. Similarly, 80% of the vimentin$^+$ cells in the cell-rich/proteoglycan-rich luminal granulation tissue associated with healing of a ruptured atherosclerotic lesion (HR) were double vimentin$^+$/αSMA$^+$.

On the basis of these observations, vimentin classified as the most inclusive lineage marker. However, we did observe a small population of spindle-shaped FAP$^+$/vimentin$^-$ cells in the cap of LFA (Figure S4.2), defying vimentin as an all-inclusive panmesenchymal marker.

Specificity of vimentin as a mesenchymal lineage marker was challenged by the diffuse presence of round, vimentin$^+$ cells in the vicinity of the vasa vasorum in the adventitia. Validation studies that included triple immunofluorescence staining for the panleucocyte marker CD45, the macrophage marker CD68, and vimentin showed subsets of triple-positive cells in the adventitia (Figure S6.1/2). This colocalization was observed for different vimentin antibodies, and confirms the expression of vimentin in subsets of macrophages. Along similar lines, we identified (small) subsets CD45$^+$/CD68$^+$ and FSP-1$^+$, Thy-1$^+$, or FAP$^+$ triple-positive cells in the adventitia, consistent with subsets of FSP-1$^+$, Thy-1$^+$, and FAP$^+$ macrophages (Figure S6.3-5).

Moreover, indications were found for vimentin expression in subsets of endothelial cells. Endothelial cell-specific expression was confirmed by CD31/vimentin double staining (Figure S7). Confocal microscopy characterized the apparent spatial associations between CD31 and FSP-1, Thy-1, and FAP as pseudocolocalization. Distinct, small populations of solitary vimentin$^+$/CD31$^+$ and vimentin$^+$/CD34$^+$ were observed in the vicinity of the adventitial vasa vasorum (Figure S8).

A third nonclassic population of vimentin$^+$ cells was observed in the granulation tissue of HR. Approximately 10% of these spindle-shaped cells were double Vim$^+$/CD45$^+$(Figure S9.1). Incidental (<5% of the population)

Table 4. Overview of Selected Potential Functional Markers

Subdivision	Antibody, Reference	Function	Tested Immunohistochemistry Suitability
Synthetic	1. Collagen type I[28,90,91]	Provides tensile strength of the arterial wall[110] In pathologic conditions, collagen contributes to plaque growth and serves as a depot for atherogenic molecules[111]	Nonspecific staining
	2. Procollagen type 1[25,92,93]	Precursor of collagen I, the most abundant collagen in ECM[112]	Weak to no staining; in higher concentrations, nonspecific staining
	3. Prolyl 4-hydroxylase β[16,33,94]	Involved in hydroxylation of prolyl residues in preprocollagen[113,114]	Works well
	4. Osteopontin[40,95,96]	Mediates cell migration, adhesion, and survival of SMCs and endothelial cells and functions as Th1 cytokine[115,116]	Works well, but extracellular presence hampers cell phenotyping
	5. Fibronectin[25,48,97]	ECM constituent with great diversity of cellular functions, including adhesion, cytoskeletal organization, migration, growth, and differentiation[117]	Works well, but extracellular presence hampers cell phenotyping
	6. Laminin[40,97,98]	ECM constituent (base membrane) with great diversity of cellular functions, including adhesion, migration, differentiation, and proliferation[118,119]	Works well, but extracellular presence hampers cell phenotyping
	7. CRBP-1[27,47,99]	Regulation of uptake, intracellular transport, and metabolism of retinol[120]	No protein expression detectable in AAA and atherosclerotic tissue
	8. PDGFR-α[43,100,101]	PDGF-α is a mitogen for mesenchymal cells and regulates proliferation, migration, and differentiation during embryonic development[121,122]	Nonspecific staining
Proinflammatory	9. NF-κB[29,102,103]	Pivotal mediator of inflammatory responses by inducing proinflammatory genes and regulating the survival, activation, and differentiation of innate immune cells and inflammatory T cells[123]	Low protein expression in vessel wall
	10. Interleukin 6[103-105]	Proangiogenic and proinflammatory/anti-inflammatory cytokine, predominantly associated with plasma cells and macrophages[124,125]	Works well
	11. MCP-1[105-107]	Regulates migration and infiltration of monocytes/macrophages[126]	No protein expression detectable in AAA and atherosclerotic tissue
	12. Interleukin 8[104,108,109]	Proangiogenic and proinflammatory cytokine, predominantly associated with lymphocytes and neutrophils; promotes neutrophil infiltration and activation, and can exert strong proangiogenic activities[127,128]	Works well

AAA, abdominal aortic aneurysm; CRBP-1 indicates cellular retinol-binding protein 1; ECM, extracellular membrane; MCP-1, monocyte chemoattractant protein 1; NF-κB, nuclear factor-κB; PDGF-α, platelet-derived growth factor α; PDGFR-α, PDGF-α receptor; SMC, smooth muscle cell; and Th1, T-helper type 1 T-cell.

double $Vim^+/CD45^+$ cells were also observed in the cap and neointima of LFA and FCP reference sections. Distinct (spindle-shaped and round) morphological features may imply distinct subpopulations (Figure S9.2/3).

Contractile/noncontractile phenotype markers

αSMA, SM-MHC (isoforms SM1 and SM2), and Smemb (embryonic form of SM-MHC) are principle parts of the contractile machinery that is characteristic for SMCs and myofibroblasts (Figure 5B).

αSMA was expressed in virtually all spindle-shaped cells in the intima, media, and adventitia. In mesenchymal cells covering the vasa vasorum, αSMA was consistently expressed. Expression of the SM-MHC isoforms and Smemb was more variable: SM-MHC (SM1) expression was notably less in the middle section of the media than in the inner and outer segments of the media, and expression of the second isoform (SM2) was limited to the outer segment of the media. Smemb expression was more pronounced in the outer medial segment than in other medial segments. A discriminatory expression profile was seen for SM-MHC/Smemb expression in the vasa vasorum with parallel expression in the thick-walled arteriole-like vessels, but Smemb single positivity was found in the thin-walled venule-like vessels.

Progressive stages of atherosclerosis showed stable αSMA expression, whereas SM-MHC and Smemb expression were negatively and positively associated, respectively, with disease progression, potentially disqualifying SM-MHC and Smemb as all-encompassing contractile markers. Smemb expression has been

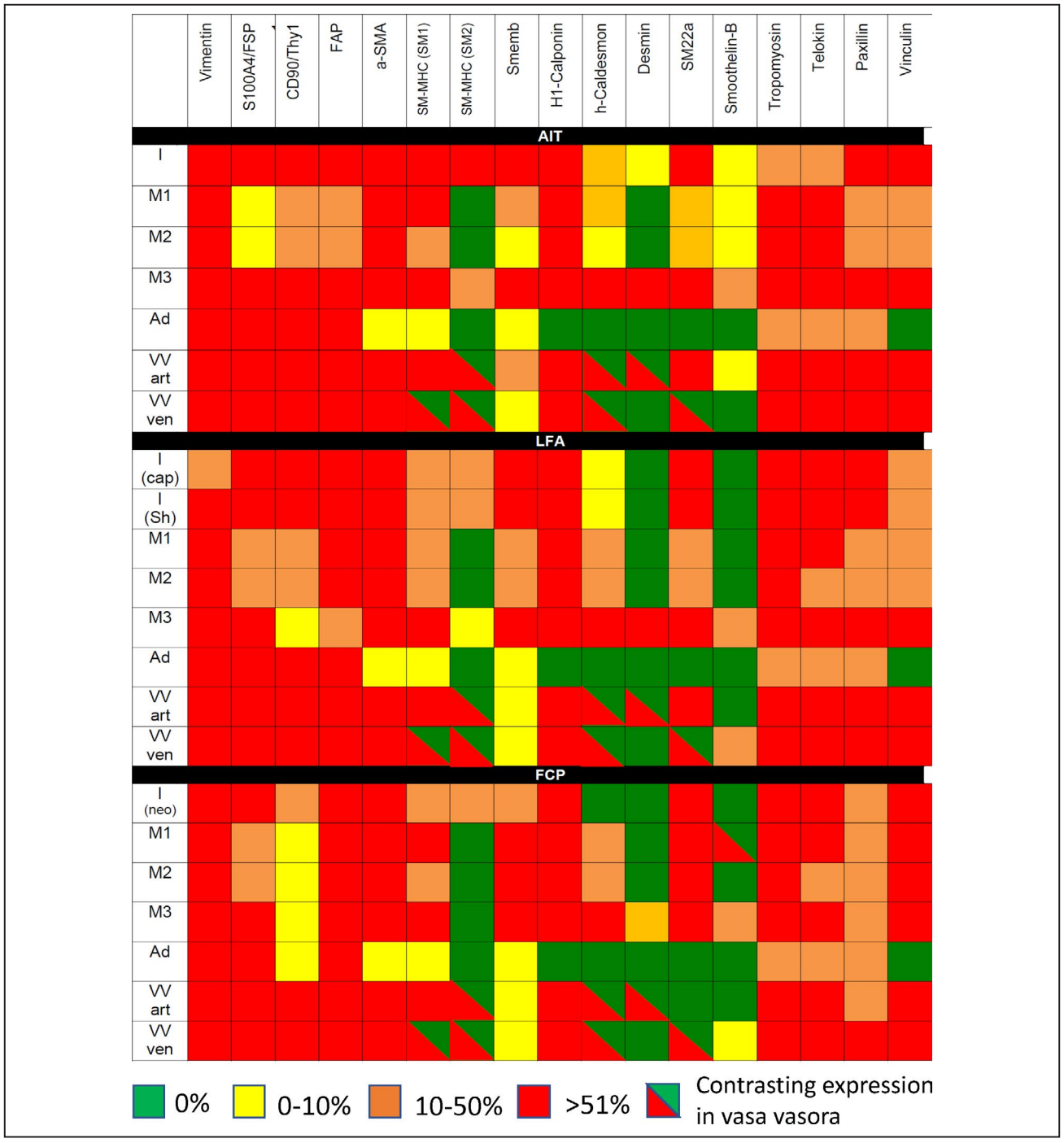

Figure 4. Semiquantitative evaluation of single immunohistochemistry (IHC) stainings.
The presence of immunohistochemical markers is appreciated in 6 zones of the vessel wall: intima (I), inner media underlying lesion (M1), middle media (M2), outer media (M3), adventitia (Ad), thin-walled, venous-type vasa vasorum (VV thin), and thick-walled artery-type vasa vasorum (VV thick). In late fibroatheroma (LFA), the intima is divided in a central cap region (Cap) and shoulder regions (Sh); and in fibrotic calcified plaque (FCP), the neointima (Neo) overlaying the fibrous cap is considered. AIT indicates adaptive intimal thickening; FAP, fibroblast activation protein; FSP, fibroblast-specific protein; α-SMA, α-smooth muscle actin; SM22α, smooth muscle protein 22α; Smemb, nonmuscle myosin heavy chain; SM-MHC, smooth muscle myosin heavy chain; and Thy1, thymocyte differentiation antigen 1.

linked to a synthetic phenotype. Indeed, most, but not all, of the Smemb+ cells in the cap and shoulder regions expressed the synthetic marker prolyl 4-hydroxylase β (P4HB) (Figure S10).

Auxiliary contractile markers

The third group of markers identified in the review consisted of a group of auxiliary molecules to the contractile machinery (SM22α [smooth muscle protein 22α],

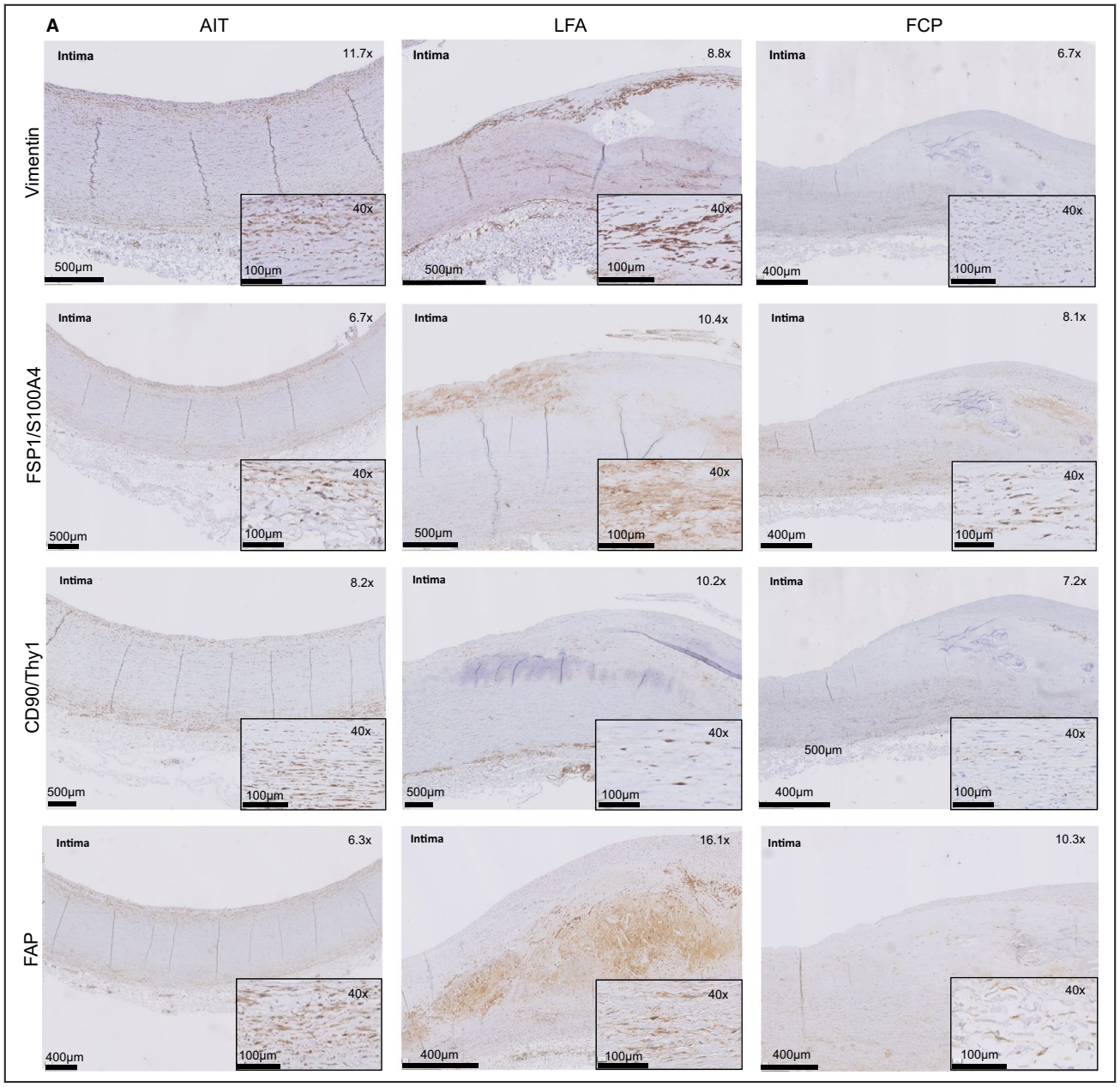

Figure 5. Histological validation of the selected immunohistochemistry (IHC) markers.
A, Mesenchymal lineage IHC markers. Overview of staining patterns in the selected representative atherosclerotic sections of adaptive intimal thickening (AIT) (early), late fibroatheroma (LFA) (progressive), and fibrotic calcified plaque (FCP) (end stage). Close ups in LFA and FCP represent cap regions and neointima, respectively. **B**, Generic contractile IHC markers. Overview of staining patterns in the selected representative atherosclerotic sections of AIT (early), LFA (progressive), and FCP (end stage). Close ups in LFA and FCP represent cap regions and neointima, respectively. **C**, Accessory contractile IHC markers. Overview of staining patterns in the selected representative atherosclerotic sections of AIT (early), LFA (progressive), and FCP (end stage). Close ups in LFA and FCP represent cap regions and neointima, respectively. **D**, Focal adhesion IHC markers. Overview of staining patterns in the selected representative atherosclerotic sections of AIT (early), LFA (progressive), and FCP (end stage). Close ups in LFA and FCP represent cap regions and neointima, respectively. **E**, Interleukin 6 (IL-6) and interleukin 8 (IL-8) staining (activation markers). Overview of staining patterns in the selected representative atherosclerotic sections of AIT (early), LFA (progressive), and FCP (end stage). Close ups in LFA and FCP represent cap regions and neointima, respectively. **F**, Prolyl 4-hydroxylase β (P4HB) staining (synthetic marker). Overview of staining patterns in the selected representative atherosclerotic sections of AIT (early), LFA (progressive), and FCP (end stage). Close ups in LFA and FCP represent cap regions and neointima, respectively. CD indicates cluster of differentiation; FAP, fibroblast activation protein; FSP, fibroblast-specific protein; α-SMA, α-smooth muscle actin; SM22α, smooth muscle protein 22α; Smemb, nonmuscle myosin heavy chain; SM-MHC, smooth muscle myosin heavy chain; and Thy1, thymocyte differentiation antigen 1.

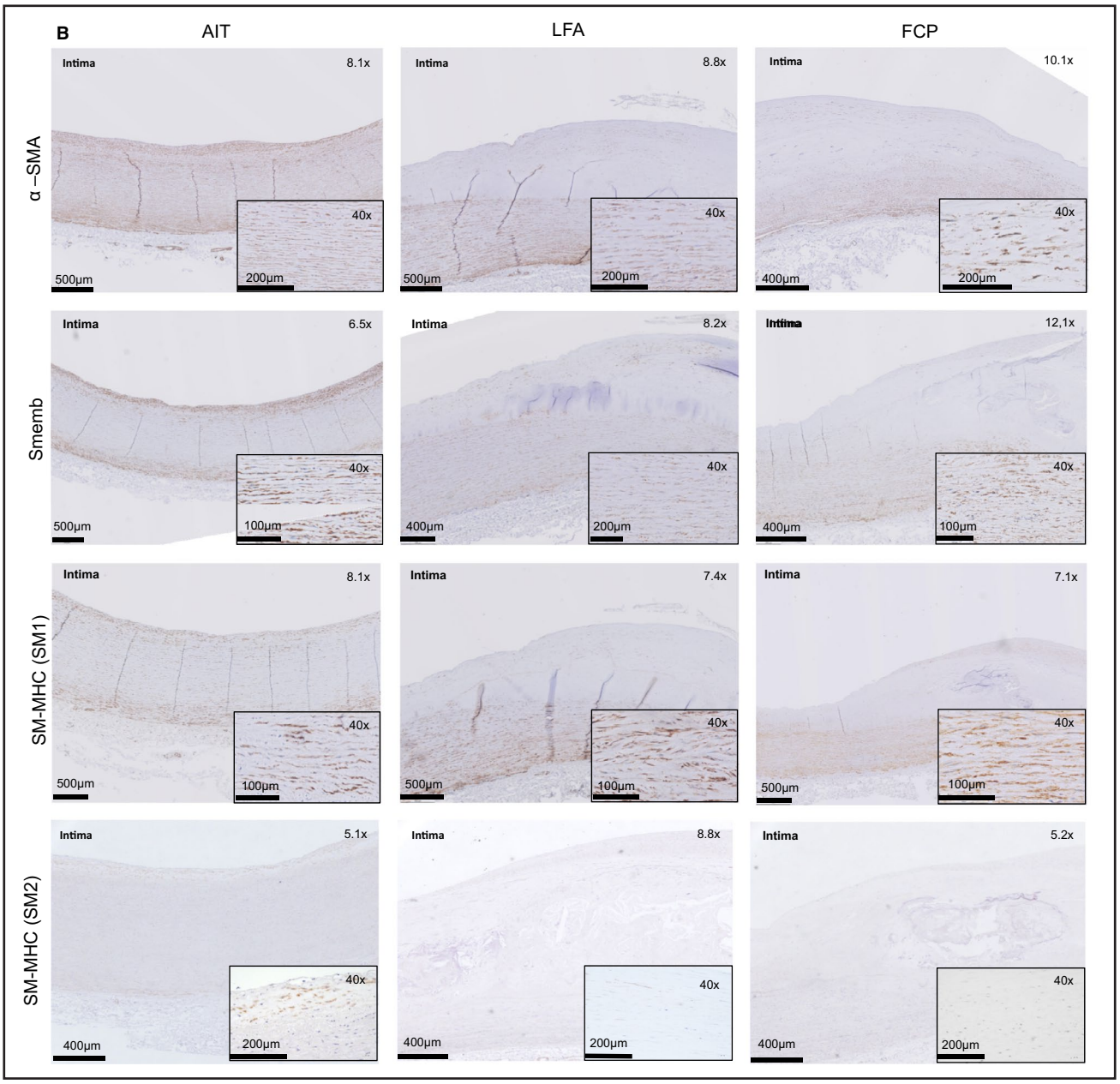

Figure 5. Continued

h1-Calponin, h-Caldesmon, Telokin, Tropomyosin, Desmin, and Smoothelin) (Figure 5C).

Spatial expression of these markers was variable: subsets of spindle-shaped cells in the intima, media, and vaso vasora were positive for SM22α and h-Caldesmon. Desmin and Smoothelin expression were both selectively expressed in the medioadventitial border zone. Desmin was selectively expressed in arteriole-type vasa vasorum, whereas Smoothelin was specifically expressed in venule-type vasa vasorum.

Although h1-Calponin was expressed in virtually all spindle-shaped cells in the intima and media in the early stages of atherosclerosis, spatial expression of h1-Calponin was more pronounced in LFA, shown by h1-Calponin^{-}/αSMA^{+} cells in the cap (Figure S11). Telokin and Tropomyosin were not fully contractile cell specific, as round triple Telokin^{+}/vimentin^{+}/CD45^{+} and Tropomyosin^{+}/vimentin^{+}/CD45^{+} cells were present in the adventitia (Figure S12.1/2).

Heterogeneous responses were seen for the auxiliary contractile markers in the context of the atherosclerotic disease progression: Smoothelin and Desmin expression related inversely to disease progression, whereas medial expression of h1-Calponin, h-Caldesmon, SM22α, Tropomyosin, and Telokin remained stable. H1-Calponin+, Tropomyosin+,

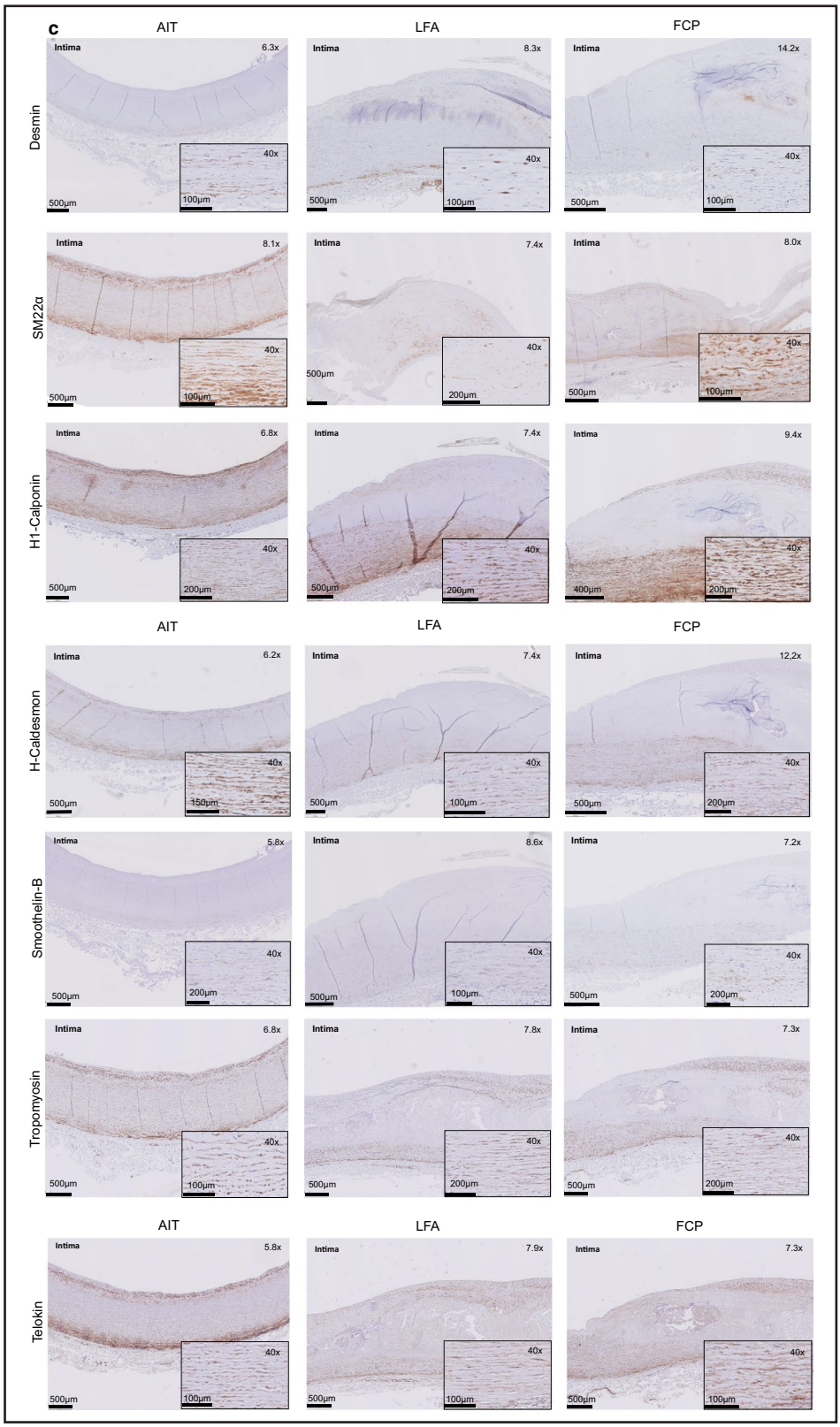

Figure 5. Continued

Telokin+, and SM22α+ were present in subsets of mesenchymal cells in the cap/shoulder, and in the neointima regions in LFA and FCP. A subpopulation (<10%) of spindle-shaped Tropomyosin^{+} αSMA^{-} cells was observed in the cap of the LFA lesion (Figure S13).

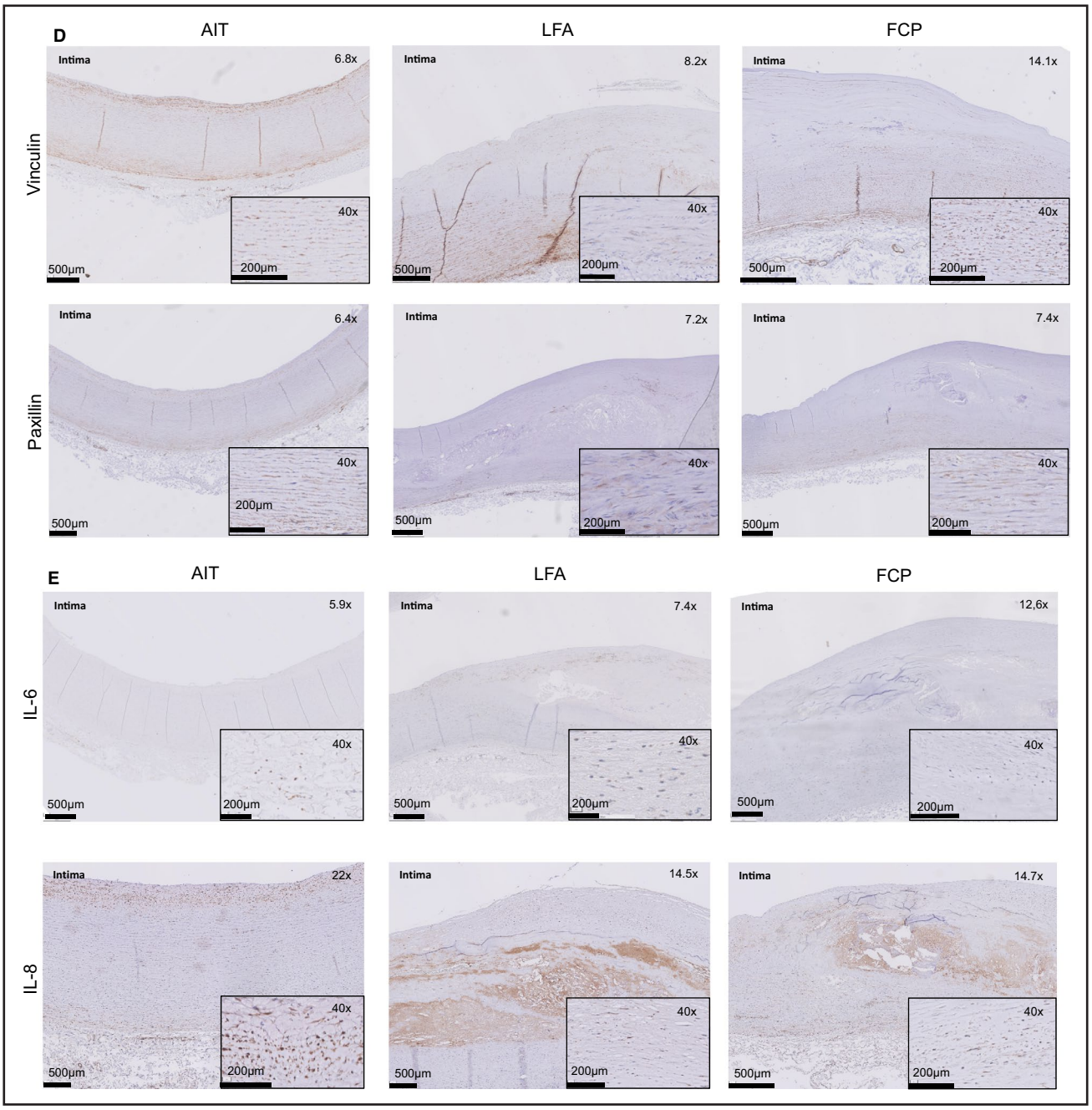

Figure 5. Continued

Focal adhesion proteins: vinculin and paxillin

The fourth cluster of markers included Vinculin and Paxillin, molecules involved in cell-cell and cell-matrix interactions (Figure 5D). In AIT, they were both abundantly expressed in the intimal and outer medial zone and to a lesser extent in the inner and middle media. Although Paxillin expression was also observed in double $CD45^{+}$/$vimentin^{+}$ cells in the adventitia (Figure S12.3), Vinculin expression was absent in the adventitia. Although Paxillin expression remained stable during atherogenic progression, Vinculin expression decreased during disease progression.

Functional markers

Apart from their phenotypical identities, mesenchymal cells can be actively involved in matrix deposition and homeostasis (synthetic phenotype), and may adapt an inflammatory phenotype. We evaluated several markers for a synthetic or an inflammatory phenotype (results are summarized in Table 4).

On the basis of an evaluation of compatibility with immunohistochemistry-based subtyping, which involved a preferably intracellular staining pattern and availability of antibodies compatible with paraffin-embedded material, the signal/background ratio, and specificity, it

Table 5. Proposed Marker Set for Standard Inventory of Mesenchymal Cell Populations in Human Vasculature

Phenotype		Function		Pathological Conditions
Generic mesenchymal: vimentin^{+}/CD31^{-}/CD45^{-}	Contractile, generic*: αSMA^{+}	Synthetic: P4HB^{+}	Proinflammatory: IL-6^{+}/IL-8^{+}	EndoMT/stem cells: CD34$^{+\dagger}$ CD31^{+}
	Noncontractile: αSMA^{-}			LeucoMT: CD45^{+}

Construction scheme of proposed mesenchymal marker set selection. Suggestions for well-working antibodies are provided in Table 1. Vimentin, in a marker set with CD31^{-}/CD45^{-}, will identify ≈95% of mesenchymal cells. αSMA will identify ≈95% of contractile mesenchymal cells. CD indicates cluster of differentiation; EndoMT, Endothelial-to-Mesenchymal cell Transition; IL-6, interleukin 6; IL-8, interleukin 8; LeucoMT, Leuccyte-to-Mesenchymal cell Transition; P4HB, prolyl 4-hydroxylase β; and αSMA, α-smooth muscle actin.

*For a list of accessory contractile and focal adhesion markers, see Table 3.

†OR,/ AND.

was decided for P4HB and interleukin 6 (IL-6) or interleukin 8 (IL-8; aka, CXCL8) as preferred markers for a secretory inflammatory phenotype. Motivations for refraining from the other candidate markers are provided in Figure S14.

IL-6 and IL-8 expression was used to visualize inflammatory status of the mesenchymal cell population (Figure 5E): in AIT, IL-6 and IL-8 expression was observed for infiltrating mesenchymal cells in the intima, and in subsets of adventitial mesenchymal cells. IL-8 was expressed in the medioadventitial border as well. Increased medial IL-6 and IL-8 expression, and significant expression of IL-6 and IL-8 in the cap and shoulder regions, was observed during atherogenic progression.

Expression of these inflammatory markers in the mesenchymal cell population may reflect the inflammatory character of atherosclerosis, an aspect that is illustrated by macrophage and T-cell stainings on the reference sections (Figure S15).

P4HB, an enzyme involved in (pre) collagen processing, was identified as preferred marker for a synthetic phenotype (Figure 5F). Expression of P4HB was confined to the intima and, with the exception of some vasa vasorum absent in the media and adventitia, in early-stage atherosclerosis. In more advanced stages of atherosclerosis, P4HB expression was observed in the cap and shoulder regions, as well as in the adventitial venule-like and arteriole-like vasa vasorum. P4HB remained absent in the entire media.

On the basis of the tentative results of the review and the inventory, a proposed marker set was compiled for an explorative evaluation of the vascular mesenchymal landscape (Tables 5 and 6).

DISCUSSION

The vascular mesenchymal landscape appears to be highly dynamic, diverse, and complex. It extends far beyond the classic tripartite classification scheme of fibroblasts, myofibroblasts, and SMCs. Furthermore, there is no evidence for a clear separation along the lines of myofibroblast and SMC populations. These findings for the human context confirm and extend observations for murine models of atherosclerosis that imply an extremely diverse spectrum of mesenchymal cells within the vessel wall.[129,130]

Mesenchymal cells are the pivotal cellular component of load-bearing structures and organs. They are the principle component of blood vessels, where they modulate vascular tone and maintain vascular integrity through deposition and maintenance of the extracellular matrix.[131,132] As a consequence, mesenchymal cells are in the center of vascular pathological conditions, such as atherosclerosis and aneurysmal disease.[133,134] In fact, mesenchymal cell activation and migration in response to intimal lipoprotein deposition is the initiating step in the human atherosclerotic process.[135] Data from murine atherosclerotic models suggest that SMCs contribute the majority of foam cells.[136] In the more

Table 6. Proposed Marker Set for Comprehensive Inventory of Mesenchymal Cell Populations in Human Vasculature

Phenotype		Function		Pathological Conditions
Generic mesenchymal: FAP^{+}/vimentin^{+}/CD31^{-}/CD45^{-}	Contractile, generic*: αSMA^{+}/tropomyosin^{+}	Synthetic: P4HB^{+}	Proinflammatory: IL-6^{+}/IL-8^{+}	EndoMT/stem cells: CD34$^{+\dagger}$ CD31^{+}
	Noncontractile: αSMA^{-}/tropomyosin^{-}			LeucoMT: CD45^{+}

Construction scheme of proposed mesenchymal marker set selection. Suggestions for well-working antibodies are provided in Table 1. To acquire ≈99% inclusivity for mesenchymal cells, a dual-marker set of vimentin^{+}/FAP^{+} (possibly as costaining, stained by the same chromogen) is needed. Likewise, for contractile mesenchymal cells, the dual-marker set αSMA/Tropomyosin reaches ≈99% inclusivity. CD indicates cluster of differentiation; EndoMT, Endothelial-to-Mesenchymal cell Transition; FAP, fibroblast activation protein; IL-6, interleukin 6; IL-8, interleukin 8; LeucoMT, Leuccyte-to-Mesenchymal cell Transition; P4HB, prolyl 4-hydroxylase β; and αSMA, α-smooth muscle actin.

*For a list of accessory contractile and focal adhesion markers, see Table 3.

†OR,/ AND.

advanced stages of atherosclerotic disease, mesenchymal cells critically contribute to plaque stability, as well as to aspects such as vascular calcification and intimal hyperplasia.[137,138] Indeed, an exploratory inventory implied clear qualitative changes in the cap during plaque progression with a nadir in cell density in thin cap lesions, but recovery of mesenchymal cell density (elongated vimentin$^+$ cells) in the cell-rich/matrix-rich granulation tissue of a healed rupture.

Along similar lines, mesenchymal cells are key players in both genetic (eg, thoracic aneurysms associated with bicuspid valve disease[139]) and degenerative aneurysms, such as the abdominal aortic aneurysm.[140] For the latter, impaired mesenchymal differentiation has been directly linked to aneurysm rupture.[141]

The vascular mesenchymal landscape is particularly complex, not only as a reflection of the heterogeneous embryological origin of the vascular tree,[142] and the vascular layers,[143] but also because SMCs are nonterminally differentiated,[144,145] thus allowing a high degree of phenotypical plasticity. Moreover, it is now clear that processes, such as endothelial-to-mesenchymal transition,[146] contribute to the vascular mesenchymal population.

Evidence was also found for the presence of fibrocytes. Ample elongated double CD45$^+$/vimentin$^+$ cells were observed in the process of cap healing following plaque rupture, and in the neointima overlaying a fibrous lesions. Moreover, we observed subpopulations of round and spindle-shaped double CD45$^+$/vimentin$^+$ cells in the cap of LFA. This observation is consistent with the (co)existence of distinct subpopulations of double CD45$^+$/vimentin$^+$ cells in the atherosclerotic process: spindle-shaped fibrocytes, which could be consistent with the phenomenon of leukocyte-mesenchymal transition,[147] and the round cells possibly representing a subclass of macrophages.[148]

The immunological field has benefited enormously from the introduction of the consensus classification of leukocyte subtypes, based on well-defined marker sets (CD markers); such classification system does not exist for mesenchymal cells. In a first attempt toward a mesenchymal cell classification for the vasculature, we inventoried candidate subtype markers through a literature review, and mapped the identified markers on a set human aorta specimens with successive stages of the atherosclerotic process.

The literature review identified 4 mesenchymal lineage markers: vimentin, FSP-1/S100A4, Thy-1/CD90, and FAP. Validation stainings disqualified FSP-1/S100A4 and Thy-1/CD90 as universal mesenchymal lineage markers. Therefore, conclusions based on studies relying on these markers may be incomplete.

On the basis of its performance in this evaluation, and on the assumption that most spindle-shaped cells are mesenchymal cells, vimentin classified as the preferred mesenchymal lineage marker for the vasculature because this was the most inclusive marker for spindle-shaped cells in the media. However, histological stainings identified small subsets of vimentin$^-$/FAP$^+$ cells in specific niches, suggesting that vimentin may not be fully inclusive and that a comprehensive appreciation of the full mesenchymal spectrum may rely on the vimentin/FAP dual-marker set.

On the same token, vimentin expression was seen in subset(s) of vascular macrophages, as well as the endothelial lining of vasa vasorum, indicating that vimentin is not fully mesenchymal cell specific, and that full specificity relies on costaining of exclusion markers (eg, CD31 and CD68). This study also identified solitary double vimentin$^+$/CD31$^+$ and vimentin$^+$/CD34$^+$ cells in the vicinity of adventitial vasa vasorum, possibly identifying vascular stem cells or cells in Endothelial-to-Mesenchymal cell Transition.[149]

Next to the lineage markers, the review identified several subclass markers. Markers for contractile phenotype were subdivided in 2 closely related subgroups: principal constituents of the contractile apparatus (αSMA, SM-MHC, and Smemb) and its auxiliary molecules (ie, actin/myosin interaction regulating [h1-Calponin, Desmin, h-Caldesmon, Tropomyosin, Telokin, Smoothelin, and SM22α]).

αSMA classified as the most inclusive marker for presence of a professional contractile machinery. However, coverage of the full spectrum of contractile mesenchymal cells may require a dual-marker set of αSMA/Tropomyosin, as the histological evaluation identified small specific niches in the cap of LFA that contained spindle-shaped αSMA$^-$/Tropomyosin$^+$ cells.

Smemb has been linked to a synthetic phenotype. Indeed, a subset of elongated Smemb$^+$ in the shoulder and cap of progressive atherosclerotic lesions also expressed P4HB. Yet, Smemb$^+$/P4HB$^-$ elongated cells were abundantly present in the media of early-stage atherosclerosis. These observations characterize Smemb as a mere differentiation marker.

A considerable degree of coexpression was observed for the auxiliary contractile markers in early atherosclerotic disease (AIT). However, increased heterogeneity was observed for the progressive stages. Clear spatial distribution of these subpopulations implies some form of synchronization in the processes of subdifferentiation. Exploration of underlying molecular synchronization pathways and functional diversity of the subdifferentiated cells is beyond the scope of this inventorying exploration.

The literature review further identified the focal adhesion proteins Vinculin and Paxillin, a binding partner of Vinculin,[150] as markers of mesenchymal differentiation. These proteins do not associate with the contractile

apparatus, but are involved in environmental sensing,[151] and are abundantly expressed by mesenchymal cells in the normal vessel wall.[152] We observed downregulation of Vinculin in spindle-shaped cells in the media during atherogenic progression, a phenomenon that has been interpreted as an indication of disturbed intermesenchymal or mesenchymal–extracellular matrix interaction.[153]

The identification of functional markers set for histological phenotyping came with several technical challenges. The inflammatory spectrum is notably broad, thus interfering with the identification of a generic marker. Moreover, by virtue of the responsive and adaptive nature of the inflammatory, protein expression can be extremely low and volatile, thus creating suboptimal conditions for immunohistochemistry. The cytokines/chemokines IL-6 and IL-8 (both essentially controlled by nuclear factor-κB activity) can be present as intracellular stores, and thus are well identifiable by immunohistochemistry staining. On this basis, we evaluated their potential as markers of (aspects of) an inflammatory phenotype. Indeed, IL-6 and IL-8 were both particularly upregulated in lesional intimas, such as the cap and shoulder regions of LFA. The dynamics of the innate and adaptive cellular immune response in human atherosclerosis have been extensively reported previously.[154,155]

Along similar lines, challenges exist for markers of a synthetic, secretory phenotype. Histological staining of deposited matrix products results in a profound extracellular staining pattern that interferes with the interpretation of intracellular stainings. Our evaluation identified the (pre)collagen processing enzyme PH4B as the optimal marker for mapping a synthetic phenotype in immunohistochemistry. In AIT, P4HB expression was confined to the intima, with the exception of some vasora, and showed upregulation during atherogenic progression in lesional intimas, such as the cap and shoulder regions in LFA.

Because our literature review did not provide conclusive evidence with respect to a discriminatory marker set identifying the classic smooth muscle phenotype and myofibroblast phenotype, it was reasoned that the arteriolar smooth muscle cell of the vasa vasorum in the adventitia constitutes the best reference to the classic, functionally contractile SMC phenotype. On basis of this premise, we could not establish a clear separation along the lines of myofibroblastic and SMC populations based on the (auxillary) contractile markers.

As (myo)fibroblastic cells are characterized by their ability to synthesize collagen, P4HB was explored as discriminative factor. However, spindle-shaped P4HB$^+$ cells covering the vasa vasorum were found as well.

This may suggest that myofibroblasts are rather cell states of fibroblastic cells or SMCs than a discrete cell type.

This evaluation of the mesenchymal landscape on the basis of a parallel evaluation of >25 markers indicates a spatially diverse, highly dynamic, and heterogeneous panorama. The spatial diversity and extreme granularity, and the relative long protein half-lives for most markers, pose particular challenges to RNA-based analysis, and to techniques relying on tissue dissection and clustering, such as single-cell analysis. Although immunohistochemistry has a clear advantage to these challenges, this explorative study has some limitations as well. First, the study is based on the results of a literature review. As such, the evaluation may be incomplete and findings from in vitro studies may not apply to the in vivo context (eg, we did not encounter a clear myofibroblast phenotype). Although specific cell isolation studies may add a further level of information about the in vivo context, studies on isolated cells were considered outside the scope of this inventory. Moreover, immunohistochemistry is semiqualitative at best, and heavily relies on the quality of the antibodies. Although quality control was performed, the specificity of antibodies for formalin-fixed, paraffin-embedded samples cannot be guaranteed. For this reason, we performed validation studies with alternative antibodies for the potentially controversial positive findings of vimentin positivity in nonmesenchymal cell lineages (fibrocytes and macrophages). Other stainings were not validated by staining with a different antibody. However, decisions to refrain from a candidate marker were only taken when multiple clones produced negative or nonspecific staining. The impact of nonspecific staining on data interpretation is clearly illustrated by the consistently observed nonspecific staining pattern when using rabbit polyclonal antibodies in concentrations beyond 1 μg/mL (1:1000 for most antibodies) on formalin-fixed, paraffin-embedded vessel sections.

The purpose of the study was to establish a marker set for mapping the mesenchymal landscape. The extreme granularity and spatial variation were unexpected. The full extent of the landscape can only be appreciated through systematic cataloging of the phenotypical diversity through a process that will rely on multiparameter imaging of samples covering the full disease spectra, targeted expression profiling, and functional evaluation. We consider this aspect beyond the scope of this inventorying study. However, this study provides the groundwork for a consensus cluster classification.

ARTICLE INFORMATION

Received April 27, 2020; accepted October 5, 2020.

Affiliations

From the Division of Vascular Surgery, Department of Surgery (L.E.B., C.M.v.R., J.F.H., J.H.L.) and Department of Pathology, Leiden University Medical Center, Leiden, The Netherlands (B.E.v.d.A.).

Acknowledgments

The authors wish to kindly thank J.W. Schoones for his assistance in composing the search strategy.

Sources of Funding

None.

Disclosures

None.

Supplementary Material

Datas S1–S3
Tables S1–S5
Figures S1–S15
References 2,3,5,23,57,61,109,133,143,156-311

REFERENCES

1. Topouzis S, Majesky M. Smooth muscle lineage diversity in the chick embryo. *Dev Biol*. 1996;178:430–445.
2. Lacolley P, Regnault V, Nicoletti A, Li Z, Michel J. The vascular smooth muscle cell in arterial pathology: a cell that can take on multiple roles. *Cardiovasc Res*. 2012;95:194–204.
3. Riches K, Clark E, Helliwell RJ, Angelini TG, Hemmings KE, Bailey MA, Bridge KI, Scott DJA, Porter KE. Progressive development of aberrant smooth muscle cell phenotype in abdominal aortic aneurysm disease. *J Vasc Res*. 2018;55:35–46.
4. Baum J, Duffy HS. Fibroblasts and myofibroblasts: what are we talking about? *J Cardiovasc Pharmacol*. 2011;57:376–379.
5. Bellini A, Mattoli S. The role of the fibrocyte, a bone marrow-derived mesenchymal progenitor, in reactive and reparative fibroses. *Lab Invest*. 2007;87:858–870.
6. Johnson RJ, Floege J, Yoshimura A, Iida H, Couser WG, Alpers CE. The activated mesangial cell: a glomerular "myofibroblast"? *J Am Soc Nephrol*. 1992;2:S190–S197.
7. Di Carlo SE, Peduto L. The perivascular origin of pathological fibroblasts. *J Clin Invest*. 2018;128:54–63.
8. Gibbons G, Dzau V. The emerging concept of vascular remodeling. *N Engl J Med*. 1994;330:1431–1438.
9. Hinz B, Phan SH, Thannickal VJ, Prunotto M, Desmoulière A, Varga J, De Wever O, Mareel M, Gabbiani G. Recent developments in myofibroblast biology: paradigms for connective tissue remodeling. *Am J Pathol*. 2012;180:1340–1355.
10. Yahagi K, Kolodgie FD, Otsuka F, Finn AV, Davis HR, Joner M, Virmani R. Pathophysiology of native coronary, vein graft, and in-stent atherosclerosis. *Nat Rev Cardiol*. 2016;13:79–98.
11. Kao HK, Chen B, Murphy GF, Li Q, Orgill DP, Guo L. Peripheral blood fibrocytes: enhancement of wound healing by cell proliferation, re-epithelialization, contraction, and angiogenesis. *Ann Surg*. 2011;254:1066–1074.
12. Chai X, Sun D, Han Q, Yi L, Wu Y, Liu X. Hypoxia induces pulmonary arterial fibroblast proliferation, migration, differentiation and vascular remodeling via the PI3K/Akt/p70S6K signaling pathway. *Int J Mol Med*. 2018;41:2461–2472.
13. Wilcox JN, Okamoto EI, Nakahara KI, Vinten-Johansen J. Perivascular responses after angioplasty which may contribute to postangioplasty restenosis: a role for circulating myofibroblast precursors? *Ann N Y Acad Sci*. 2001;947:68–90.
14. Onuta G, van Ark J, Rienstra H, Boer MW, Klatter FA, Bruggeman CA, Zeebregts CJ, Rozing J, Hillebrands JL. Development of transplant vasculopathy in aortic allografts correlates with neointimal smooth muscle cell proliferative capacity and fibrocyte frequency. *Atherosclerosis*. 2010;209:393–402.
15. Kuwabara JT, Tallquist MD. Tracking adventitial fibroblast contribution to disease: a review of current methods to identify resident fibroblasts. *Arterioscler Thromb Vasc Biol*. 2017;37:1598–1607.
16. Witt W, Büttner P, Jannasch A, Matschke K, Waldow T. Reversal of myofibroblastic activation by polyunsaturated fatty acids in valvular interstitial cells from aortic valves: role of RhoA/G-actin/MRTF signalling. *J Mol Cell Cardiol*. 2014;74:127–138.
17. Wang G, Jacquet L, Karamariti E, Xu Q. Origin and differentiation of vascular smooth muscle cells. *J Physiol*. 2015;593:3013–3030.
18. Covas DT, Panepucci RA, Fontes AM, Silva WA Jr, Orellana MD, Freitas MC, Neder L, Santos AR, Peres LC, Jamur MC, et al. Multipotent mesenchymal stromal cells obtained from diverse human tissues share functional properties and gene-expression profile with CD146$^+$ perivascular cells and fibroblasts. *Exp Hematol*. 2008;36:642–654.
19. Qian J, Tian W, Jiang X, Tamosiuniene R, Sung YK, Shuffle EM, Tu AB, Valenzuela A, Jiang S, Zamanian RT, et al. Leukotriene B4 activates pulmonary artery adventitial fibroblasts in pulmonary hypertension. *Hypertension*. 2015;66:1227–1239.
20. Kovacic JC, Dimmeler S, Harvey RP, Finkel T, Aikawa E, Krenning G, Baker AH. Endothelial to mesenchymal transition in cardiovascular disease: JACC state-of-the-art review. *J Am Coll Cardiol*. 2019;73:190–209.
21. Evrard SM, Lecce L, Michelis KC, Nomura-Kitabayashi A, Pandey G, Purushothaman KR, D'Escamard V, Li JR, Hadri L, Fujitani K, et al. Endothelial to mesenchymal transition is common in atherosclerotic lesions and is associated with plaque instability. *Nat Commun*. 2016;7:11853.
22. Kahounová Z, Kurfürstová D, Bouchal J, Kharaishvili G, Navrátil J, Remšík J, Šimečková Š, Študent V, Kozubík A, Souček K. The fibroblast surface markers FAP, anti-fibroblast, and FSP are expressed by cells of epithelial origin and may be altered during epithelial-to-mesenchymal transition. *Cytometry A*. 2018;93:941–951.
23. Barron L, Gharib SA, Duffield JS. Lung pericytes and resident fibroblasts: busy multitaskers. *Am J Pathol*. 2016;186:2519–2531.
24. Kalajzic I, Kalajzic Z, Wang L, Jiang X, Lamothe K, San Miguel SM, Aguila HL, Rowe DW. Pericyte/myofibroblast phenotype of osteoprogenitor cell. *J Musculoskelet Neuronal Interact*. 2007;7:320–322.
25. Frid MG, Brunetti JA, Burke DL, Carpenter TC, Davie NJ, Stenmark KR. Circulating mononuclear cells with a dual, macrophage-fibroblast phenotype contribute robustly to hypoxia-induced pulmonary adventitial remodeling. *Chest*. 2005;128:583S–584S.
26. Sartore S, Chiavegato A, Faggin E, Franch R, Puato M, Ausoni S, Pauletto P. Contribution of adventitial fibroblasts to neointima formation and vascular remodeling: from innocent bystander to active participant. *Circ Res*. 2001;89:1111–1121.
27. Beamish JA, He P, Kottke-Marchant K, Marchant RE. Molecular regulation of contractile smooth muscle cell phenotype: implications for vascular tissue engineering. *Tissue Eng Part B Rev*. 2010;16:467–491.
28. Karamariti E, Zhai C, Yu B, Qiao L, Wang Z, Potter CMF, Wong MM, Simpson RML, Zhang Z, Wang X, et al. DKK3 (Dickkopf 3) alters atherosclerotic plaque phenotype involving vascular progenitor and fibroblast differentiation into smooth muscle cells. *Arterioscler Thromb Vasc Biol*. 2018;38:425–437.
29. Starke RM, Thompson JW, Ali MS, Pascale CL, Martinez Lege A, Ding D, Chalouhi N, Hasan DM, Jabbour P, Owens GK, et al. Cigarette smoke initiates oxidative stress-induced cellular phenotypic modulation leading to cerebral aneurysm pathogenesis. *Arterioscler Thromb Vasc Biol*. 2018;38:610–621.
30. Hirai H, Yang B, Garcia-Barrio MT, Rom O, Ma PX, Zhang J, Chen YE. Direct reprogramming of fibroblasts into smooth muscle-like cells with defined transcription factors-brief report. *Arterioscler Thromb Vasc Biol*. 2018;38:2191–2197.
31. Cheng SL, Shao JS, Behrmann A, Krchma K, Towler DA. Dkk1 and MSX2-Wnt7b signaling reciprocally regulate the endothelial-mesenchymal transition in aortic endothelial cells. *Arterioscler Thromb Vasc Biol*. 2013;33:1679–1689.
32. Casella S, Bielli A, Mauriello A, Orlandi A. Molecular pathways regulating macrovascular pathology and vascular smooth muscle cells phenotype in type 2 diabetes. *Int J Mol Sci*. 2015;16:24353–24368.
33. Plekhanova OS, Stepanova VV, Ratner EI, Bobik A, Tkachuk VA, Parfyonova YV. Urokinase plasminogen activator in injured adventitia increases the number of myofibroblasts and augments early proliferation. *J Vasc Res*. 2006;43:437–446.

34. Wilcox JN, Cipolla GD, Martin FH, Simonet L, Dunn B, Ross CE, Scott NA. Contribution of adventitial myofibroblasts to vascular remodeling and lesion formation after experimental angioplasty in pig coronary arteries. *Ann N Y Acad Sci*. 1997;811:437–447.
35. Holm A, Heumann T, Augustin HG. Microvascular mural cell organotypic heterogeneity and functional plasticity. *Trends Cell Biol*. 2018;28:302–316.
36. Lepreux S, Guyot C, Billet F, Combe C, Balabaud C, Bioulac-Sage P, Desmoulière A. Smoothelin, a new marker to determine the origin of liver fibrogenic cells. *World J Gastroenterol*. 2013;19:9343–9350.
37. van Eys GJ, Niessen PM, Rensen SS. Smoothelin in vascular smooth muscle cells. *Trends Cardiovasc Med*. 2007;17:26–30.
38. Alexander MR, Owens GK. Epigenetic control of smooth muscle cell differentiation and phenotypic switching in vascular development and disease. *Annu Rev Physiol*. 2012;74:13–40.
39. Owens GK. Regulation of differentiation of vascular smooth muscle cells. *Physiol Rev*. 1995;75:487–517.
40. Cecchettini A, Rocchiccioli S, Boccardi C, Citti L. Vascular smooth-muscle-cell activation: proteomics point of view. *Int Rev Cell Mol Biol*. 2011;288:43–99.
41. Kawai-Kowase K, Owens GK. Multiple repressor pathways contribute to phenotypic switching of vascular smooth muscle cells. *Am J Physiol Cell Physiol*. 2007;292:C59–C69.
42. Owens GK, Kumar MS, Wamhoff BR. Molecular regulation of vascular smooth muscle cell differentiation in development and disease. *Physiol Rev*. 2004;84:767–801.
43. Shi N, Chen SY. Smooth muscle cell differentiation: model systems, regulatory mechanisms, and vascular diseases. *J Cell Physiol*. 2016;231:777–787.
44. Tang DD, Gerlach BD. The roles and regulation of the actin cytoskeleton, intermediate filaments and microtubules in smooth muscle cell migration. *Respir Res*. 2017;18:54.
45. Régent A, Ly KH, Groh M, Khifer C, Lofek S, Clary G, Chafey P, Baud V, Broussard C, Federici C, et al. Molecular analysis of vascular smooth muscle cells from patients with giant cell arteritis: targeting endothelin-1 receptor to control proliferation. *Autoimmun Rev*. 2017;16:398–406.
46. Lefebvre P, Nusgens BV, Lapière CM. Cultured myofibroblasts display a specific phenotype that differentiates them from fibroblasts and smooth muscle cells. *Dermatology*. 1994;189:65–67.
47. Yoshida T, Owens GK. Molecular determinants of vascular smooth muscle cell diversity. *Circ Res*. 2005;96:280–291.
48. Malashicheva A, Kostina D, Kostina A, Irtyuga O, Voronkina I, Smagina L, Ignatieva E, Gavriliuk N, Uspensky V, Moiseeva O. Phenotypic and functional changes of endothelial and smooth muscle cells in thoracic aortic aneurysms. *Int J Vasc Med*. 2016;2016:3107879.
49. Ding Y, Zhang M, Zhang W, Lu Q, Cai Z, Song P, Okon IS, Xiao L, Zou MH. AMP-activated protein kinase alpha 2 deletion induces VSMC phenotypic switching and reduces features of atherosclerotic plaque stability. *Circ Res*. 2016;119:718–730.
50. Pilling D, Fan T, Huang D, Kaul B, Gomer RH. Identification of markers that distinguish monocyte-derived fibrocytes from monocytes, macrophages, and fibroblasts. *PLoS One*. 2009;4:e7475.
51. Liu T, Guevara OE, Warburton RR, Hill NS, Gaestel M, Kayyali US. Regulation of vimentin intermediate filaments in endothelial cells by hypoxia. *Am J Physiol Cell Physiol*. 2010;299:C363–C373.
52. Coen M, Burkhardt K, Bijlenga P, Gabbiani G, Schaller K, Kövari E, Rüfenacht DA, Ruíz DS, Pizzolato G, Bochaton-Piallat ML. Smooth muscle cells of human intracranial aneurysms assume phenotypic features similar to those of the atherosclerotic plaque. *Cardiovasc Pathol*. 2013;22:339–344.
53. Chaabane C, Heizmann CW, Bochaton-Piallat ML. Extracellular S100A4 induces smooth muscle cell phenotypic transition mediated by RAGE. *Biochim Biophys Acta*. 2015;1853:2144–2157.
54. Brisset AC, Hao H, Camenzind E, Bacchetta M, Geinoz A, Sanchez JC, Chaponnier C, Gabbiani G, Bochaton-Piallat ML. Intimal smooth muscle cells of porcine and human coronary artery express S100A4, a marker of the rhomboid phenotype in vitro. *Circ Res*. 2007;100:1055–1062.
55. Martínez-González J, Berrozpe M, Varela O, Badimon L. Heterogeneity of smooth muscle cells in advanced human atherosclerotic plaques: intimal smooth muscle cells expressing a fibroblast surface protein are highly activated by platelet-released products. *Eur J Clin Invest*. 2001;31:939–949.
56. Powell DW, Pinchuk IV, Saada JI, Chen X, Mifflin RC. Mesenchymal cells of the intestinal lamina propria. *Annu Rev Physiol*. 2011;73:213–237.
57. Rajkumar VS, Howell K, Csiszar K, Denton CP, Black CM, Abraham DJ. Shared expression of phenotypic markers in systemic sclerosis indicates a convergence of pericytes and fibroblasts to a myofibroblast lineage in fibrosis. *Arthritis Res Ther*. 2005;7:R1113–R1123.
58. Chung KM, Hsu SC, Chu YR, Lin MY, Jiaang WT, Chen RH, Chen X. Fibroblast activation protein (FAP) is essential for the migration of bone marrow mesenchymal stem cells through RhoA activation. *PLoS One*. 2014;9:e88772.
59. Tchou J, Zhang PJ, Bi Y, Satija C, Marjumdar R, Stephen TL, Lo A, Chen H, Mies C, June CH, et al. Fibroblast activation protein expression by stromal cells and tumor-associated macrophages in human breast cancer. *Hum Pathol*. 2013;44:2549–2557.
60. Prunotto M, Bruschi M, Gunning P, Gabbiani G, Weibel F, Ghiggeri G, Petretto A, Scaloni A, Bonello T, Schevzov G, et al. Stable incorporation of α-smooth muscle actin into stress fibers is dependent on specific tropomyosin isoforms. *Cytoskeleton*. 2015;62:257–267.
61. Gomez D, Owens G. Smooth muscle cell phenotypic switching in atherosclerosis. *Cardiovasc Res*. 2012;95:156–164.
62. Mack C, Thompson M, Lawrenz-Smith S, Owens G. Smooth muscle α-actin CArG elements coordinate formation of a smooth muscle cell-selective, serum response factor-containing activation complex. *Circ Res*. 2002;86:221–232.
63. Allahverdian S, Chehroudi AC, McManus BM, Abraham T, Francis GA. Contribution of intimal smooth muscle cells to cholesterol accumulation and macrophage-like cells in human atherosclerosis. *Circulation*. 2014;129:1551–1559.
64. Sandison ME, Dempster J, McCarron JG. The transition of smooth muscle cells from a contractile to a migratory, phagocytic phenotype: direct demonstration of phenotypic modulation. *J Physiol*. 2016;594:6189–6209.
65. Frangogiannis NG, Michael LH, Entman ML. Myofibroblasts in reperfused myocardial infarcts express the embryonic form of smooth muscle myosin heavy chain (SMemb). *Cardiovasc Res*. 2000;48:89–100.
66. Aikawa M, Sivam PN, Kuro-o M, Kimura K, Nakahara K, Takewaki S, Ueda M, Yamaguchi H, Yazaki Y, Periasamy M, et al. Human smooth muscle myosin heavy chain isoforms as molecular markers for vascular development and atherosclerosis. *Circ Res*. 1993;73:1000–1012.
67. Garanich JS, Mathura RA, Shi ZD, Tarbell JM. Effects of fluid shear stress on adventitial fibroblast migration: implications for flow-mediated mechanisms of arterialization and intimal hyperplasia. *Am J Physiol Heart Circ Physiol*. 2007;292:H3128–H3135.
68. Madsen CS, Regan CP, Hungerford JE, White SL, Manabe I, Owens GK. Smooth muscle-specific expression of the smooth muscle myosin heavy chain gene in transgenic mice requires 5'-flanking and first intronic DNA sequence. *Circ Res*. 1998;82:908–917.
69. Liu R, Jin JP. Calponin isoforms CNN1, CNN2 and CNN3: regulators for actin cytoskeleton functions in smooth muscle and non-muscle cells. *Gene*. 2016;585:143–153.
70. Miano JM, Olson EN. Expression of the smooth muscle cell calponin gene marks the early cardiac and smooth muscle cell lineages during mouse embryogenesis. *J Biol Chem*. 1996;271:7095–7103.
71. Frid MG, Shekhonin BV, Koteliansky VE, Glukhova MA. Phenotypic changes of human smooth muscle cells during development: late expression of heavy caldesmon and calponin. *Dev Biol*. 1992;153:185–193.
72. Perez-Montiel MD, Plaza JA, Dominguez-Malagon H, Suster S. Differential expression of smooth muscle myosin, smooth muscle actin, H-caldesmon, and calponin in the diagnosis of myofibroblastic and smooth muscle lesions of skin and soft tissue. *Am J Dermatopathol*. 2006;28:105–111.
73. Bär H, Strelkov SV, Sjöberg G, Aebi U, Herrmann H. The biology of desmin filaments: how do mutations affect their structure, assembly, and organisation? *J Struct Biol*. 2004;148:137–152.
74. Singh SR, Robbins J. Desmin and cardiac disease: an unfolding story. *Circ Res*. 2018;122:1324–1326.
75. Paulin D, Li Z. Desmin: a major intermediate filament protein essential for the structural integrity and function of muscle. *Exp Cell Res*. 2004;301:1–7.
76. Kaplan-Albuquerque N, Garat C, Van Putten V, Nemenoff RA. Regulation of SM22 alpha expression by arginine vasopressin and PDGF-BB in vascular smooth muscle cells. *Am J Physiol Heart Circ Physiol*. 2003;285:H1444–H1452.

77. Zhong L, He X, Si X, Wang H, Li B, Hu Y, Li M, Chen X, Liao W, Liao Y, et al. SM22α (smooth muscle 22α) prevents aortic aneurysm formation by inhibiting smooth muscle cell phenotypic switching through suppressing reactive oxygen species/NF-κB (nuclear factor-κB). *Arterioscler Thromb Vasc Biol*. 2019;39:e10–e25.
78. Han M, Dong LH, Zheng B, Shi JH, Wen JK, Cheng Y. Smooth muscle 22 alpha maintains the differentiated phenotype of vascular smooth muscle cells by inducing filamentous actin bundling. *Life Sci*. 2009;84:394–401.
79. Coco DP, Hirsch MS, Hornick JL. Smoothelin is a specific marker for smooth muscle neoplasms of the gastrointestinal tract. *Am J Surg Pathol*. 2009;33:1795–1801.
80. Van Eys G, Niessen P, Rensen S. Smoothelin in vascular smooth muscle cells. *Trends Cardiovasc Med*. 2007;17:26–30.
81. Hitchcock-DeGregori SE, Barua B. Tropomyosin structure, function, and interactions: a dynamic regulator. *Subcell Biochem*. 2017;82:253–284.
82. Marston S, El-Mezgueldi M. Role of tropomyosin in the regulation of contraction in smooth muscle. *Adv Exp Med Biol*. 2008;644:110–123.
83. Herring BP, Smith AF. Telokin expression is mediated by a smooth muscle cell-specific promoter. *Am J Physiol*. 1996;270:C1656–C1665.
84. Madden JA, Dantuma MW, Sorokina EA, Weihrauch D, Kleinman JG. Telokin expression and the effect of hypoxia on its phosphorylation status in smooth muscle cells from small and large pulmonary arteries. *Am J Physiol Lung Cell Mol Physiol*. 2008;294:L1166–L1173.
85. Herring BP, El-Mounayri O, Gallagher PJ, Yin F, Zhou J. Regulation of myosin light chain kinase and telokin expression in smooth muscle tissues. *Am J Physiol Cell Physiol*. 2006;291:C817–C827.
86. Schaller MD. Paxillin: a focal adhesion-associated adaptor protein. *Oncogene*. 2001;20:6459–6472.
87. Yuminamochi T, Yatomi Y, Osada M, Ohmori T, Ishii Y, Nakazawa K, Hosogaya S, Ozaki Y. Expression of the LIM proteins paxillin and Hic-5 in human tissues. *J Histochem Cytochem*. 2003;51:513–521.
88. Peng X, Nelson ES, Maiers JL, DeMali KA. New insights into vinculin function and regulation. *Int Rev Cell Mol Biol*. 2011;287:191–231.
89. Belkin AM, Ornatsky OI, Kabakov AE, Glukhova MA, Koteliansky VE. Diversity of vinculin/meta-vinculin in human tissues and cultivated cells: expression of muscle specific variants of vinculin in human aorta smooth muscle cells. *J Biol Chem*. 1988;263:6631–6635.
90. Chen D, Ma L, Tham EL, Maresh S, Lechler RI, McVey JH, Dorling A. Fibrocytes mediate intimal hyperplasia post-vascular injury and are regulated by two tissue factor-dependent mechanisms. *J Thromb Haemost*. 2013;11:963–974.
91. Stenmark KR, Gerasimovskaya E, Nemenoff RA, Das M. Hypoxic activation of adventitial fibroblasts: role in vascular remodeling. *Chest*. 2002;122:326S–334S.
92. Imoto K, Okada M, Yamawaki H. Characterization of fibroblasts from hypertrophied right ventricle of pulmonary hypertensive rats. *Pflugers Arch*. 2018;470:1405–1417.
93. Rodriguez A, Karen J, Gardner H, Gerdin B, Rubin K, Sundberg C. Integrin alpha1beta1 is involved in the differentiation into myofibroblasts in adult reactive tissues in vivo. *J Cell Mol Med*. 2009;13:3449–3462.
94. Messier RH Jr, Bass BL, Aly HM, Jones JL, Domkowski PW, Wallace RB, Hopkins RA. Dual structural and functional phenotypes of the porcine aortic valve interstitial population: characteristics of the leaflet myofibroblast. *J Surg Res*. 1994;57:1–21.
95. Jin X, Fu GX, Li XD, Zhu DL, Gao PJ. Expression and function of osteopontin in vascular adventitial fibroblasts and pathological vascular remodeling. *PLoS One*. 2011;6:e23558.
96. Hu WY, Fukuda N, Ikeda Y, Suzuki R, Tahira Y, Takagi H, Matsumoto K, Kanmatsuse K, Mugishima H. Human-derived vascular smooth muscle cells produce angiotensin II by changing to the synthetic phenotype. *J Cell Physiol*. 2003;196:284–292.
97. Khaw BA, Carrio I, Pieri PL, Narula J. Radionuclide imaging of the synthetic smooth muscle cell phenotype in experimental atherosclerotic lesions. *Trends Cardiovasc Med*. 1996;6:226–232.
98. Kudryavtseva O, Aalkjaer C, Matchkov VV. Vascular smooth muscle cell phenotype is defined by Ca^{2+}-dependent transcription factors. *FEBS J*. 2013;280:5488–5499.
99. Karoor V, Fini MA, Loomis Z, Sullivan T, Hersh LB, Gerasimovskaya E, Irwin D, Dempsey EC. Sustained activation of Rho GTPases promotes a synthetic pulmonary artery smooth muscle cell phenotype in neprilysin null mice. *Arterioscler Thromb Vasc Biol*. 2018;38:154–163.
100. Saleh Al-Shehabi T, Iratni R, Eid AH. Anti-atherosclerotic plants which modulate the phenotype of vascular smooth muscle cells. *Phytomedicine*. 2016;23:1068–1081.
101. Petsophonsakul P, Furmanik M, Forsythe R, Dweck M, Schurink GW, Natour E, Reutelingsperger C, Jacobs M, Mees B, Schurgers L. Role of vascular smooth muscle cell phenotypic switching and calcification in aortic aneurysm formation. *Arterioscler Thromb Vasc Biol*. 2019;39:1351–1368.
102. Chistiakov DA, Orekhov AN, Bobryshev YV. Vascular smooth muscle cell in atherosclerosis. *Acta Physiol (Oxf)*. 2015;214:33–50.
103. Furgeson SB, Simpson PA, Park I, Vanputten V, Horita H, Kontos CD, Nemenoff RA, Weiser-Evans MC. Inactivation of the tumour suppressor, PTEN, in smooth muscle promotes a pro-inflammatory phenotype and enhances neointima formation. *Cardiovasc Res*. 2010;86:274–282.
104. Chen PY, Simons M. Fibroblast growth factor-transforming growth factor beta dialogues, endothelial cell to mesenchymal transition, and atherosclerosis. *Curr Opin Lipidol*. 2018;29:397–403.
105. Villeneuve LM, Reddy MA, Lanting LL, Wang M, Meng L, Natarajan R. Epigenetic histone H3 lysine 9 methylation in metabolic memory and inflammatory phenotype of vascular smooth muscle cells in diabetes. *Proc Natl Acad Sci USA*. 2008;105:9047–9052.
106. Zhang Y, Bao S, Kuang Z, Ma Y, Hu Y, Mao Y. Urotensin II promotes monocyte chemoattractant protein-1 expression in aortic adventitial fibroblasts of rat. *Chin Med J (Engl)*. 2014;127:1907–1912.
107. Allahverdian S, Chaabane C, Boukais K, Francis GA, Bochaton-Piallat ML. Smooth muscle cell fate and plasticity in atherosclerosis. *Cardiovasc Res*. 2018;114:540–550.
108. Orr AW, Hastings NE, Blackman BR, Wamhoff BR. Complex regulation and function of the inflammatory smooth muscle cell phenotype in atherosclerosis. *J Vasc Res*. 2010;47:168–180.
109. Chung SW, Park JW, Lee SA, Eo SK, Kim K. Thrombin promotes proinflammatory phenotype in human vascular smooth muscle cell. *Biochem Biophys Res Commun*. 2010;396:748–754.
110. Kwansa AL, De Vita R, Freeman JW. Tensile mechanical properties of collagen type I and its enzymatic crosslinks. *Biophys Chem*. 2016;214–215:1–10.
111. Nadkarni SK, Bouma BE, de Boer J, Tearney GJ. Evaluation of collagen in atherosclerotic plaques: the use of two coherent laser-based imaging methods. *Lasers Med Sci*. 2009;24:439–445.
112. Rekhter MD. Collagen synthesis in atherosclerosis: too much and not enough. *Cardiovasc Res*. 1999;41:376–384.
113. Frantz C, Stewart KM, Weaver VM. The extracellular matrix at a glance. *J Cell Sci*. 2010;123:4195–4200.
114. Liu X, Huang X, Chen L, Zhang Y, Li M, Wang L, Ge C, Wang H, Zhang M. Mechanical stretch promotes matrix metalloproteinase-2 and prolyl-4-hydroxylase α1 production in human aortic smooth muscle cells via Akt-p38 MAPK-JNK signaling. *Int J Biochem Cell Biol*. 2015;62:15–23.
115. Lund SA, Giachelli CM, Scatena M. The role of osteopontin in inflammatory processes. *J Cell Commun Signal*. 2009;3:311–322.
116. Icer MA, Gezmen-Karadag M. The multiple functions and mechanisms of osteopontin. *Clin Biochem*. 2018;59:17–24.
117. Pankov R, Yamada KM. Fibronectin at a glance. *J Cell Sci*. 2002;115:3861–3863.
118. Hamill KJ, Kligys K, Hopkinson SB, Jones JC. Laminin deposition in the extracellular matrix: a complex picture emerges. *J Cell Sci*. 2009;122:4409–4417.
119. Hallmann R, Horn N, Selg M, Wendler O, Pausch F, Sorokin LM. Expression and function of laminins in the embryonic and mature vasculature. *Physiol Rev*. 2005;85:979–1000.
120. Uchio K, Tuchweber B, Manabe N, Gabbiani G, Rosenbaum J, Desmoulière A. Cellular retinol-binding protein-1 expression and modulation during in vivo and in vitro myofibroblastic differentiation of rat hepatic stellate cells and portal fibroblasts. *Lab Invest*. 2002;82:619–628.
121. Liu T, Ma W, Xu H, Huang M, Zhang D, He Z, Zhwang L, Brem S, O'Rourke D, Gong Y, et al. PDGF-mediated mesenchymal transformation renders endothelial resistance to anti-VEGF treatment in glioblastoma. *Nat Commun*. 2018;9:3439.
122. Kimani PW, Holmes AJ, Grossmann RE, McGowan S. PDGF-Rα gene expression predicts proliferation, but PDGF-A suppresses transdifferentiation of neonatal mouse lung myofibroblasts. *Respir Res*. 2009;10:119.

123. Liu T, Zhang L, Joo D. NF-κB signaling in inflammation. *Signal Transduct Target Ther*. 2017;2:17–23.
124. Reiss A, Siegart N, De Leon J. Interleukin-6 in atherosclerosis: atherogenic or atheroprotective? *Clin Lipidol*. 2017;12:14–23.
125. Hunter C, Jones S. IL-6 as a keystone cytokine in health and disease. *Nat Immunol*. 2015;16:448–457.
126. Van der Velde AR, Meijers WC, de Boer RA. Cardiovascular biomarkers: translational aspects of hypertension, atherosclerosis, and heart failure in drug development. In: Wehling M, ed. *Principles of Translational Science in Medicine*, 2nd ed. Amsterdam: Elsevier; 2015:167–183.
127. Bester J, Pretorius E. Effects of IL-1β, IL-6 and IL-8 on erythrocytes, platelets and clot viscoelasticity. *Sci Rep*. 2016;6:32188.
128. Lindeman JH, Abdul-Hussien H, Schaapherder AF, Van Bockel JH, Von der Thüsen JH, Roelen DL, Kleemann R. Enhanced expression and activation of pro-inflammatory transcription factors distinguish aneurysmal from atherosclerotic aorta: IL-6- and IL-8-dominated inflammatory responses prevail in the human aneurysm. *Clin Sci (Lond)*. 2008;114:687–697.
129. Wirka RC, Wagh D, Paik DT, et al. Atheroprotective roles of smooth muscle cell phenotypic modulation and the TCF21 disease gene as revealed by single-cell analysis. *Nat Med*. 2019;25:1280–1289.
130. Feil S, Fehrenbacher B, Lukowski R, Essmann F, Schulze-Osthoff K, Schaller M, Feil R. Transdifferentiation of vascular smooth muscle cells to macrophage-like cells during atherogenesis. *Circ Res*. 2014;115:662–667.
131. Humphrey JD, Dufresne ER, Schwartz MA. Mechanotransduction and extracellular matrix homeostasis. *Nat Rev Mol Cell Biol*. 2014;15:802–812.
132. Bochaton-Piallat ML, Bäck M. Novel concepts for the role of smooth muscle cells in vascular disease: towards a new smooth muscle cell classification. *Cardiovasc Res*. 2018;114:477–480.
133. Bennett MR, Sinha S, Owens GK. Vascular smooth muscle cells in atherosclerosis. *Circ Res*. 2016;118:692–702.
134. Lindeman JH. The pathophysiologic basis of abdominal aortic aneurysm progression: a critical appraisal. *Expert Rev Cardiovasc Ther*. 2015;13:839–851.
135. Doran AC, Meller N, McNamara CA. Role of smooth muscle cells in the initiation and early progression of atherosclerosis. *Arterioscler Thromb Vasc Biol*. 2008;28:812–819.
136. Wang Y, Dubland JA, Allahverdian S, Asonye E, Sahin B, Jaw JE, Sin DD, Seidman MA, Leeper NJ, Francis GA. Smooth muscle cells contribute the majority of foam cells in ApoE (apolipoprotein E)-deficient mouse atherosclerosis. *Arterioscler Thromb Vasc Biol*. 2019;39:876–887.
137. Evrard SM, Lecce L, Michelis KC, et al. Endothelial to mesenchymal transition is common in atherosclerotic lesions and is associated with plaque instability. *Nat Commun*. 2016;7:11853.
138. Otsuka F, Sakakura K, Yahagi K, Joner M, Virmani R. Has our understanding of calcification in human coronary atherosclerosis progressed? *Arterioscler Thromb Vasc Biol*. 2014;34:724–736.
139. Grewal N, Gittenberger-de Groot AC, Poelmann RE, Klautz RJ, Lindeman JH, Goumans MJ, Palmen M, Mohamed SA, Sievers HH, Bogers AJ, et al. Ascending aorta dilation in association with bicuspid aortic valve: a maturation defect of the aortic wall. *J Thorac Cardiovasc Surg*. 2014;148:1583–1590.
140. Kim HW, Weintraub NL. Aortic aneurysm: in defense of the vascular smooth muscle cell. *Arterioscler Thromb Vasc Biol*. 2016;36:2138–2140.
141. Doderer SA, Gäbel G, Kokje VBC, Northoff BH, Holdt LM, Hamming JF, Lindeman JHN. Adventitial adipogenic degeneration is an unidentified contributor to aortic wall weakening in the abdominal aortic aneurysm. *J Vasc Surg*. 2018;67:1891–1900.
142. Roostalu U, Wong JK. Arterial smooth muscle dynamics in development and repair. *Dev Biol*. 2018;435:109–121.
143. Gittenberger-de Groot AC, DeRuiter MC, Bergwerff M, Poelmann RE. Smooth muscle cell origin and its relation to heterogeneity in development and disease. *Arterioscler Thromb Vasc Biol*. 1999;19:1589–1594.
144. Madsen CS, Hershey JC, Hautmann MB, White SL, Owens GK. Expression of the smooth muscle myosin heavy chain gene is regulated by a negative-acting GC-rich element located between two positive-acting serum response factor-binding elements. *J Biol Chem*. 1997;272:6332–6340.
145. Nguyen AT, Gomez D, Bell RD, Campbell JH, Clowes AW, Gabbiani G, Giachelli CM, Parmacek MS, Raines EW, Rusch NJ, et al. Smooth muscle cell plasticity: fact or fiction? *Circ Res*. 2013;112:17–22.
146. Gäbel G, Northoff BH, Weinzierl I, Ludwig S, Hinterseher I, Wilfert W, Teupser D, Doderer SA, Bergert H, Schönleben F, et al. Molecular fingerprint for terminal abdominal aortic aneurysm disease. *J Am Heart Assoc*. 2017;6:e006798. DOI: 10.1161/JAHA.117.006798.
147. Reilkoff RA, Bucala R, Herzog EL. Fibrocytes: emerging effector cells in chronic inflammation. *Nat Rev Immunol*. 2011;11:427–435.
148. Håversen L, Sundelin JP, Mardinoglu A, Rutberg M, Ståhlman M, Wilhelmsson U, Hultén LM, Pekny M, Fogelstrand P, Bentzon JF, et al. Vimentin deficiency in macrophages induces increased oxidative stress and vascular inflammation but attenuates atherosclerosis in mice. *Sci Rep*. 2018;8:16973.
149. Piera-Velazquez S, Jimenez SA. Endothelial to mesenchymal transition: role in physiology and in the pathogenesis of human diseases. *Physiol Rev*. 2019;99:1281–1324.
150. Ziegler WH, Liddington RC, Critchley DR. The structure and regulation of vinculin. *Trends Cell Biol*. 2006;16:453–460.
151. Huveneers S, Oldenburg J, Spanjaard E, van der Krogt G, Grigoriev I, Akhmanova A, Rehmann H, de Rooij J. Vinculin associates with endothelial VE-cadherin junctions to control force-dependent remodeling. *J Cell Biol*. 2012;196:641–652.
152. Fang S, Sharma RV, Bhalla RC. Enhanced recovery of injury-caused downregulation of paxillin protein by eNOS gene expression in rat carotid artery: mechanism of NO inhibition of intimal hyperplasia? *Arterioscler Thromb Vasc Biol*. 1999;19:147–152.
153. von Essen M, Rahikainen R, Oksala N, et al. Talin and vinculin are downregulated in atherosclerotic plaque: Tampere Vascular Study. *Atherosclerosis*. 2016;255:43–53.
154. van Dijk RA, Rijs K, Wezel A, Hamming JF, Kolodgie FD, Virmani R, Schaapherder AF, Lindeman JHN. Systematic evaluation of the cellular innate immune response during the process of human atherosclerosis. *J Am Heart Assoc*. 2016;5:e002860. DOI: 10.1161/JAHA.115.002860.
155. van Dijk RA, Duinisveld AJ, Schaapherder AF, Mulder-Stapel A, Hamming JF, Kuiper J, de Boer OJ, van der Wal AC, Kolodgie FD, Virmani R, et al. A change in inflammatory footprint precedes plaque instability: a systematic evaluation of cellular aspects of the adaptive immune response in human atherosclerosis. *J Am Heart Assoc*. 2015;4:e001403. DOI: 10.1161/JAHA.114.001403.
156. Moher D, Shamseer L, Clarke M, Ghersi D, Liberati A, Petticrew M, Shekelle P, Stewart LA. Preferred reporting items for systematic review and meta-analysis protocols (PRISMA-P) 2015 statement. *Syst Rev*. 2015;4:1.
157. Moher D, Liberati A, Tetzlaff J, Altman DG; The PRISMA Group. Preferred reporting items for systematic reviews and meta-analyses: the PRISMA statement. *PLoS Med*. 2009;6:e1000097.
158. Pi Y, Zhang LL, Li BH, Guo L, Cao XJ, Gao CY, Li JC. Inhibition of reactive oxygen species generation attenuates TLR4-mediated proinflammatory and proliferative phenotype of vascular smooth muscle cells. *Lab Invest*. 2013;93:880–887.
159. Sava P, Ramanathan A, Dobronyi A, Peng X, Sun H, Ledesma-Mendoza A, Herzog EL, Gonzalez AL. Human pericytes adopt myofibroblast properties in the microenvironment of the IPF lung. *JCI Insight*. 2017;2:e96352.
160. Xu JY, Chang NB, Li T, Jiang R, Sun XL, He YZ, Jiang J. Endothelial cells inhibit the angiotensin II induced phenotypic modulation of rat vascular adventitial fibroblasts. *J Cell Biochem*. 2017;118:1921–1927.
161. Majesky MW, Horita H, Ostriker A, Lu S, Regan JN, Bagchi A, Dong XR, Poczobutt J, Nemenoff RA, Weiser-Evans MC. Differentiated smooth muscle cells generate a subpopulation of resident vascular progenitor cells in the adventitia regulated by Klf4. *Circ Res*. 2017;120:296–311.
162. Hegner B, Schaub T, Catar R, Kusch A, Wagner P, Essin K, Lange C, Riemekasten G, Dragun D. Intrinsic deregulation of vascular smooth muscle and myofibroblast differentiation in mesenchymal stromal cells from patients with systemic sclerosis. *PLoS One*. 2016;11:e0153101.
163. Bahnson ES, Vavra AK, Flynn ME, Vercammen JM, Jiang Q, Schwartz AR, Kibbe MR. Long-term effect of PROLI/NO on cellular proliferation and phenotype after arterial injury. *Free Radic Biol Med*. 2016;90:272–286.
164. An SJ, Liu P, Shao TM, Wang ZJ, Lu HG, Jiao Z, Li X, Fu JQ. Characterization and functions of vascular adventitial fibroblast subpopulations. *Cell Physiol Biochem*. 2015;35:1137–1150.

165. Wang Z, Ren Z, Hu Z, Hu X, Zhang H, Wu H, Zhang M. Angiotensin-II induces phosphorylation of ERK1/2 and promotes aortic adventitial fibroblasts differentiating into myofibroblasts during aortic dissection formation. *J Mol Histol*. 2014;45:401–412.
166. Chen WD, Chu YF, Liu JJ, Hong MN, Gao PJ. RhoA-Rho kinase signaling pathway mediates adventitial fibroblasts differentiation to myofibroblasts induced by TGF-β1. *Sheng Li Xue Bao*. 2013;65:113–121.
167. Li Y, Tao J, Zhang J, Tian X, Liu S, Sun M, Zhang X, Yan C, Han Y. Cellular repressor E1A-stimulated genes controls phenotypic switching of adventitial fibroblasts by blocking p38MAPK activation. *Atherosclerosis*. 2012;225:304–314.
168. Forte A, Della Corte A, Grossi M, Bancone C, Provenzano R, Finicelli M, De Feo M, De Santo LS, Nappi G, Cotrufo M, et al. Early cell changes and TGFβ pathway alterations in the aortopathy associated with bicuspid aortic valve stenosis. *Clin Sci (Lond)*. 2013;124:97–108.
169. Zhang YG, Hu YC, Mao YY, Wei RH, Bao SL, Wu LB, Kuang ZJ. Transforming growth factor-β1 involved in urotensin II-induced phenotypic differentiation of adventitial fibroblasts from rat aorta. *Chin Med J (Engl)*. 2010;123:3634–3639.
170. Chen YT, Chang FC, Wu CF, Chou YH, Hsu HL, Chiang WC, Shen J, Chen YM, Wu KD, Tsai TJ, et al. Platelet-derived growth factor receptor signaling activates pericyte-myofibroblast transition in obstructive and post-ischemic kidney fibrosis. *Kidney Int*. 2011;80:1170–1181.
171. Zheng L, Xu CC, Chen WD, Shen WL, Ruan CC, Zhu LM, Zhu DL, Gao PJ. MicroRNA-155 regulates angiotensin II type 1 receptor expression and phenotypic differentiation in vascular adventitial fibroblasts. *Biochem Biophys Res Commun*. 2010;400:483–488.
172. Ji J, Xu F, Li L, Chen R, Wang J, Hu WC. Activation of adventitial fibroblasts in the early stage of the aortic transplant vasculopathy in rat. *Transplantation*. 2010;89:945–953.
173. Gan Q, Yoshida T, Li J, Owens GK. Smooth muscle cells and myofibroblasts use distinct transcriptional mechanisms for smooth muscle alpha-actin expression. *Circ Res*. 2007;101:883–892.
174. Guo SJ, Wu LY, Shen WL, Chen WD, Wei J, Gao PJ, Zhu DL. Gene profile for differentiation of vascular adventitial myofibroblasts. *Sheng Li Xue Bao*. 2006;58:337–344.
175. Butcher JT, Barrett BC, Nerem RM. Equibiaxial strain stimulates fibroblastic phenotype shift in smooth muscle cells in an engineered tissue model of the aortic wall. *Biomaterials*. 2006;27:5252–5258.
176. Jiang YL, Dai AG, Li QF, Hu RC. Transforming growth factor-beta1 induces transdifferentiation of fibroblasts into myofibroblasts in hypoxic pulmonary vascular remodeling. *Acta Biochim Biophys Sin (Shanghai)*. 2006;38:29–36.
177. Miyazaki H, Hayashi K, Hasegawa Y. Tensile properties of fibroblasts and vascular smooth muscle cells. *Biorheology*. 2003;40:207–212.
178. Das M, Dempsey EC, Reeves JT, Stenmark KR. Selective expansion of fibroblast subpopulations from pulmonary artery adventitia in response to hypoxia. *Am J Physiol Lung Cell Mol Physiol*. 2002;282:L976–L986.
179. Zhong A, Mirzaei Z, Simmons CA. The roles of matrix stiffness and ß-catenin signaling in endothelial-to-mesenchymal transition of aortic valve endothelial cells. *Cardiovasc Eng Technol*. 2018;9:158–167.
180. Zhang L, Chen Y, Li G, Chen M, Huang W, Liu Y, Li Y. TGF-β1/FGF-2 signaling mediates the 15-HETE-induced differentiation of adventitial fibroblasts into myofibroblasts. *Lipids Health Dis*. 2016;15:2.
181. Castellano G, Franzin R, Stasi A, Divella C, Sallustio F, Pontrelli P, Lucarelli G, Battaglia M, Staffieri F, Crovace A, et al. Complement activation during ischemia/reperfusion injury induces pericyte-to-myofibroblast transdifferentiation regulating peritubular capillary lumen reduction through pERK signaling. *Front Immunol*. 2018;9:1002.
182. Chen C, Han X, Fan F, Liu Y, Wang T, Wang J, Hu P, Ma A, Tian H. Serotonin drives the activation of pulmonary artery adventitial fibroblasts and TGF-β1/Smad3-mediated fibrotic responses through 5-HT(2A) receptors. *Mol Cell Biochem*. 2014;397:267–276.
183. Lin S, Ma S, Lu P, Cai W, Chen Y, Sheng J. Effect of CTRP3 on activation of adventitial fibroblasts induced by TGF-β1 from rat aorta in vitro. *Int J Clin Exp Pathol*. 2014;7:2199–2208.
184. Okayama K, Azuma J, Dosaka N, Iekushi K, Sanada F, Kusunoki H, Iwabayashi M, Rakugi H, Taniyama Y, Morishita R. Hepatocyte growth factor reduces cardiac fibrosis by inhibiting endothelial-mesenchymal transition. *Hypertension*. 2012;59:958–965.
185. Yang W, Zhang J, Wang H, Gao P, Singh M, Shen K, Fang N. Angiotensin II downregulates catalase expression and activity in vascular adventitial fibroblasts through an AT1R/ERK1/2-dependent pathway. *Mol Cell Biochem*. 2011;358:21–29.
186. Jones JA, Beck C, Barbour JR, Zavadzkas JA, Mukherjee R, Spinale FG, Ikonomidis JS. Alterations in aortic cellular constituents during thoracic aortic aneurysm development: myofibroblast-mediated vascular remodeling. *Am J Pathol*. 2009;175:1746–1756.
187. Che ZQ, Gao PJ, Shen WL, Fan CL, Liu JJ, Zhu DL. Angiotensin II-stimulated collagen synthesis in aortic adventitial fibroblasts is mediated by connective tissue growth factor. *Hypertens Res*. 2008;31:1233–1240.
188. Cushing MC, Mariner PD, Liao JT, Sims EA, Anseth KS. Fibroblast growth factor represses Smad-mediated myofibroblast activation in aortic valvular interstitial cells. *FASEB J*. 2008;22:1769–1777.
189. Merryman WD, Lukoff HD, Long RA, Engelmayr GC Jr, Hopkins RA, Sacks MS. Synergistic effects of cyclic tension and transforming growth factor-beta1 on the aortic valve myofibroblast. *Cardiovasc Pathol*. 2007;16:268–276.
190. An SJ, Boyd R, Zhu M, Chapman A, Pimentel DR, Wang HD. NADPH oxidase mediates angiotensin II-induced endothelin-1 expression in vascular adventitial fibroblasts. *Cardiovasc Res*. 2007;75:702–709.
191. Jiang Z, Yu P, Tao M, Fernandez C, Ifantides C, Moloye O, Schultz GS, Ozaki CK, Berceli SA. TGF-beta- and CTGF-mediated fibroblast recruitment influences early outward vein graft remodeling. *Am J Physiol Heart Circ Physiol*. 2007;293:H482–H488.
192. Karasek MA. Does transformation of microvascular endothelial cells into myofibroblasts play a key role in the etiology and pathology of fibrotic disease? *Med Hypotheses*. 2007;68:650–655.
193. Davie NJ, Gerasimovskaya EV, Hofmeister SE, Richman AP, Jones PL, , Reeves JT, Stenmark KR. Pulmonary artery adventitial fibroblasts cooperate with vasa vasorum endothelial cells to regulate vasa vasorum neovascularization: a process mediated by hypoxia and endothelin-1. *Am J Pathol*. 2006;168:1793–1807.
194. Tomas JJ, Stark VE, Kim JL, Wolff RA, Hullett DA, Warner TF, Hoch JR. Beta-galactosidase-tagged adventitial myofibroblasts tracked to the neointima in healing rat vein grafts. *J Vasc Res*. 2003;40:266–275.
195. Siow RC, Mallawaarachchi CM, Weissberg PL. Migration of adventitial myofibroblasts following vascular balloon injury: insights from in vivo gene transfer to rat carotid arteries. *Cardiovasc Res*. 2003;59:212–221.
196. Frid MG, Kale VA, Stenmark KR. Mature vascular endothelium can give rise to smooth muscle cells via endothelial-mesenchymal transdifferentiation: in vitro analysis. *Circ Res*. 2002;90:1189–1196.
197. Hartlapp I, Abe R, Saeed RW, Peng T, Voelter W, Bucala R, Metz CN. Fibrocytes induce an angiogenic phenotype in cultured endothelial cells and promote angiogenesis in vivo. *FASEB J*. 2001;15:2215–2224.
198. Hirose M, Kosugi H, Nakazato K, Hayashi T. Restoration to a quiescent and contractile phenotype from a proliferative phenotype of myofibroblast-like human aortic smooth muscle cells by culture on type IV collagen gels. *J Biochem*. 1999;125:991–1000.
199. Shi Y, O'Brien JE Jr, Fard A, Zalewski A. Transforming growth factor-beta 1 expression and myofibroblast formation during arterial repair. *Arterioscler Thromb Vasc Biol*. 1996;16:1298–1305.
200. Shi Y, O'Brien JE, Fard A, Mannion JD, Wang D, Zalewski A. Adventitial myofibroblasts contribute to neointimal formation in injured porcine coronary arteries. *Circulation*. 1996;94:1655–1664.
201. Zhang YG, Li J, Li YG, Wei RH. Urotensin II induces phenotypic differentiation, migration, and collagen synthesis of adventitial fibroblasts from rat aorta. *J Hypertens*. 2008;26:1119–1126.
202. Patel S, Shi Y, Niculescu R, Chung EH, Martin JL, Zalewski A. Characteristics of coronary smooth muscle cells and adventitial fibroblasts. *Circulation*. 2000;101:524–532.
203. Frösen J, Joutel A. Smooth muscle cells of intracranial vessels: from development to disease. *Cardiovasc Res*. 2018;114:501–512.
204. Majesky MW. Vascular smooth muscle cells. *Arterioscler Thromb Vasc Biol*. 2016;36:e82–e86.
205. Yuan SM. α-Smooth muscle actin and ACTA2 gene expressions in vasculopathies. *Braz J Cardiovasc Surg*. 2015;30:644–649.
206. Lao KH, Zeng L, Xu Q. Endothelial and smooth muscle cell transformation in atherosclerosis. *Curr Opin Lipidol*. 2015;26:449–456.
207. Chaabane C, Coen M, Bochaton-Piallat ML. Smooth muscle cell phenotypic switch: implications for foam cell formation. *Curr Opin Lipidol*. 2014;25:374–379.
208. Davis-Dusenbery BN, Wu C, Hata A. Micromanaging vascular smooth muscle cell differentiation and phenotypic modulation. *Arterioscler Thromb Vasc Biol*. 2011;31:2370–2377.

209. Chan-Park MB, Shen JY, Cao Y, Xiong Y, Liu Y, Rayatpisheh S, Kang GC, Greisler HP. Biomimetic control of vascular smooth muscle cell morphology and phenotype for functional tissue-engineered small-diameter blood vessels. *J Biomed Mater Res A*. 2009;88:1104–1121.
210. Morrow D, Guha S, Sweeney C, Birney Y, Walshe T, O'Brien C, Walls D, Redmond EM, Cahill PA. Notch and vascular smooth muscle cell phenotype. *Circ Res*. 2008;103:1370–1382.
211. Halka AT, Turner NJ, Carter A, Ghosh J, Murphy MO, Kirton JP, Kielty CM, Walker MG. The effects of stretch on vascular smooth muscle cell phenotype in vitro. *Cardiovasc Pathol*. 2008;17:98–102.
212. Rzucidlo EM, Martin KA, Powell RJ. Regulation of vascular smooth muscle cell differentiation. *J Vasc Surg*. 2007;45(suppl A):A25–A32.
213. McDonald OG, Owens GK. Programming smooth muscle plasticity with chromatin dynamics. *Circ Res*. 2007;100:1428–1441.
214. Iyemere VP, Proudfoot D, Weissberg PL, Shanahan CM. Vascular smooth muscle cell phenotypic plasticity and the regulation of vascular calcification. *J Intern Med*. 2006;260:192–210.
215. Stegemann JP, Hong H, Nerem RM. Mechanical, biochemical, and extracellular matrix effects on vascular smooth muscle cell phenotype. *J Appl Physiol*. 2005;98:2321–2327.
216. Hao H, Gabbiani G, Bochaton-Piallat ML. Arterial smooth muscle cell heterogeneity: implications for atherosclerosis and restenosis development. *Arterioscler Thromb Vasc Biol*. 2003;23:1510–1520.
217. Stenmark KR, Frid MG. Smooth muscle cell heterogeneity: role of specific smooth muscle cell subpopulations in pulmonary vascular disease. *Chest*. 1998;114:82S–90S.
218. Shanahan CM, Weissberg PL. Smooth muscle cell heterogeneity: patterns of gene expression in vascular smooth muscle cells in vitro and in vivo. *Arterioscler Thromb Vasc Biol*. 1998;18:333–338.
219. Frid MG, Dempsey EC, Durmowicz AG, Stenmark KR. Smooth muscle cell heterogeneity in pulmonary and systemic vessels: importance in vascular disease. *Arterioscler Thromb Vasc Biol*. 1997;17:1203–1209.
220. Archer SL. Diversity of phenotype and function of vascular smooth muscle cells. *J Lab Clin Med*. 1996;127:524–529.
221. Thyberg J. Differentiated properties and proliferation of arterial smooth muscle cells in culture. *Int Rev Cytol*. 1996;169:183–265.
222. Sartore S, Scatena M, Chiavegato A, Faggin E, Giuriato L, Pauletto P. Myosin isoform expression in smooth muscle cells during physiological and pathological vascular remodeling. *J Vasc Res*. 1994;31:61–81.
223. Harrison OJ, Visan AC, Moorjani N, Modi A, Salhiyyah K, Torrens C, Ohri S, Cagampang FR. Defective NOTCH signaling drives increased vascular smooth muscle cell apoptosis and contractile differentiation in bicuspid aortic valve aortopathy: a review of the evidence and future directions. *Trends Cardiovasc Med*. 2019;29:61–68.
224. Walsh K, Takahashi A. Transcriptional regulation of vascular smooth muscle cell phenotype. *Z Kardiol*. 2001;90(suppl 3):12–16.
225. Shanahan CM, Weissberg PL. Smooth muscle cell phenotypes in atherosclerotic lesions. *Curr Opin Lipidol*. 1999;10:507–513.
226. Vendrov AE, Sumida A, Canugovi C, Lozhkin A, Hayami T, Madamanchi NR, Runge MS. NOXA1-dependent NADPH oxidase regulates redox signaling and phenotype of vascular smooth muscle cell during atherogenesis. *Redox Biol*. 2019;21:101063.
227. Sun QR, Zhang X, Fang K. Phenotype of vascular smooth muscle cells (VSMCs) is regulated by miR-29b by targeting sirtuin 1. *Med Sci Monit*. 2018;24:6599–6607.
228. Zeng M, Luo Y, Xu C, Li R, Chen N, Deng X, Fang D, Wang L, Wu J, Luo M. Platelet-endothelial cell interactions modulate smooth muscle cell phenotype in an in vitro model of type 2 diabetes mellitus. *Am J Physiol Cell Physiol*. 2019;316:C186–C197.
229. Yi B, Shen Y, Tang H, Wang X, Li B, Zhang Y. Stiffness of aligned fibers regulates the phenotypic expression of vascular smooth muscle cells. *ACS Appl Mater Interfaces*. 2019;11:6867–6880.
230. Wu W, Zhang W, Choi M, Zhao J, Gao P, Xue M, Singer HA, Jourd'heuil D, Long X. Vascular smooth muscle-MAPK14 is required for neointimal hyperplasia by suppressing VSMC differentiation and inducing proliferation and inflammation. *Redox Biol*. 2019;22:101137.
231. Wirka RC, Wagh D, Paik DT, Pjanic M, Nguyen T, Miller CL, Kundu R, Nagao M, Coller J, Koyano TK, et al. Atheroprotective roles of smooth muscle cell phenotypic modulation and the TCF21 disease gene as revealed by single-cell analysis. *Nat Med*. 2019;25:1280–1289.
232. Malhotra R, Mauer AC, Lino Cardenas CL, Guo X, Yao J, Zhang X, Wunderer F, Smith AV, Wong Q, Pechlivanis S, et al. HDAC9 is implicated in atherosclerotic aortic calcification and affects vascular smooth muscle cell phenotype. *Nat Genet*. 2019;51:1580–1587.
233. Sun L, Zhao M, Liu A, Lv M, Zhang J, Li Y, Yang X, Wu Z. Shear stress induces phenotypic modulation of vascular smooth muscle cells via AMPK/mTOR/ULK1-mediated autophagy. *Cell Mol Neurobiol*. 2018;38:541–548.
234. Wu B, Zhang L, Zhu YH, Zhang YE, Zheng F, Yang JY, Guo LY, Li XY, Wang L, Tang JM, et al. Mesoderm/mesenchyme homeobox gene l promotes vascular smooth muscle cell phenotypic modulation and vascular remodeling. *Int J Cardiol*. 2018;251:82–89.
235. Fu Y, Chang Y, Chen S, Li Y, Chen Y, Sun G, Yu S, Ye N, Li C, Sun Y. BAG3 promotes the phenotypic transformation of primary rat vascular smooth muscle cells via TRAIL. *Int J Mol Med*. 2018;41:2917–2926.
236. Charles R, Bourmoum M, Claing A. ARF GTPases control phenotypic switching to vascular smooth muscle cells through the regulation of actin function and actin dependent gene expression. *Cell Signal*. 2018;46:64–75.
237. Zhang L, Xu Z, Wu Y, Liao J, Zeng F, Shi L. Akt/eNOS and MAPK signaling pathways mediated the phenotypic switching of thoracic aorta vascular smooth muscle cells in aging/hypertensive rats. *Physiol Res*. 2018;67:543–553.
238. Rizzo S, Coen M, Sakic A, De Gaspari M, Thiene G, Gabbiani G, Basso C, Bochaton-Piallat ML. Sudden coronary death in the young: evidence of contractile phenotype of smooth muscle cells in the culprit atherosclerotic plaque. *Int J Cardiol*. 2018;264:1–6.
239. Davis-Knowlton J, Turner JE, Turner A, Damian-Loring S, Hagler N, Henderson T, Emery IF, Bond K, Duarte CW, Vary CPH, et al. Characterization of smooth muscle cells from human atherosclerotic lesions and their responses to Notch signaling. *Lab Invest*. 2019;99:290–304.
240. Misra A, Feng Z, Chandran RR, Kabir I, Rotllan N, Aryal B, Sheikh AQ, Ding L, Qin L, Fernández-Hernando C, et al. Integrin beta3 regulates clonality and fate of smooth muscle-derived atherosclerotic plaque cells. *Nat Commun*. 2018;9:2073.
241. Smyth LCD, Rustenhoven J, Scotter EL, Schweder P, Faull RLM, Park TIH, Dragunow M. Markers for human brain pericytes and smooth muscle cells. *J Chem Neuroanat*. 2018;92:48–60.
242. Gao P, Wu W, Ye J, Lu YW, Adam AP, Singer HA, Long X. Transforming growth factor β1 suppresses proinflammatory gene program independent of its regulation on vascular smooth muscle differentiation and autophagy. *Cell Signal*. 2018;50:160–170.
243. Ma S, Motevalli SM, Chen J, Xu MQ, Wang Y, Feng J, Qiu Y, Han D, Fan M, Ding M, et al. Precise theranostic nanomedicines for inhibiting vulnerable atherosclerotic plaque progression through regulation of vascular smooth muscle cell phenotype switching. *Theranostics*. 2018;8:3693–3706.
244. Liu Z, Zhang M, Zhou T, Shen Q, Qin X. Exendin-4 promotes the vascular smooth muscle cell re-differentiation through AMPK/SIRT1/FOXO3a signaling pathways. *Atherosclerosis*. 2018;276:58–66.
245. Xie SA, Zhang T, Wang J, Zhao F, Zhang YP, Yao WJ, Hur SS, Yeh YT, Pang W, Zheng LS, et al. Matrix stiffness determines the phenotype of vascular smooth muscle cell in vitro and in vivo: role of DNA methyltransferase 1. *Biomaterials*. 2018;155:203–216.
246. Dale M, Fitzgerald MP, Liu Z, Meisinger T, Karpisek A, Purcell LN, Carson JS, Harding P, Lang H, Koutakis P, et al. Premature aortic smooth muscle cell differentiation contributes to matrix dysregulation in Marfan syndrome. *PLoS One*. 2017;12:e0186603.
247. Lakhkar A, Dhagia V, Joshi SR, Gotlinger K, Patel D, Sun D, Wolin MS, Schwartzman ML, Gupte SA. 20-HETE-induced mitochondrial superoxide production and inflammatory phenotype in vascular smooth muscle is prevented by glucose-6-phosphate dehydrogenase inhibition. *Am J Physiol Heart Circ Physiol*. 2016;310:H1107–H1117.
248. Yang X, Coriolan D, Murthy V, Schultz K, Golenbock DT, Beasley D. Proinflammatory phenotype of vascular smooth muscle cells: role of efficient Toll-like receptor 4 signaling. *Am J Physiol Heart Circ Physiol*. 2005;289:H1069–H1076.
249. Krug AW, Allenhöfer L, Monticone R, Spinetti G, Gekle M, Wang M, Lakatta EG. Elevated mineralocorticoid receptor activity in aged rat vascular smooth muscle cells promotes a proinflammatory phenotype via extracellular signal-regulated kinase 1/2 mitogen-activated protein kinase and epidermal growth factor receptor-dependent pathways. *Hypertension*. 2010;55:1476–1483.
250. Liu R, Lo L, Lay AJ, Zhao Y, Ting KK, Robertson EN, Sherrah AG, Jarrah S, Li H, Zhou Z, et al. ARHGAP18 protects against thoracic

aortic aneurysm formation by mitigating the synthetic and proinflammatory smooth muscle cell phenotype. *Circ Res*. 2017;121:512–524.
251. Csiszar A, Sosnowska D, Wang M, Lakatta EG, Sonntag WE, Ungvari Z. Age-associated proinflammatory secretory phenotype in vascular smooth muscle cells from the non-human primate *Macaca mulatta*: reversal by resveratrol treatment. *J Gerontol A Biol Sci Med Sci*. 2012;67:811–820.
252. Schultz K, Murthy V, Tatro JB, Beasley D. Endogenous interleukin-1 alpha promotes a proliferative and proinflammatory phenotype in human vascular smooth muscle cells. *Am J Physiol Heart Circ Physiol*. 2007;292:H2927–H2934.
253. Yang X, Murthy V, Schultz K, Tatro JB, Fitzgerald KA, Beasley D. Toll-like receptor 3 signaling evokes a proinflammatory and proliferative phenotype in human vascular smooth muscle cells. *Am J Physiol Heart Circ Physiol*. 2006;291:H2334–H2343.
254. Zucker MM, Wujak L, Gungl A, Didiasova M, Kosanovic D, Petrovic A, Klepetko W, Schermuly RT, Kwapiszewska G, Schaefer L, et al. LRP1 promotes synthetic phenotype of pulmonary artery smooth muscle cells in pulmonary hypertension. *Biochim Biophys Acta Mol Basis Dis*. 2019;1865:1604–1616.
255. Yang L, Gao L, Nickel T, Yang J, Zhou J, Gilbertsen A, Geng Z, Johnson C, Young B, Henke C, et al. Lactate promotes synthetic phenotype in vascular smooth muscle cells. *Circ Res*. 2017;121:1251–1262.
256. Patel R, Cardneau JD, Colles SM, Graham LM. Synthetic smooth muscle cell phenotype is associated with increased nicotinamide adenine dinucleotide phosphate oxidase activity: effect on collagen secretion. *J Vasc Surg*. 2006;43:364–371.
257. Rama A, Matsushita T, Charolidi N, Rothery S, Dupont E, Severs NJ. Up-regulation of connexin43 correlates with increased synthetic activity and enhanced contractile differentiation in TGF-beta-treated human aortic smooth muscle cells. *Eur J Cell Biol*. 2006;85:375–386.
258. Acampora KB, Nagatomi J, Langan EM III, LaBerge M. Increased synthetic phenotype behavior of smooth muscle cells in response to in vitro balloon angioplasty injury model. *Ann Vasc Surg*. 2010;24:116–126.
259. Augstein A, Mierke J, Poitz DM, Strasser RH. Sox9 is increased in arterial plaque and stenosis, associated with synthetic phenotype of vascular smooth muscle cells and causes alterations in extracellular matrix and calcification. *Biochim Biophys Acta Mol Basis Dis*. 2018;1864:2526–2537.
260. Alshanwani AR, Riches-Suman K, O'Regan DJ, Wood IC, Turner NA, Porter KE. MicroRNA-21 drives the switch to a synthetic phenotype in human saphenous vein smooth muscle cells. *IUBMB Life*. 2018;70:649–657.
261. Thyberg J, Blomgren K, Roy J, Tran PK, Hedin U. Phenotypic modulation of smooth muscle cells after arterial injury is associated with changes in the distribution of laminin and fibronectin. *J Histochem Cytochem*. 1997;45:837–846.
262. Thyberg J, Hultgårdh-Nilsson A. Fibronectin and the basement membrane components laminin and collagen type IV influence the phenotypic properties of subcultured rat aortic smooth muscle cells differently. *Cell Tissue Res*. 1994;276:263–271.
263. Anwar A, Li M, Frid MG, Kumar B, Gerasimovskaya EV, Riddle SR, McKeon BA, Thukaram R, Meyrick BO, Fini MA, et al. Osteopontin is an endogenous modulator of the constitutively activated phenotype of pulmonary adventitial fibroblasts in hypoxic pulmonary hypertension. *Am J Physiol Lung Cell Mol Physiol*. 2012;303:L1–L11.
264. Giachelli C, Bae N, Lombardi D, Majesky M, Schwartz S. Molecular cloning and characterization of 2B7, a rat mRNA which distinguishes smooth muscle cell phenotypes in vitro and is identical to osteopontin (secreted phosphoprotein I, 2aR). *Biochem Biophys Res Commun*. 1991;177:867–873.
265. Okada Y, Katsuda S, Matsui Y, Watanabe H, Nakanishi I. Collagen synthesis by cultured arterial smooth muscle cells during spontaneous phenotypic modulation. *Acta Pathol Jpn*. 1990;40:157–164.
266. Ang AH, Tachas G, Campbell JH, Bateman JF, Campbell GR. Collagen synthesis by cultured rabbit aortic smooth-muscle cells: alteration with phenotype. *Biochem J*. 1990;265:461–469.
267. Chiarini A, Onorati F, Marconi M, Pasquali A, Patuzzo C, Malashicheva A, Irtyega O, Faggian G, Pignatti PF, Trabetti E, et al. Studies on sporadic non-syndromic thoracic aortic aneurysms, 1: deregulation of Jagged/Notch 1 homeostasis and selection of synthetic/secretor phenotype smooth muscle cells. *Eur J Prev Cardiol*. 2018;25:42–50.
268. Denger S, Jahn L, Wende P, Watson L, Gerber SH, Kübler W, Kreuzer J. Expression of monocyte chemoattractant protein-1 cDNA in vascular smooth muscle cells: induction of the synthetic phenotype: a possible clue to SMC differentiation in the process of atherogenesis. *Atherosclerosis*. 1999;144:15–23.
269. Wang TM, Chen KC, Hsu PY, Lin HF, Wang YS, Chen CY, Liao YC, Juo SH. microRNA let-7g suppresses PDGF-induced conversion of vascular smooth muscle cell into the synthetic phenotype. *J Cell Mol Med*. 2017;21:3592–3601.
270. Pahk K, Joung C, Jung SM, Young Song H, Yong Park J, Woo Byun J, Lee YS, Chul Paeng J, Kim C, Kim S, et al. Visualization of synthetic vascular smooth muscle cells in atherosclerotic carotid rat arteries by F-18 FDG PET. *Sci Rep*. 2017;7:6989.
271. Ghosh S, Kollar B, Nahar T, Suresh Babu S, Wojtowicz A, Sticht C, Gretz N, Wagner AH, Korff T, Hecker M. Loss of the mechanotransducer zyxin promotes a synthetic phenotype of vascular smooth muscle cells. *J Am Heart Assoc*. 2015;4:e001712. DOI: 10.1161/JAHA.114.001712.
272. Lee HS, Yun SJ, Ha JM, Jin SY, Ha HK, Song SH, Kim CD, Bae SS. Prostaglandin D2 stimulates phenotypic changes in vascular smooth muscle cells. *Exp Mol Med*. 2019;51:1–10.
273. Jaminon A, Reesink K, Kroon A, Schurgers L. The role of vascular smooth muscle cells in arterial remodeling: focus on calcification-related processes. *Int J Mol Sci*. 2019;20:5694.
274. Clement M, Chappell J, Raffort J, Lareyre F, Vandestienne M, Taylor AL, Finigan A, Harrison J, Bennett MR, Bruneval P, et al. Vascular smooth muscle cell plasticity and autophagy in dissecting aortic aneurysms. *Arterioscler Thromb Vasc Biol*. 2019;39:1149–1159.
275. Owens GK, Pasterkamp G. PlaqOmics Leducq Fondation Trans-Atlantic Network: defining the roles of smooth muscle cells and other extracellular matrix-producing cells in late-stage atherosclerotic plaque pathogenesis. *Circ Res*. 2019;124:1297–1299.
276. Liu M, Gomez D. Smooth muscle cell phenotypic diversity. *Arterioscler Thromb Vasc Biol*. 2019;39:1715–1723.
277. Yuan SM, Wu N. Aortic alpha-smooth muscle actin expressions in aortic disorders and coronary artery disease: an immunohistochemical study. *Anatol J Cardiol*. 2018;19:11–16.
278. Lin CS, Hsieh PS, Hwang LL, Lee YH, Tsai SH, Tu YC, Hung YW, Liu CC, Chuang YP, Liao MT, et al. The CCL5/CCR5 axis promotes vascular smooth muscle cell proliferation and atherogenic phenotype switching. *Cell Physiol Biochem*. 2018;47:707–720.
279. Zhong L, He X, Si X, Wang H, Li B, Hu Y, Li M, Chen X, Liao W, Liao Y, et al. SM22 (smooth muscle 22) prevents aortic aneurysm formation by inhibiting smooth muscle cell phenotypic switching through suppressing reactive oxygen species/NF-kappaB (nuclear factor-kappaB). *Arterioscler Thromb Vasc Biol*. 2019;39:e10–e25.
280. Choi S, Park M, Kim J, Park W, Kim S, Lee DK, Hwang JY, Choe J, Won MH, Ryoo S, et al. TNF-alpha elicits phenotypic and functional alterations of vascular smooth muscle cells by miR-155-5p-dependent down-regulation of cGMP-dependent kinase 1. *J Biol Chem*. 2018;293:14812–14822.
281. Schwartz SM, Virmani R, Majesky MW. An update on clonality: what smooth muscle cell type makes up the atherosclerotic plaque? *F1000Res*. 2018;7:F1000 Faculty Rev-1969.
282. Goikuria H, del Mar FM, Manrique RV, Sastre M, Elizagaray E, Lorenzo A, Vandenbroeck K, Alloza I. Characterization of carotid smooth muscle cells during phenotypic transition. *Cells*. 2018;7:23.
283. Rensen SSM, Doevendans PAFM, Van Eys GJJM. Regulation and characteristics of vascular smooth muscle cell phenotypic diversity. *Neth Heart J*. 2007;15:100–108.
284. Mahoney WM Jr, Schwartz SM. Defining smooth muscle cells and smooth muscle injury. *J Clin Invest*. 2005;115:221–224.
285. Li J, Zhang YG, Luo LM, Dong X, Ding WH, Dang SY. Urotensin II promotes aldosterone expression in rat aortic adventitial fibroblasts. *Mol Med Rep*. 2018;17:2921–2928.
286. Yin L, Cai W, Sheng J, Sun Y. Hypoxia induced changes of SePP1 expression in rat preadipocytes and its impact on vascular fibroblasts. *Int J Clin Exp Med*. 2014;7:41–50.
287. Brittan M, Chance V, Elia G, Poulsom R, Alison MR, MacDonald TT, Wright NA. A regenerative role for bone marrow following experimental colitis: contribution to neovasculogenesis and myofibroblasts. *Gastroenterology*. 2005;128:1984–1995.
288. Banks MF, Gerasimovskaya EV, Tucker DA, Frid MG, Carpenter TC, Stenmark KR. Egr-1 antisense oligonucleotides inhibit hypoxia-induced

proliferation of pulmonary artery adventitial fibroblasts. *J Appl Physiol (1985)*. 2005;98:732–738.
289. Gerasimovskaya EV, Tucker DA, Stenmark KR. Activation of phosphatidylinositol 3-kinase, Akt, and mammalian target of rapamycin is necessary for hypoxia-induced pulmonary artery adventitial fibroblast proliferation. *J Appl Physiol (1985)*. 2005;98:722–731.
290. Das M, Stenmark KR, Dempsey EC. Enhanced growth of fetal and neonatal pulmonary artery adventitial fibroblasts is dependent on protein kinase C. *Am J Physiol Lung Cell Mol Physiol*. 1995;269:L660–L667.
291. Moulton KS, Li M, Strand K, Burgett S, McClatchey P, Tucker R, Furgeson SB, Lu S, Kirkpatrick B, Cleveland JC, et al. PTEN deficiency promotes pathological vascular remodeling of human coronary arteries. *JCI Insight*. 2018;3:e97228.
292. Wesseling M, Sakkers TR, de Jager SCA, Pasterkamp G, Goumans MJ. The morphological and molecular mechanisms of epithelial/endothelial-to-mesenchymal transition and its involvement in atherosclerosis. *Vasc Pharmacol*. 2018;106:1–8.
293. Kim M, Choi SH, Jin YB, Lee HJ, Ji YH, Kim J, Lee YS, Lee YJ. The effect of oxidized low-density lipoprotein (ox-LDL) on radiation-induced endothelial-to-mesenchymal transition. *Int J Radiat Biol*. 2013;89:356–363.
294. Tang R, Li Q, Lv L, Dai H, Zheng M, Ma K, Liu B. Angiotensin II mediates the high-glucose-induced endothelial-to-mesenchymal transition in human aortic endothelial cells. *Cardiovasc Diabetol*. 2010;9:31.
295. Muchaneta-Kubara EC, El Nahas AM. Myofibroblast phenotypes expression in experimental renal scarring. *Nephrol Dial Transplant*. 1997;12:904–915.
296. Ikawati M, Kawaichi M, Oka C. Loss of HtrA1 serine protease induces synthetic modulation of aortic vascular smooth muscle cells. *PLoS One*. 2018;13:e0196628.
297. Foster LC, Arkonac BM, Sibinga NES, Shi C, Perrella MA, Haber E. Regulation of CD44 gene expression by the proinflammatory cytokine interleukin-1beta in vascular smooth muscle cells. *J Biol Chem*. 1998;273:20341–20346.
298. Clement N, Gueguen M, Glorian M, Blaise R, Andreani M, Brou C, Bausero P, Limon I. Notch3 and IL-1beta exert opposing effects on a vascular smooth muscle cell inflammatory pathway in which NF-kappaB drives crosstalk. *J Cell Sci*. 2007;120:3352–3361.
299. Maiellaro K, Taylor WR. The role of the adventitia in vascular inflammation. *Cardiovasc. Res*. 2007;75:640–648.
300. Orekhov AN, Bobryshev YV, Chistiakov DA. The complexity of cell composition of the intima of large arteries: focus on pericyte-like cells. *Cardiovasc Res*. 2014;103:438–451.
301. Murashov IS, Volkov AM, Kazanskaya GM, Kliver EE, Savchenko SV, Klochkova SV, Lushnikova EL. Immunohistochemical phenotypes of stable and unstable occlusive atherosclerotic plaques in coronary arteries. *Bull Exp Biol Med*. 2018;165:798–802.
302. Okamoto E, Suzuki T, Aikawa M, Imataka K, Fujii J, Kuro-o M, Nakahara K, Hasegawa A, Yazaki Y, Nagai R. Diversity of the synthetic-state smooth-muscle cells proliferating in mechanically and hemodynamically injured rabbit arteries. *Lab Invest*. 1996;74:120–128.
303. Yutani C, Fujita H, Takaichi S, Yamamoto A. The role of vascular smooth muscle cell phenotypic modulation at the aortic branch in atherogenesis. *Front Med Biol Eng*. 1993;5:143–146.
304. Owens GK, Wise G. Regulation of differentiation/maturation in vascular smooth muscle cells by hormones and growth factors. *Agents Actions Suppl*. 1997;48:3–24.
305. Forte A, Della Corte A, Grossi M, Bancone C, Maiello C, Galderisi U, Cipollaro M. Differential expression of proteins related to smooth muscle cells and myofibroblasts in human thoracic aortic aneurysm. *Histol Histopathol*. 2013;28:795–803.
306. Thyberg J. Phenotypic modulation of smooth muscle cells during formation of neointimal thickenings following vascular injury. *Histol Histopathol*. 1998;13:871–891.
307. Weissberg PL, Cary NR, Shanahan CM. Gene expression and vascular smooth muscle cell phenotype. *Blood Press Suppl*. 1995;2:68–73.
308. Ci W, Wang T, Li T, Wan J. T-614 inhibits human aortic adventitial fibroblast proliferation and promotes interleukin-8 production in vitro. *Vascular*. 2020;28:314–320.
309. Kuro-o M, Nagai R, Nakahara K, Katoh H, Tsai RC, Tsuchimochi H, Yazaki Y, Ohkubo A, Takaku F. cDNA cloning of a myosin heavy chain isoform in embryonic smooth muscle and its expression during vascular development and in arteriosclerosis. *J Biol Chem*. 1991;266:3768–3773.
310. Aslam MI, Hettmer S, Abraham J, Latocha D, Soundararajan A, Huang ET, Goros MW, Michalek JE, Wang S, Mansoor A. Dynamic and nuclear expression of PDGFRα and IGF-1R in alveolar rhabdomyoscarcoma. *Mol Cancer Res*. 2013;11:1303–1313.
311. Endale M, Ahlfeld S, Bao E, Chen X, Green J, Bess Z, Weirauch MT, Xu Y, Per AK. Temporal, spatial and phenotypical changes of PDGFRα expressing fibroblasts during late lung development. *Dev Biol*. 2017;425:161–175.

SUPPLEMENTAL MATERIAL

Data S1. Systematic Search Protocol for most commonly used phenotypical and functional mesenchymal markers in the vascular research field[160,161]

Administrative information

Authors- contact and contributions:

1. J.H. Lindeman. Dept. of Surgery, Division of Vascular Surgery, Leiden University Medical Center. J.H.N.Lindeman@lumc.nl

2. L.E. Bruijn: Dept. of Surgery, Division of Vascular Surgery, Leiden University Medical Center. L.E.Bruijn@lumc.nl

Contributions:

Both authors reviewed the titles, abstracts and full-texts for eligibility independently, based on the search strategy developed by author L.E. Bruijn in collaboration with search specialist J.W. Schoones, LUMC.

Financial support: none

Methods

Information sources: Pubmed and Embase

Pubmed search strategy:

(("Phenotype"[mesh:noexp] OR phenotyp*[tiab] OR "phenotypic modulation"[tw] OR "phenotypic regulation"[tw] OR "phenotypic differentiation"[tw] OR "phenotypic characterization"[tw] OR "phenotypic characterisation"[tw] OR "phenotypic diversity"[tw] OR "phenotypic heterogeneity"[tw] OR phenotypic modulat*[tw] OR

phenotypic regulat*[tw] OR phenotypic different*[tw] OR phenotypic character*[tw] OR phenotypic divers*[tw] OR phenotypic heterog*[tw] OR (("phenotypic"[ti] OR "pheno"[ti]) AND ("modulation"[ti] OR "regulation"[ti] OR "differentiation"[ti] OR "characterization"[ti] OR "characterisation"[ti] OR "diversity"[ti] OR "heterogeneity"[ti])) OR "vascular remodeling"[tw] OR "vascular remodelling"[tw]) AND ("Fibroblasts"[majr] OR "Myofibroblasts"[majr] OR "fibroblast"[ti] OR "fibroblasts"[ti] OR fibroblast*[ti] OR "myofibroblast"[ti] OR "myofibroblasts"[ti] OR myofibroblast*[ti] OR "Myocytes, Smooth Muscle"[majr] OR "smooth muscle cell"[ti] OR "smooth muscle cells"[ti]) AND ("Blood Vessels"[majr] OR "blood vessels"[ti] OR "blood vessel"[ti] OR "artery"[ti] OR "arteries"[ti] OR "aorta"[ti] OR "aortic"[ti] OR "Arteriosclerosis"[majr] OR "Atherosclerosis"[majr] OR atherosclero*[ti] OR arteriosclero*[ti] OR "coronary artery disease"[ti] OR "coronary artery diseases"[ti] OR "AAA"[ti] OR "Aortic Aneurysm, Abdominal"[majr] OR "Abdominal Aortic Aneurysm"[ti] OR "Abdominal Aortic Aneurysms"[ti]) NOT ("mesenchymal stem cells"[ti] OR "mesenchymal stem cell"[ti] OR "Mesenchymal Stromal Cells"[Majr]) AND ("1990/01/01"[PDAT] : "3000/12/31"[PDAT]) AND (english[la] OR dutch[la]))

Total number of references: 2698

Date: 9-12-2019

Data S2. Embase search strategy.

('Phenotype'/ OR Phenotyp*.ti,ab. OR 'Phenotypic modulation.mp. OR 'Phenotypic regulation'.mp. OR 'Phenotypic differentiation'.mp. OR 'Phenotypic characterization'.mp. OR 'Phenotypic characterisation'.mp. OR 'Phenotypic diversity'.mp. OR 'Phenotypic heterogeneity'.mp. OR Phenotypic modulat*.mp. OR Phenotypic regulat*.mp. OR Phenotypic different*.mp. OR Phenotypic character*.mp. OR Phenotypic divers*.mp. OR Phenotypic heterog*.mp. OR (('Phenotypic'.ti. OR 'Pheno'.ti.) AND ('Modulation'.ti. OR 'Regulation'.ti. OR 'Differentiation'.ti. OR 'Characterization'.ti. OR 'Characterisation'.ti. OR 'Diversity'.ti. OR 'Heterogeneity'.ti.)) OR 'Vascular Remodeling'.mp. OR 'Vascular Remodelling'.mp.) AND ('Fibroblasts'/ OR 'Myofibroblasts'/ OR 'Smooth Muscle cell'/ OR 'Fibroblast'.ti. OR 'Fibroblasts'.ti. OR Fibroblast*.ti. OR 'Myofibroblast'.ti. OR 'Myofibroblasts'.ti. OR Myofibroblast*.ti. OR 'Smooth muscle cell'.ti. OR 'Smooth muscle cells'.ti.) AND ('Blood Vessels'/ OR 'Arteriosclerosis'/ OR 'Atherosclerosis'/ OR 'Abdominal aortic aneurysm'/ OR 'Blood vessels'.ti. OR 'Blood vessel'.ti. OR 'artery'.ti. OR 'Arteries'.ti. OR 'Aorta'.ti. OR 'Aortic'.ti. OR Atherosclero*.ti. OR Arteriosclero*.ti. OR 'Coronary artery disease'.ti. OR 'Coronary artery diseases'.ti. OR 'AAA'.ti. OR 'Abdominal Aortic Aneurysm'.ti. OR 'Abdominal Aortic Aneurysms'.ti.) NOT 'Mesenchymal stroma cell'/ OR 'Mesenchymal stem cell'.ti. OR 'Mesenchymal stem cells'.ti.

Total number of references: 1371

Date: 10-12-2019

Data management: References were stored in a PDF-file.

Selection and data collection process: author L.E. Bruijn retrieved all included articles on 09-12-2019 in Pubmed and Embase with the search strategy. Gray literature was not located for this study. Next, the two reviewers independently undertook the initial selection based upon title, abstract and keywords. In case of disagreement, the two reviewers discussed whether the study should be included or excluded based on the initial selection. Subsequently, full texts were reviewed when eligibility was considered either definite or ambiguous.

Outcomes and prioritization:

Potential relevant differentiation/functional markers were extracted from the included studies for the qualitative synthesis. Studies were not assessed for quality as our research question was which mesenchymal and functional markers are most commonly used in the vascular research field and quality of the studies was therefore irrelevant.

Data S3. Movat Pentachrome Protocol.

Working solutions:

(A) 1% Alcian Blue Solution: 1 g Alcian Blue 8 GX (Merck, Burlington, US), 100 ml distilled water, 1 ml Glacial Acetic Acid (Sigma Aldrich, Saint Louis, US)

(B) Alkaline Alcohol solution: 10 ml Ammonium Hydroxide (Merck, Burlington, US), 90 ml Ethanol 100%.

(C) Elastic Hematoxylin Solution: 25 ml 10% Alcoholic Hematoxylin **(J)**, 25 ml Ethanol 100%, 25 ml 10% Ferric Chloride **(D)**, 25 ml Verhoeff's Iodine Solution **(K)**.

(D) 10% Ferric Chloride Solution: 10 g Ferric Chloride (Sigma Aldrich, Saint Louis, US), 100 ml distilled water

(E) 5% Sodium Thiosulfate Solution: 5g Sodium Thiosulfate (Sigma Aldrich, Saint Louis, US), 100 ml distilled water

(F) Biebrich Scarlet/Acid Fuchsin solution: pre-made from ScyTek Laboratories (Logan, United States).

(G) 1% Acetic Acid Solution: 1 ml Glacial Acetic Acid, 99 ml distilled water

(H) 5% Aqueous Phosphotungstic Acid solution: 5 g Phosphotungstic Acid (Sigma Aldrich, Saint Louis, US), 100 ml distilled water

(I) 4% Alcoholic Saffron Solution: 4 g Saffron (Safranor Safran du Gâtinais, Échilleuses, France), 100 ml Ethanol 100%.

(J) 10% Alcoholic Hematoxylin Solution: 10 g Hematoxylin (Merck, Burlington, US), 100 ml Ethanol 100%

(K) Verhoeff's Iodine Solution: 2 g Iodine Crystals (Sigma Aldrich, Saint Louis, US), 4 g Potassium Iodide (Sigma Aldrich, Saint Louis, US), 100 ml distilled water

Protocol:

1. Deparaffinization and rehydration of slides. 2. Rinse slides in distilled water. 3. Stain in 2 changes with **(A)** , both times for 15-25 minutes. 4. Rinse slides in running warm to hot water until clear. 5. Place slides in **(B)** for 30 minutes, then rinse in running tap water. 6. Stain in **(C)** for 20 minutes. 7. Rinse in running warm tap water. 8. Differentiate in 2% aqueous **(D)** for 5 seconds-2 minutes. 9. Place slides in **(E)** for about 1 minute. 10. Wash in running tap water and rinse in distilled water. 11. Stain in **(F)** for 1-1.5 minutes. 12. Rinse in distilled water. 13. Rinse in **(G)** for 7-12 seconds. 14. Place slides in **(H)** for 7-12 minutes. 15. Rinse in distilled water. 16. Rinse in **(G)** for 8-10 seconds. 17. Place in 2 changes of Ethanol 100%. 18. Stain in **(I)** for 1.5 minute and quickly rinse in Ethanol 100%. 19. Dehydration of slides.

Table S1. Excluded full-texts in Systematic Search.

Number	Publication	Reason
1	Owens GK. Molecular control of vascular smooth muscle cell differentiation and phenotypic plasticity. *Novartis Found Symp.* 2007;283:174-91.	Conference proceeding.
2	Bentzon JF, Majesky MW. Lineage tracking of origin and fate of smooth muscle cells in atherosclerosis. *Cardiovasc Res*. 2018;114(4):492-500.	No marker proteins for differentiation described.
3	Maegdefessel L, Rayner KJ, Leeper NJ. MicroRNA regulation of vascular smooth muscle function and phenotype: early career committee contribution. *Arterioscler Thromb Vasc Biol.* 2015;35(1):2-6.	No marker proteins for differentiation described.
4	Matchkov VV, Kudryavtseva O, Aalkjaer C. Intracellular Ca^{2+} signalling and phenotype of vascular smooth muscle cells. *Basic Clin Pharmacol Toxicol*. 2012;110(1):42-8.	No marker proteins for differentiation described.
5	Song Z, Li G. Role of specific microRNAs in regulation of vascular smooth muscle cell differentiation and the response to injury. *J Cardiovasc Transl Res*. 2010;3(3):246-50.	No marker proteins for differentiation described.
6	Erlinge D. Extracellular ATP: a central player in the regulation of vascular smooth muscle phenotype. Focus on "Dual role of PKA in phenotype modulation of vascular smooth muscle cells by extracellular ATP". *Am J Physiol Cell Physiol.* 2004;287(2):C260-2.	No marker proteins for differentiation described.
7	Bochaton-Piallat ML, Bäck M. Novel concepts for the role of smooth muscle cells in vascular disease: towards a new smooth muscle cell classification. Cardiovasc Res. 2018;114(4):477-480.	No marker proteins for differentiation described.
8	Shi N, Mei X, Chen SY. Smooth Muscle Cells in Vascular Remodeling. *Arterioscler. Thromb. Vasc. Biol*. 2019;39(12):e247-e252.	No marker proteins for differentiation described.
9	Basatemur GL, Jørgensen HF, Clarke MCH, Bennett MR, Mallat Z. Vascular smooth muscle cells in atherosclerosis. *Nat Rev Cardiol.* 2019;16(12):727-744.	No full-text available in Leiden University Medical Library collection.
10	Kannenberg F, Gorzelniak K, Jager K, Fobker M, Rust S, Repa J, Roth M, Bjorkhem I, Walter M. Characterization of cholesterol homeostasis in telomerase immortalized tangier disease fibroblasts reveals marked phenotype variability. *J. Biol. Chem.* 2013;288(52):36936-36947.	No marker proteins for differentiation described.

Table S2. Excluded phenotypical markers identified with Systematic Search.

Protein marker	Reason for exclusion
DDR2[15,310]	<3 references
NGS[97]	Primarily pericyte marker
Anti-reticular fibroblast marker (RFM)[97]	<3 references
MHC class II[302]	<3 references
CD4[302]	<3 references
Acting binding proteins Cofilin[16] Profilin[16] Talin[176]	<3 references
MYPT-1[16]	<3 references
Cytoskeleton proteins Tubulin[98] Metavinculin[40,42,111]	<3 references Vinculin selected
Leiomodin-1[111]	<3 references
Integrins (A1,A7,B1)[211,294]	<3 references
Myocardin[211,222,294]	Master regulator of SMC differentiation. Panel of contractile markers included yet.
N-Cadherin/T-Cadherin[86,294]	<3 references
Calmodulin[111,214,249]	Telokin selected
LPP[38]	<3 references
Myosin light chains (LC17a en LC17b)[39]	<3 references
Cysteine- and glycine-rich protein 1[91]	<3 references
1E12[226]	<3 references
Phospholamban[228,300]	Expressed specifically in cardiac muscle.
Aquaporin-1[228,300]	<3 references
Osteoglycin[228]	<3 references
Ubiquitin[228]	<3 references
APEG-1[294]	<3 references
CRP-2[294]	<3 references
MAS5[300]	<3 references

Table S3. Excluded full-texts in synthetic/inflammatory marker search.

Number	Publication	Reason
1	Owens GK. Molecular control of vascular smooth muscle cell differentiation and phenotypic plasticity. *Novartis Found Symp*. 2007;283:174-91.	Conference proceeding.
2	Bentzon JF, Majesky MW. Lineage tracking of origin and fate of smooth muscle cells in atherosclerosis. *Cardiovasc Res.* 2018;114(4):492-500.	No marker proteins for differentiation described.
3	Maegdefessel L, Rayner KJ, Leeper NJ. MicroRNA regulation of vascular smooth muscle function and phenotype: early career committee contribution. *Arterioscler Thromb Vasc Biol*. 2015 Jan;35(1):2-6.	No marker proteins for differentiation described.
4	Matchkov VV, Kudryavtseva O, Aalkjaer C. Intracellular Ca^{2+} signalling and phenotype of vascular smooth muscle cells. *Basic Clin Pharmacol Toxicol.* 2012;110(1):42-8.	No marker proteins for differentiation described.
5	Song Z, Li G. Role of specific microRNAs in regulation of vascular smooth muscle cell differentiation and the response to injury. *J Cardiovasc Transl Res*. 2010;3(3):246-50.	No marker proteins for differentiation described.
6	Erlinge D. Extracellular ATP: a central player in the regulation of vascular smooth muscle phenotype. Focus on "Dual role of PKA in phenotype modulation of vascular smooth muscle cells by extracellular ATP". *Am J Physiol Cell Physiol.* 2004;287(2):C260-2.	No marker proteins for differentiation described.
7	Bochaton-Piallat ML, Bäck M. Novel concepts for the role of smooth muscle cells in vascular disease: towards a new smooth muscle cell classification. *Cardiovasc Res.* 2018;114(4):477-480.	No marker proteins for differentiation described.
8	Shi N., Mei X., Chen S.-Y. Smooth Muscle Cells in Vascular Remodeling. *Arterioscler. Thromb. Vasc. Biol.* 2019;39(12):e247-e252.	No marker proteins for differentiation described.
9	Basatemur GL, Jørgensen HF, Clarke MCH, Bennett MR, Mallat Z. Vascular smooth muscle cells in atherosclerosis. *Nat Rev Cardiol.* 2019;16(12):727-744.	No full-text available in Leiden University Medical Library collection.
10	Reddy MA, Villeneuve LM, Wang M, Lanting L, Natarajan R. Role of the lysine-specific demethylase 1 in the proinflammatory phenotype of vascular smooth muscle cells of diabetic mice. *Circ Res*. 2008;103(6):615-23. Retraction in: *Circ Res.* 2009;105(6):e9.	Retracted publication.
11	Ramos KS, Weber TJ, Liau G. Altered protein secretion and extracellular matrix deposition is associated with the proliferative phenotype induced by allylamine in aortic smooth muscle cells. *Biochem J.* 1993;289.	No protein markers for differentiation or proliferative/ synthetic features described.
12	5. Stengel D, O'Neil C, Brochériou I, Karabina SA, Durand H, Caplice NM, Pickering JG, Ninio E. PAF-receptor is preferentially expressed in a distinct synthetic phenotype of smooth muscle cells cloned from human internal thoracic artery: functional implications in cell migration. *Biochem Biophys Res Commun*.2006;346(3):693-9.	No protein markers for differentiation or proliferative/ synthetic features described.
13	Liu L, Abramowitz J, Askari A, Allen JC. Role of caveolae in ouabain-induced proliferation of cultured vascular smooth muscle cells of the synthetic phenotype. *Am J Physiol Heart Circ Physiol.* 2004;287(5):H2173-82.	No protein markers for differentiation or proliferative/ synthetic features described.
14	Rybalkin SD, Bornfeldt KE, Sonnenburg WK, Rybalkina IG, Kwak KS, Hanson K, Krebs EG, Beavo JA. Calmodulin-stimulated cyclic nucleotide phosphodiesterase (PDE1C) is induced in human	No protein markers for differentiation or proliferative/

	arterial smooth muscle cells of the synthetic, proliferative phenotype. *J Clin Invest*. 1997;100(10):2611-21.	synthetic features described.
15	Wang Y, Lindstedt KA, Kovanen PT. Phagocytosis of mast cell granule remnant-bound LDL by smooth muscle cells of synthetic phenotype: a scavenger receptor-mediated process that effectively stimulates cytoplasmic cholesteryl ester synthesis. *J Lipid Res.* 1996;37(10):2155-66.	No protein markers for differentiation or proliferative/ synthetic features described.
16	Kannenberg F, Gorzelniak K, Jager K, Fobker M, Rust S, Repa J, Roth M, Bjorkhem I, Walter M. Characterization of cholesterol homeostasis in telomerase immortalized tangier disease fibroblasts reveals marked phenotype variability. *J. Biol. Chem. 2013*;288(52):36936-36947	No marker proteins for differentiation described.

Table S4. Excluded synthetic IHC markers.

Marker	Reason for exclusion
(pro-)Collagen II, III, VIII[40,208,268]	Among all the collagen subtypes, type I collagen is considered to be most abundant in vascular fibrous pathology.
Collagenase IV[294]	<3 references
Heat shock protein 47 (Hsp47)[195]	<3 references
ECM components Chondroitin sulfate[98] Vitronectin[40] Tenascin[232] Tropoelastin[232] Fibrillin[233] Osteoglycin[235] Syndecan-1/4[104,294] Versican[20] Aortic-carboxypeptidase-like protein (ALCP)[42,91]	<3 references
Matrix Gla Protein (MGP)[232,235,317]	Predominantly extracellular protein
TGN46[278]	<3 references
Intermediate filaments GFAP[278] Cytokeratin 8 and 18[111,232]	<3 references
Cyclophilin A[281]	<3 references
Zona occludens 2- protein[111]	<3 references
Cingulin[111]	<3 references
uPa[111]	<3 references
tPA[111]	<3 references
Connexin 43[104,194]	<3 references
IGF-BP2[102]	<3 references
TSP-1[40]	<3 references
Cytochrome P-45OIAI[232]	<3 references
Osteoprotegerin[241]	<3 references
SMPD3[105]	<3 references
Sortilin-1[105]	<3 references

Table S5. Excluded pro-inflammatory IHC markers.

Marker	Reason for exclusion
IL-1a[259,263]	<3 references
IL-1β[106,112,162]	Not detectable at protein level[294]
TNF-α[106,112,162]	Very low expression at protein level[294]
MCSF[109]	<3 references
TGF-β[177]	<3 references
Cell activation markers (ICAM-1, VCAM-1, E-selectin, MMP-2, MMP-3, MMP-7, MMP-9)[29,106,112,177,203,260,318]	NF-κB selected as central regulator
CCR2[19]	<3 references
MHCII[14]	<3 references
CXCL1[107,239]	<3 references

Figure S1. Defining the regions of interest within atherosclerotic lesions for semi-quantitative scoring system.

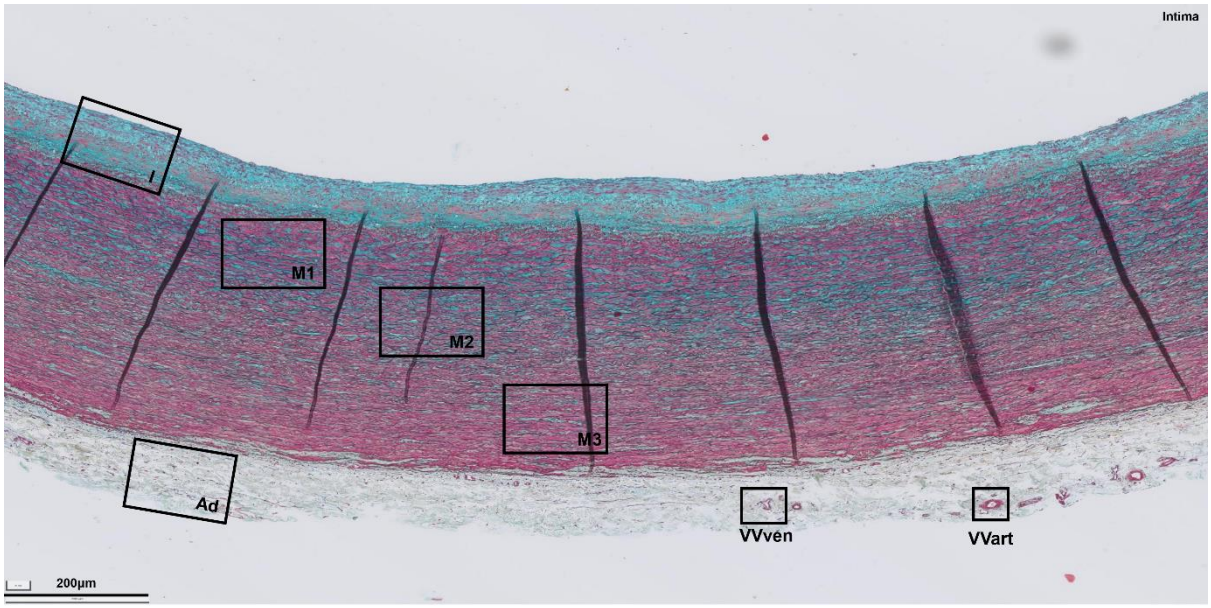

Abbreviations: I. Intima **M1.** Inner media zone **M2.** Middle media zone **M3.** Outer media zone **Ad.** Adventitia **VVven.** Venule-like vasa vasora **VVart.** Arteriole-like vasa vasora.

Figure S2. Rabbit IgG in concentrations higher than 1 µm/mL produce significant background.

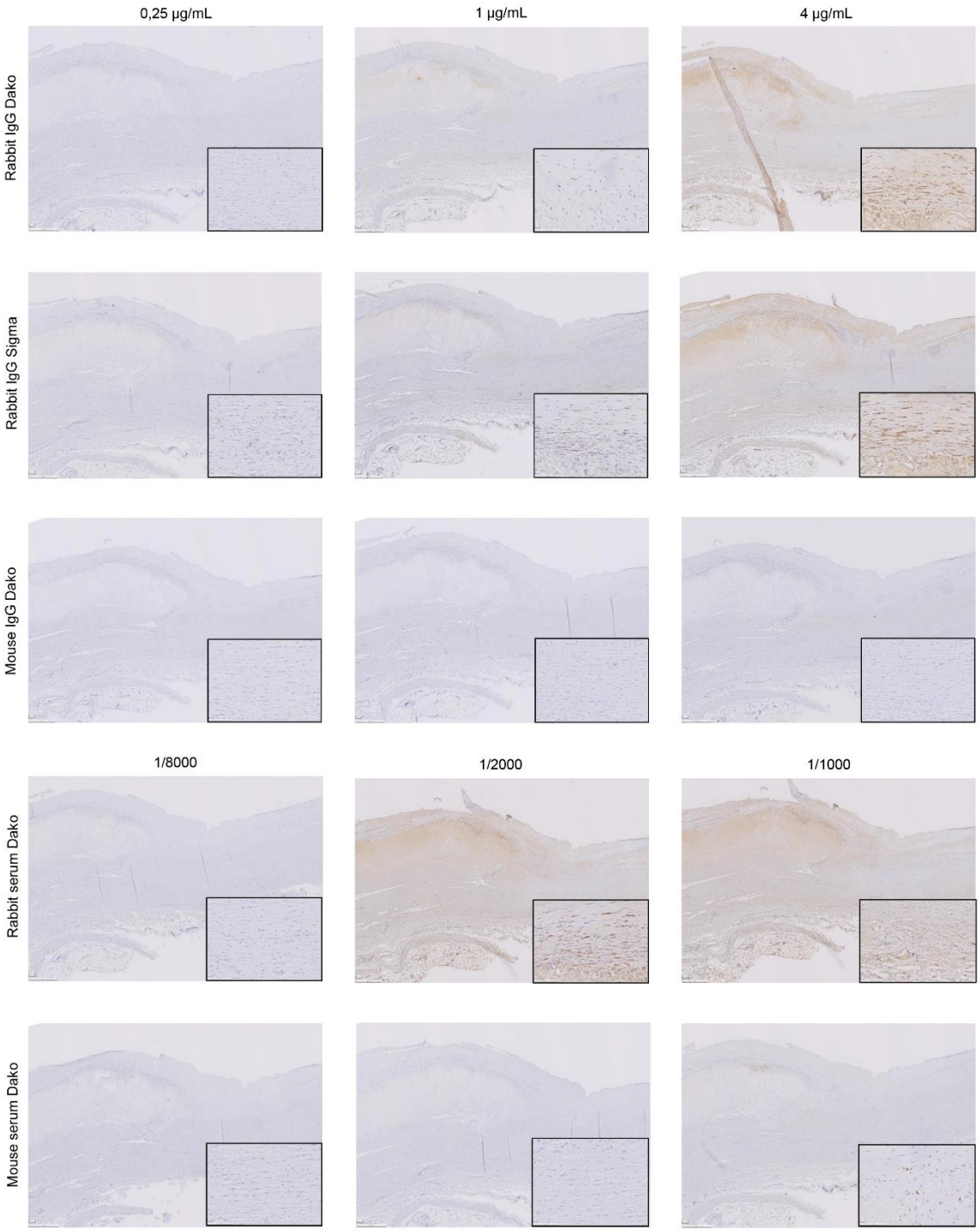

Overview of rabbit isotype controls in several concentrations (on early fibroatheroma (EFA); 2,5x and 26x magnification). Non-specific binding of rabbit IgG is significantly increased in rabbit IgG concentrations of 1 µg/mL or higher. This phenomenon was not observed in mouse IgG or mouse sera.

Figure S3. Disqualification of Thy-1/CD90 and FSP-1/S100A4 as universal mesenchymal lineage markers.

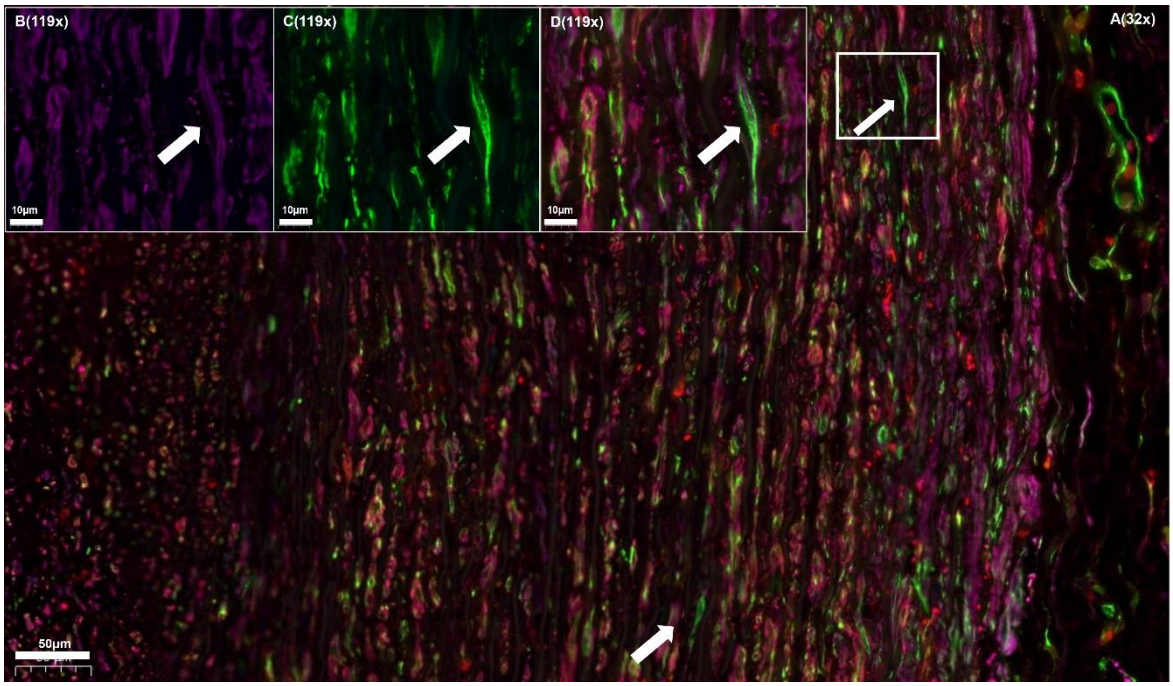

Fig S3.1. A. The majority of spindle shaped cells in the media of AIT are triple positive for Vimentin^{+} (in *green*; AF488; FITC-channel), FSP-1^{+} (in *red*; AF546; TRITC-channel) and αSMA^{+} (in *magenta*; AF647; Cy5-channel). The inserts show single channel signals for αSMA^{+} (**B**) and Vimentin^{+} (**C**). Insert (**D**) shows the presence of αSMA^{+}/Vimentin^{+}/FSP-1^{-} double positive subpopulation.

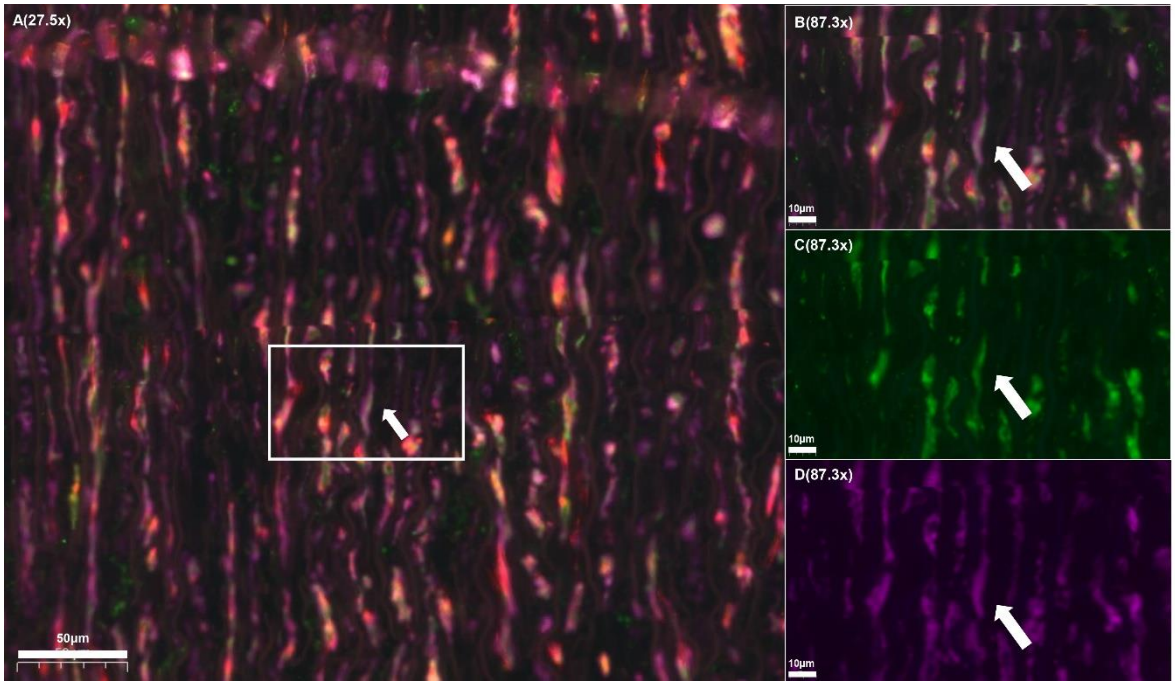

Fig S3.2. A. The majority of spindle shaped cells in the media of AIT are triple positive for Vimentin^{+} (in *green*; AF488; FITC-channel), CD90^{+} (in *red*; AF546; TRITC-channel) and αSMA^{+} (in *magenta*; AF647; Cy5-channel). The inserts show single channel signals for Vimentin^{+} (**C**) and αSMA^{+} (**D**). Insert (**B**) shows the presence of αSMA^{+}/Vimentin^{+}/CD90^{-} double positive subpopulation.

Figure S4. Challenging Vimentin as an all-inclusive panmesenchymal marker.

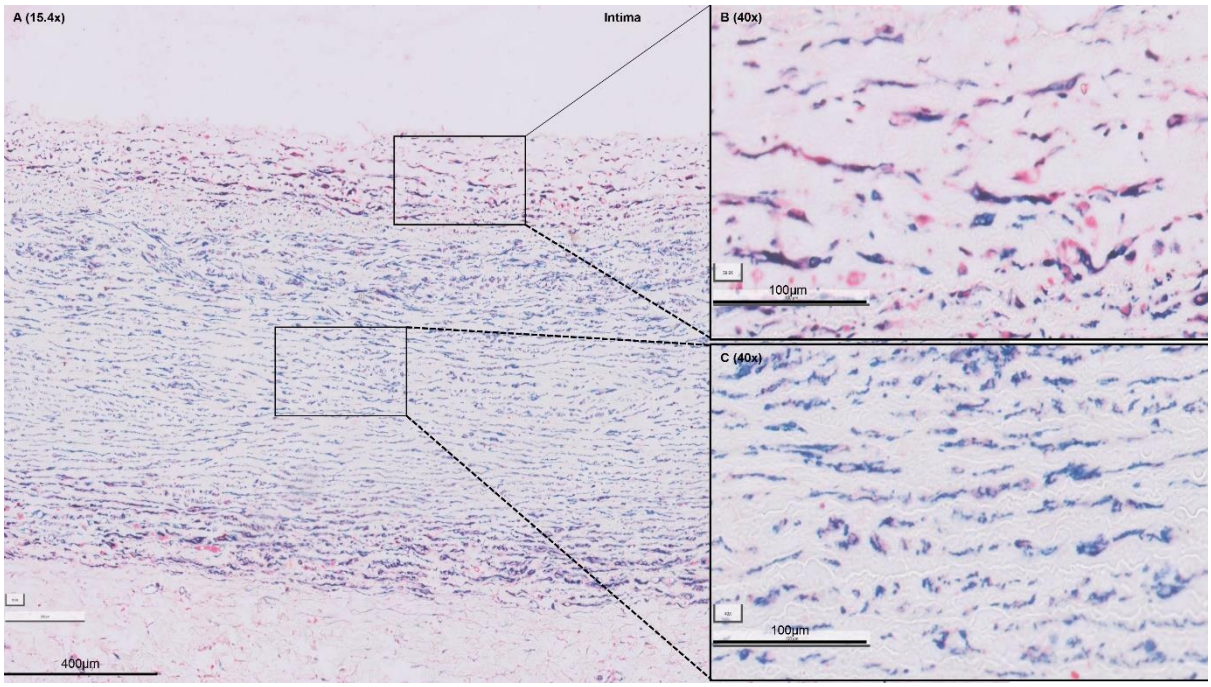

Figure S4.1: A. Adaptive Intimal Thickening (AIT) section double IHC stained for FAP (in *red*) and Vimentin (in *blue*). In AIT, FAP and Vimentin show almost complete (**B**/**C**; in *purple*).

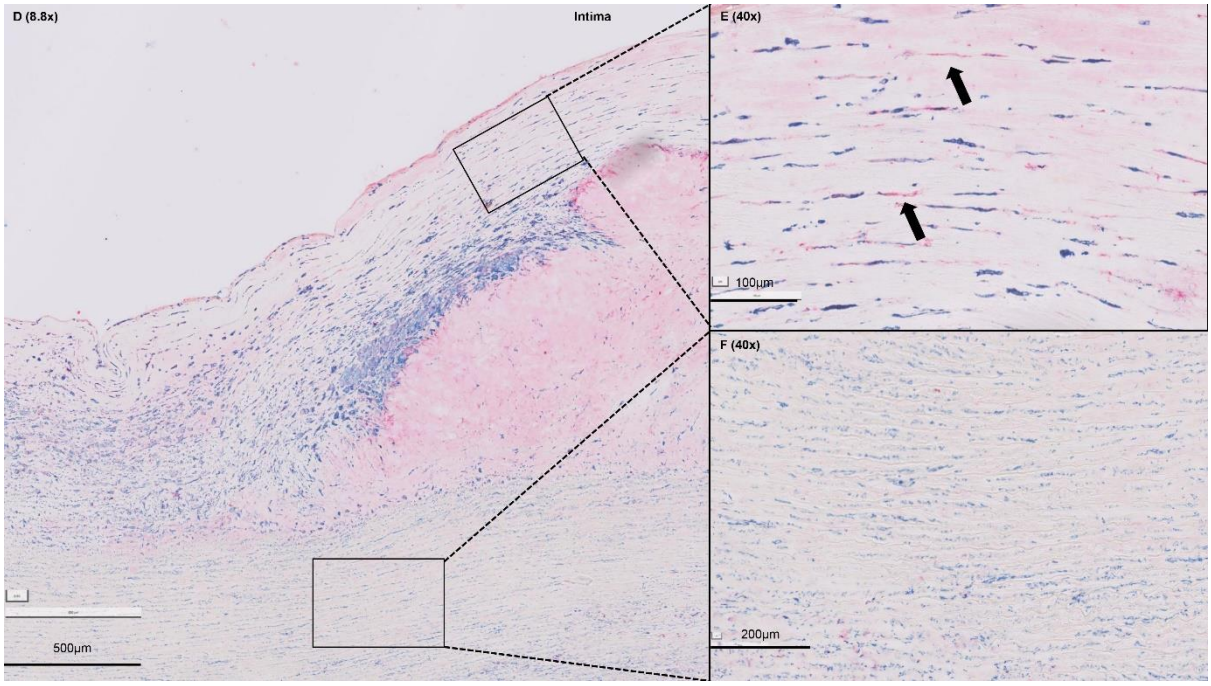

Figure S4.2. A. Late Fibroatheroma (LFA) section double IHC stained for FAP (in *red*) and Vimentin (in *blue*). During atherogenic progression, although FAP expression remained stable in the medial zones (**F**), FAP expression is unstable in the cap region, shown by spindle-shaped single FAP^{+} cells (**E; arrows,** *in red*), challenging Vimentin as an all-inclusive panmesenchymal marker.

Figure S5. Double Vimentin^{+}/αSMA^{+} cells in the cap of progressive atherosclerotic lesions (LFA and TCFA) and stabilized atherosclerotic lesions (HR).

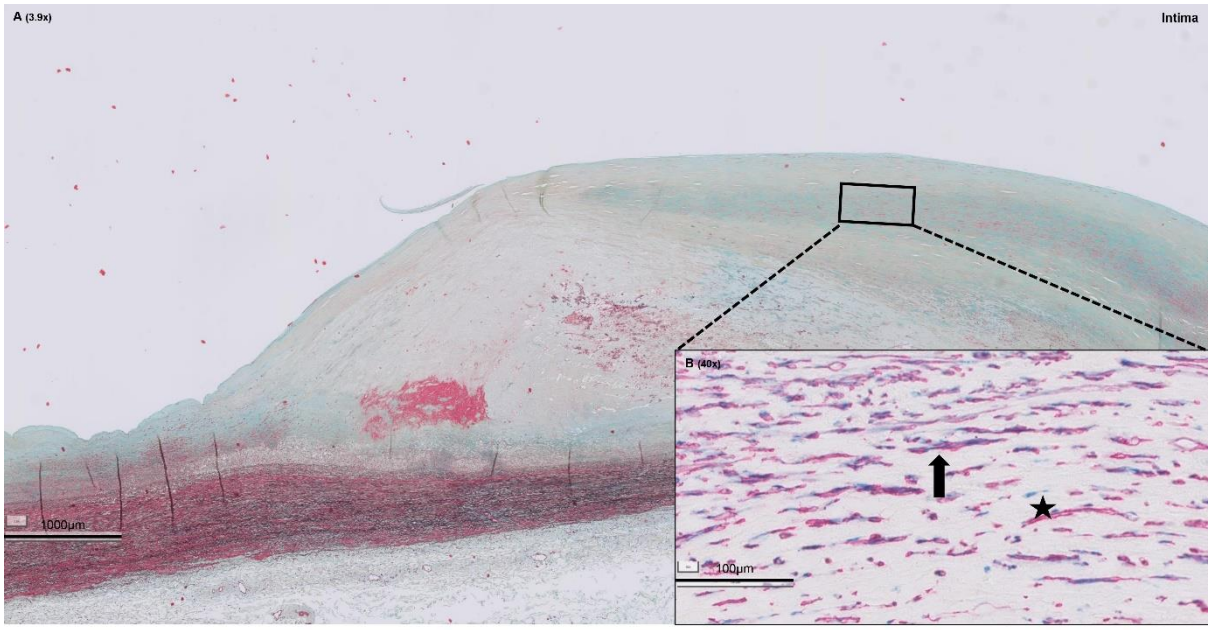

Figure S5.1: **A.** Movat Pentachrome staining of LFA (Late Fibroatheroma).

Legend: *red*, smooth muscle cells/fibrin; *violet*: leukocytes; *black*: elastin; *blue*: proteoglycans/mucins; *yellow*: collagen. Various shades of green reflect colocalization of collagen (*yellow*) and proteoglycans (*blue*).

B. Insert of the cap double IHC stained for Vimentin (in *blue*) and αSMA (in *red*), showing that the cap is mesenchymal cell (Vimentin+) rich. Approximately 80% of the Vimentin^{+} cells were double Vimentin^{+}/αSMA^{+} (**arrow in B**, in *purple*; star indicates a single Vimentin^{+}/αSMA^{-} cell).

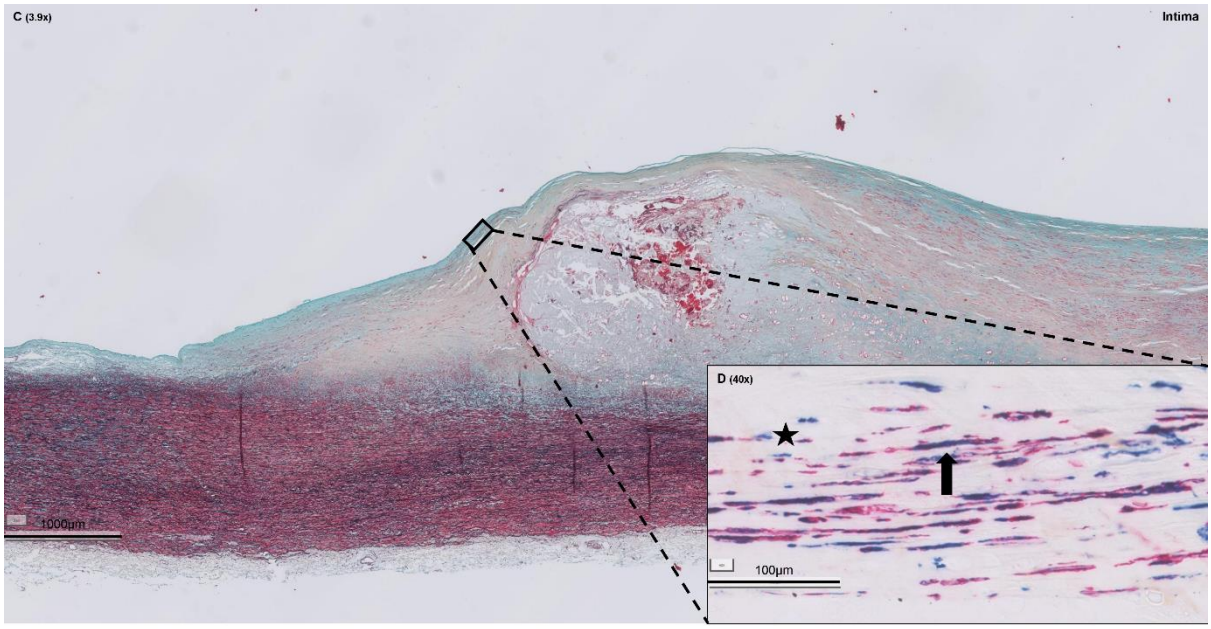

Figure S5.2: C. Movat Pentachrome staining of TCFA (Thin cap fibroatheroma). For legend see Figure S5.1.

D. Insert of the cap double IHC stained for Vimentin (in *blue*) and αSMA (in *red*). Transition from a LFA to a TCFA was associated with a clear decrease in cell density. Approximately 80% of the Vimentin^{+} cells were double Vimentin^{+}/αSMA^{+} (**arrow in D**, in *purple*; star indicates a single Vimentin^{+}/αSMA^{-} cell).

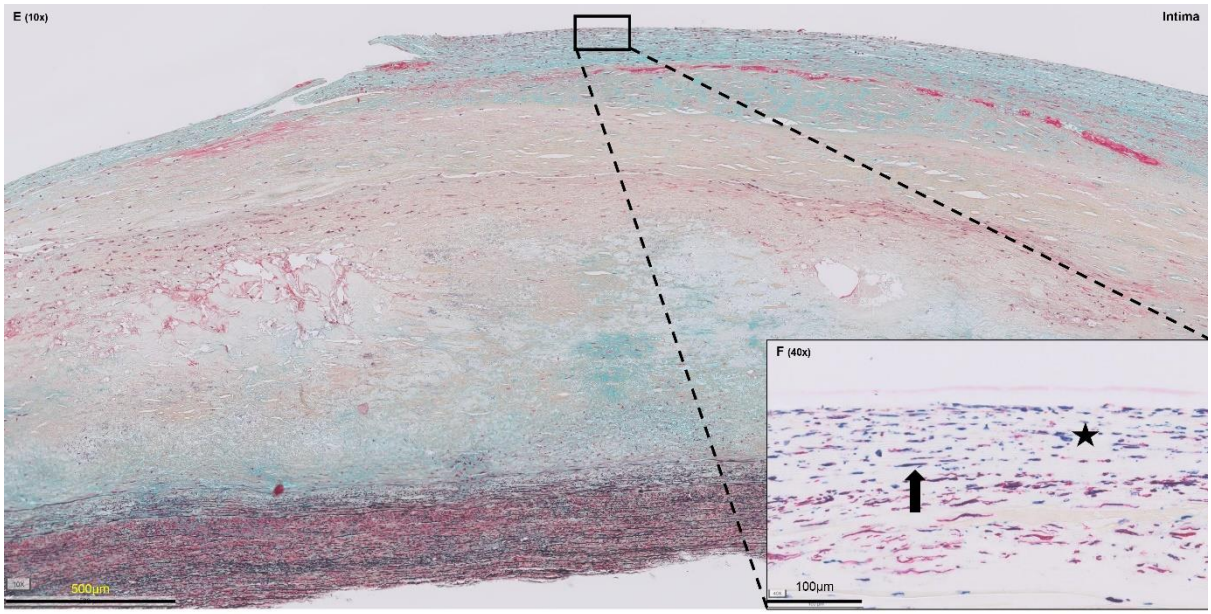

Figure S5.3: E. Movat Pentachrome staining of HR (Thin cap fibroatheroma). For legend see Figure S5.1.

F. Within the cell-rich/proteoglycan-rich luminal granulation tissue that is associated with healing of a ruptured atherosclerotic lesions (HR), approximately 80% of the Vimentin$^+$ cells (in *blue*) were double Vimentin$^+$/αSMA$^+$ (**arrow in D**, in *purple*; star indicates a single Vimentin$^+$/αSMA$^-$ cell).

Figure S6. Vimentin, Thy-1/CD90, S100A4/FSP-1 and FAP are limited in mesenchymal lineage specificity: expression in monocytic cells.

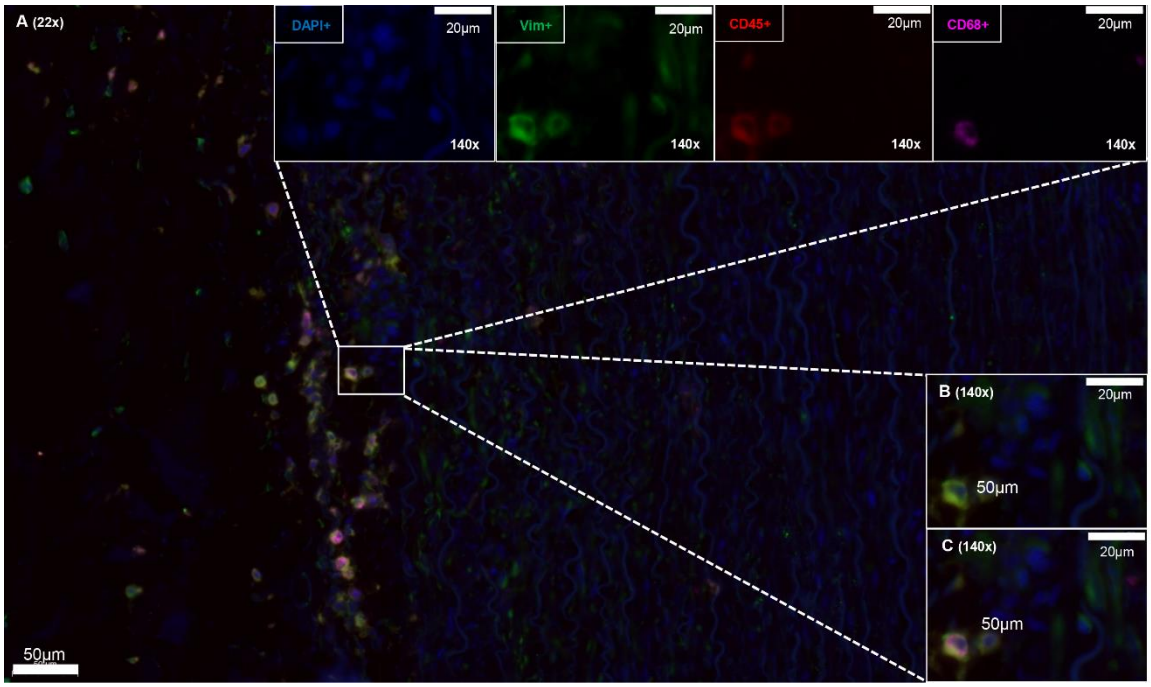

Figure S6.1: A. Triple IF staining of Vimentin (Vim), clone 1A4, (in *green*; AF488; FITC-channel), CD45 (in *red*; Vulcan Red; TRITC-channel) and CD68 (in *magenta*; AF647; Cy5-channel) in the adventitia. Nuclei are DAPI-stained (*blue*). Arterial elastic laminae in the medial layer are occasionally visible in greenblue due to auto-fluorescence. The four top inserts show the single channel information for Dapi, Vimentin, CD45 and CD68 (from left to right). Inserts on the down right show overlay information for **(B)** $CD45^+/Vimentin^+$ cells, respectively of which a part is $CD68^+/Vimentin^+/CD45^+$**(C)**.

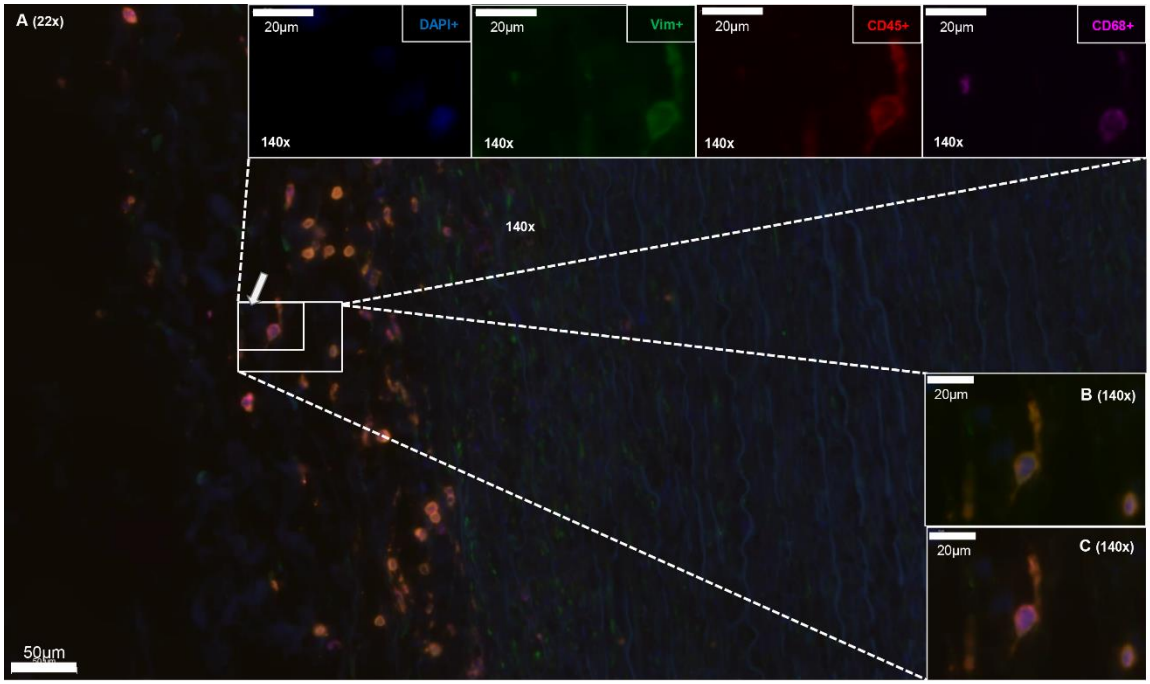

Figure S6.2: A. Triple IF staining of Vimentin (Vim), clone VI-10, (in *green*; AF488; FITC-channel), CD45 (in *red*; Vulcan Red; TRITC-channel) and CD68 (in *magenta*; AF647; Cy5-channel) in the adventitia. Nuclei are DAPI-stained (*blue*). Arterial elastic laminae in the medial layer are occasionally visible in greenblue due to auto-fluorescence. The four top inserts show the single channel information for Dapi, Vimentin, CD45 and CD68 (from left to right). Inserts on the down right show overlay information for **(B)** $CD45^{+}$/$Vimentin^{+}$ cells, respectively of which a part is $CD68^{+}$/$Vimentin^{+}$/$CD45^{+}$**(C)**.

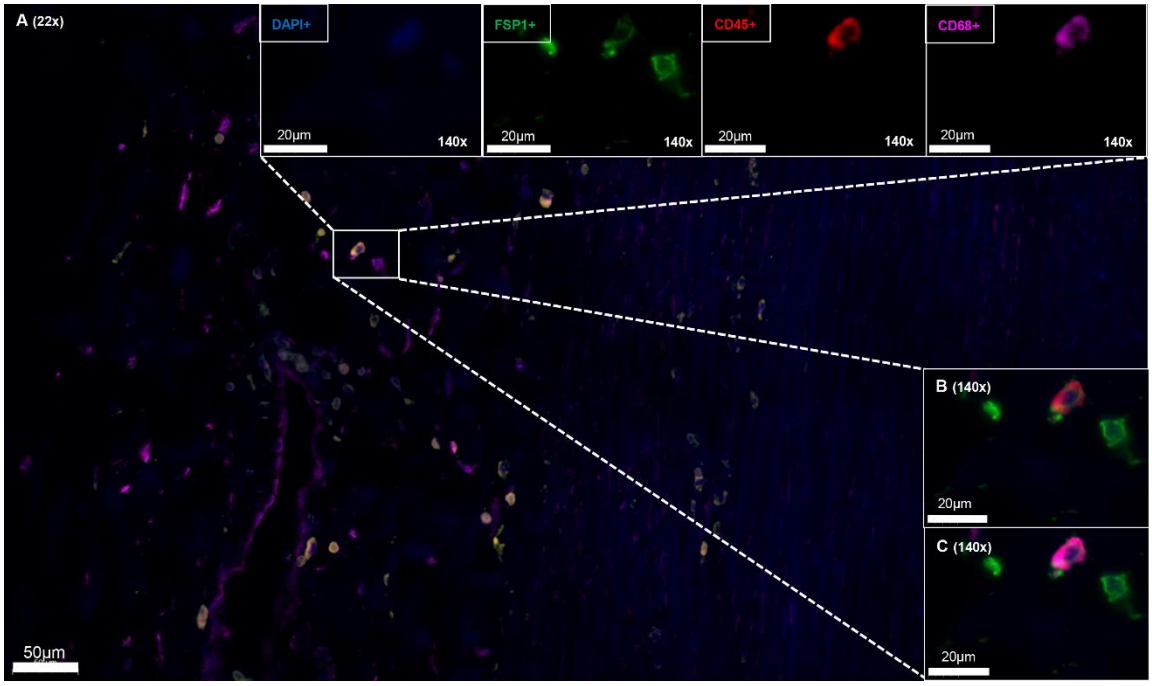

FigureS6.3: A. Triple IF staining of FSP-1 (in *green*; AF647; Cy5-channel), CD45 (in *red*; Vulcan Red; TRITC-channel) and CD68 (in *magenta*; AF488; FITC-channel) in the adventitia. Nuclei are DAPI-stained (*blue*). Arterial elastic laminae in the medial layer are occasionally visible in greenblue due to auto-fluorescence. The four top inserts show the single channel information for Dapi, FSP-1, CD45 and CD68 (from left to right). Inserts on the down right show overlay information for **(B)** $CD45^+/FSP\text{-}1^+$ cells, respectively of which a part is $CD68^+/FSP\text{-}1^+/CD45^+$**(C)**.

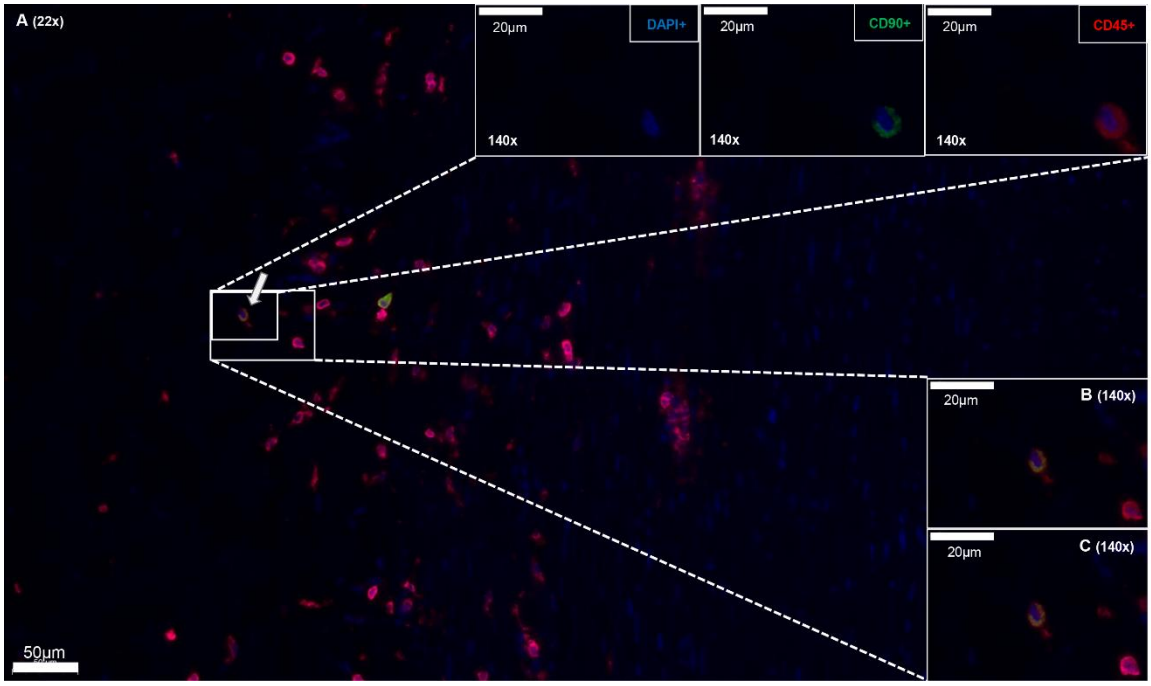

Figure S6.4: A. Triple IF staining of CD90 (in *green*; AF488; FITC-channel), CD45 (in *red*; Vulcan Red; TRITC-channel) and CD68 (in *magenta*; AF647; Cy5-channel) in the adventitia. Nuclei are DAPI-stained (*blue*). Arterial elastic laminae in the medial layer are occasionally visible in greenblue due to auto-fluorescence. The four top inserts show the single channel information for Dapi, CD90, CD45 and CD68 (from left to right). Inserts on the down right show overlay information for **(B)** $CD45^+/CD90^+$ cells, respectively of which a part is $CD68^+/CD90^+/CD45^+$**(C)**.

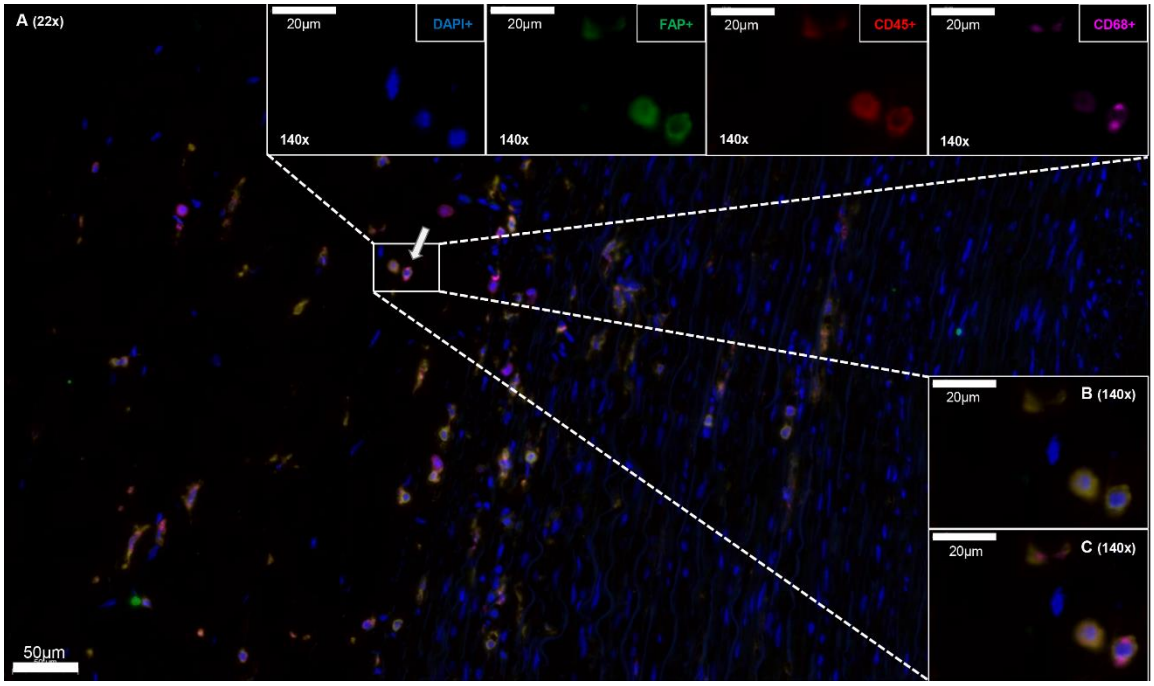

Figure S6.5: A. Triple IF staining of FAP (in *green*; AF488; FITC-channel), CD45 (in *red*; Vulcan Red; TRITC-channel) and CD68 (in *magenta*; AF647; Cy5-channel) in the adventitia. Nuclei are DAPI-stained (*blue*). Arterial elastic laminae in the medial layer are occasionally visible in greenblue due to auto-fluorescence. **(B)** The four top inserts show the single channel information for Dapi, FAP, CD45 and CD68 (from left to right). Inserts on the down right show overlay information for **(B)** $CD45^+/FAP^+$ cells, respectively of which a part is $CD68^+/FAP^+/CD45^+$**(C)**.

Figure S7. Limited mesenchymal lineage specificity of Vimentin: expression in endothelial cells. Thy-1/CD90, S100A4/FSP-1 and FAP are not expressed in endothelial cells.

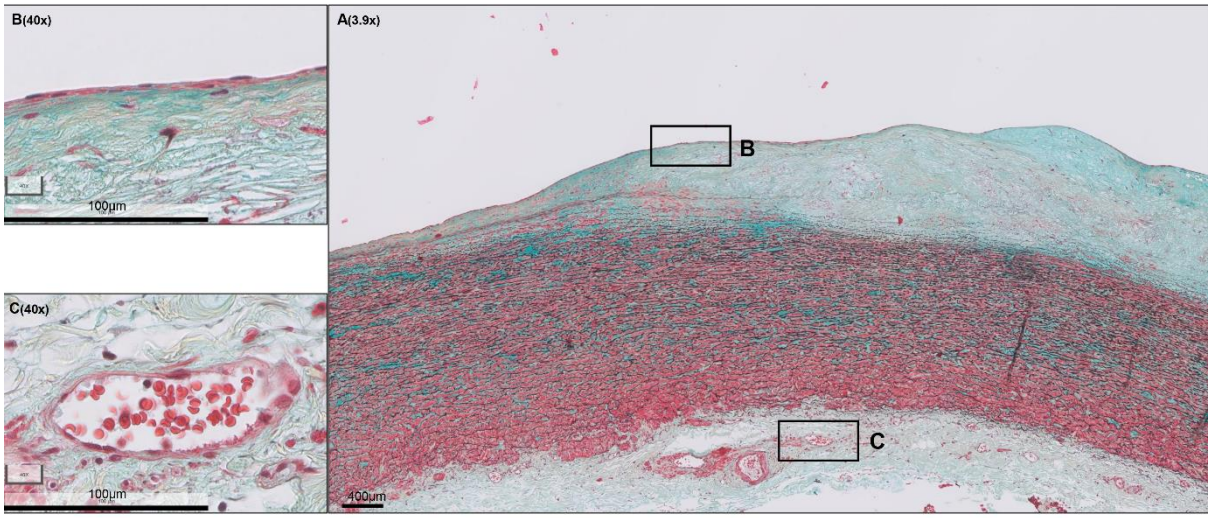

Figure S7.1: **A**. Movat Pentachrome staining of EFA (Early Fibroatheroma). Legend: *red*, smooth muscle cells/fibrin; *violet*: leukocytes; *black*: elastin; *blue*: proteoglycans/mucins; *yellow*: collagen. Various shades of green reflect colocalization of collagen (*yellow*) and proteoglycans (*blue*). **B**. Close up of intact endothelium in the arterial wall and of endothelial cells in a vasum vasorum (**C**).

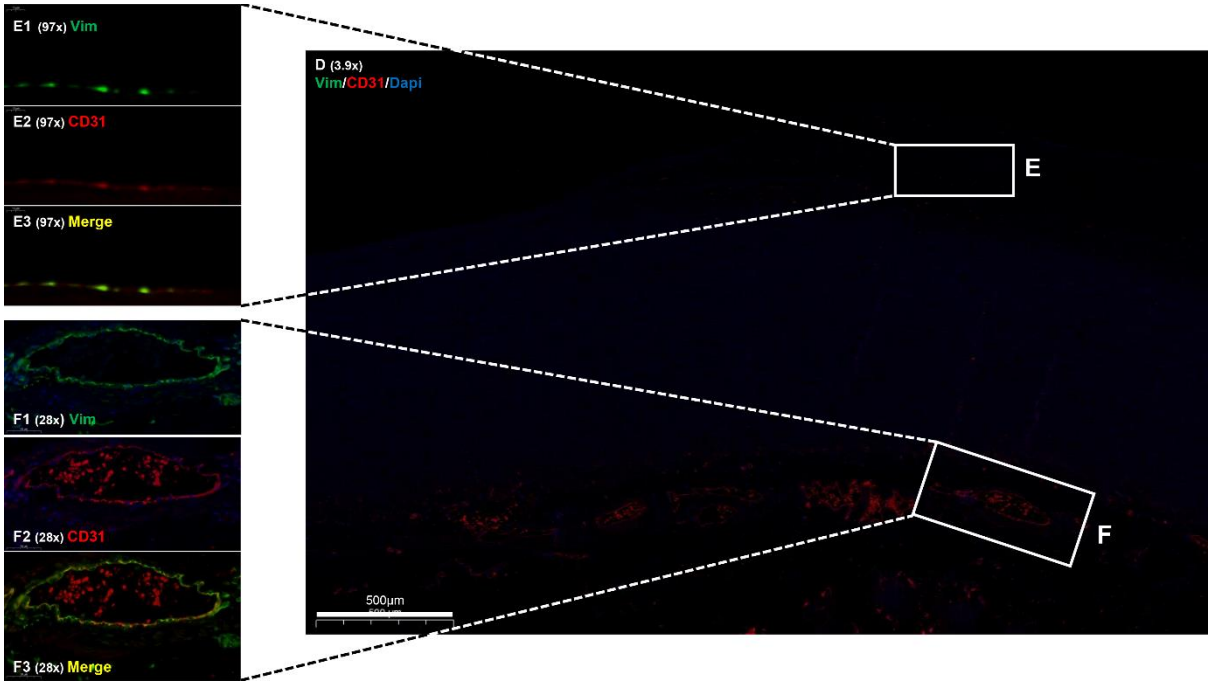

Figure S7.2: **D**. Double IF staining of Vimentin (cytoplasma staining, in *green*; AF488; FITC-channel) and CD31 (plasma membrane and cell junction staining, in *red*; Vulcan Red; TRITC-channel) of a consecutive section of the EFA shown in **A**. Nuclei are DAPI-stained (in *blue*).

The inserts on the left shown single channel information for Vimentin (**E1/F1**) and CD31 (**E2/F2**). Vimentin and CD31 colocalize in the arterial intima (**E3**) and in endothelial cells in the vasa vasora (**F3**).

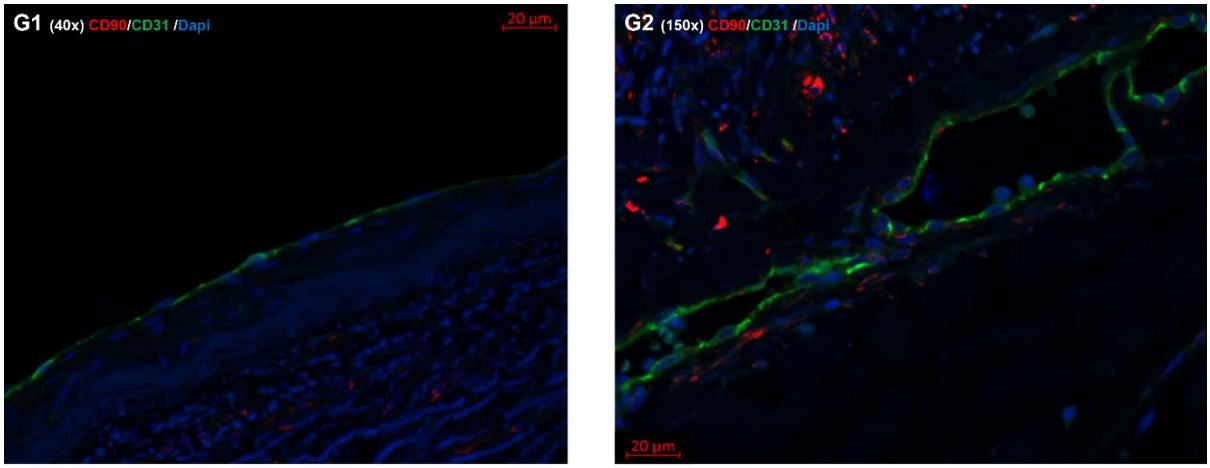

Figure S7.3: **G1**. Close up of single positive $CD31^+$ (in *green*; AF488; FITC-channel; plasma membrane and cell junction staining)/$CD90^-$ endothelial cells in the arterial wall. **G2**. Close up of $CD90^+/CD31^-$ cells (in *red*; Vulcan Red; TRITC-channel; plasma membrane staining) that are in close proximity of $CD31^+$ endothelial cells (in *green*; AF488; FITC-channel; plasma membrane and cell junction staining) in vasa vasora. Nuclei are DAPI-stained (in *blue*).

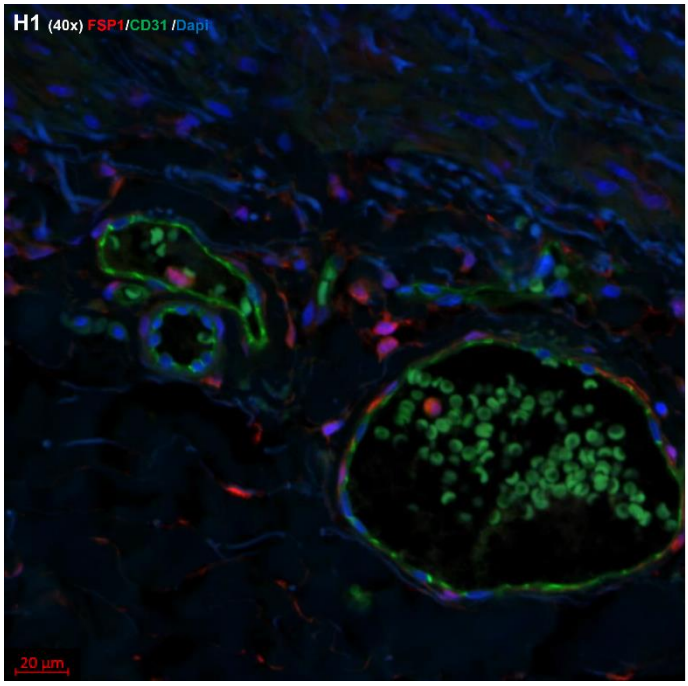

Figure S7.4: H1. Close up of FSP-1^{+} cells (in *red*; Vulcan Red; TRITC-channel, nucleus and cytoplasm staining) are in close proximity of single CD31^{+} endothelial cells (in *green*; AF488; FITC-channel; plasma membrane and cell junction staining) in vasa vasora. Nuclei are DAPI-stained (in *blue*).

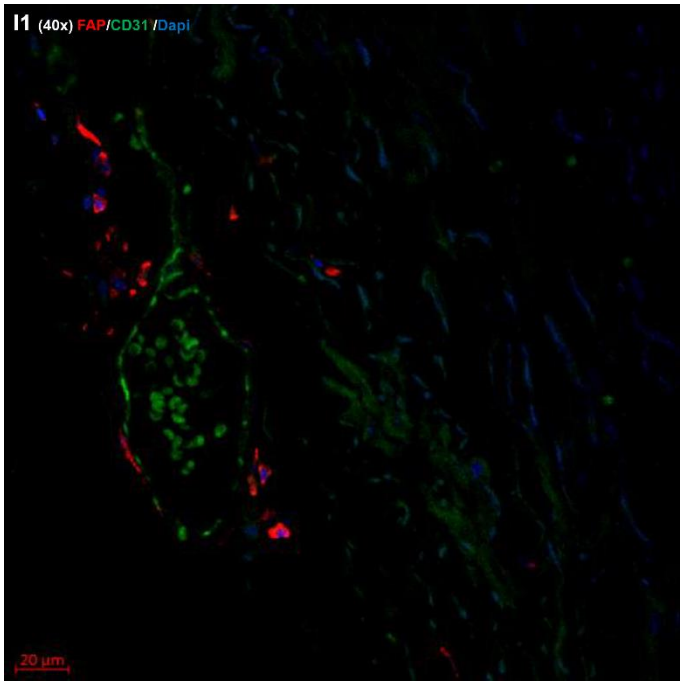

Figure S7.5: H1. Close up of single FAP$^+$ cells (in *red*; Vulcan Red; TRITC-channel, nucleus and cytoplasm staining) that are in close proximity of CD31$^+$ endothelial cells (in *green*; AF488; FITC-channel; plasma membrane and cell junction staining) in vasa vasora. Nuclei are DAPI-stained (in *blue*).

Figure S8. Role for EndoMT/ stem cells in vascular pathology.

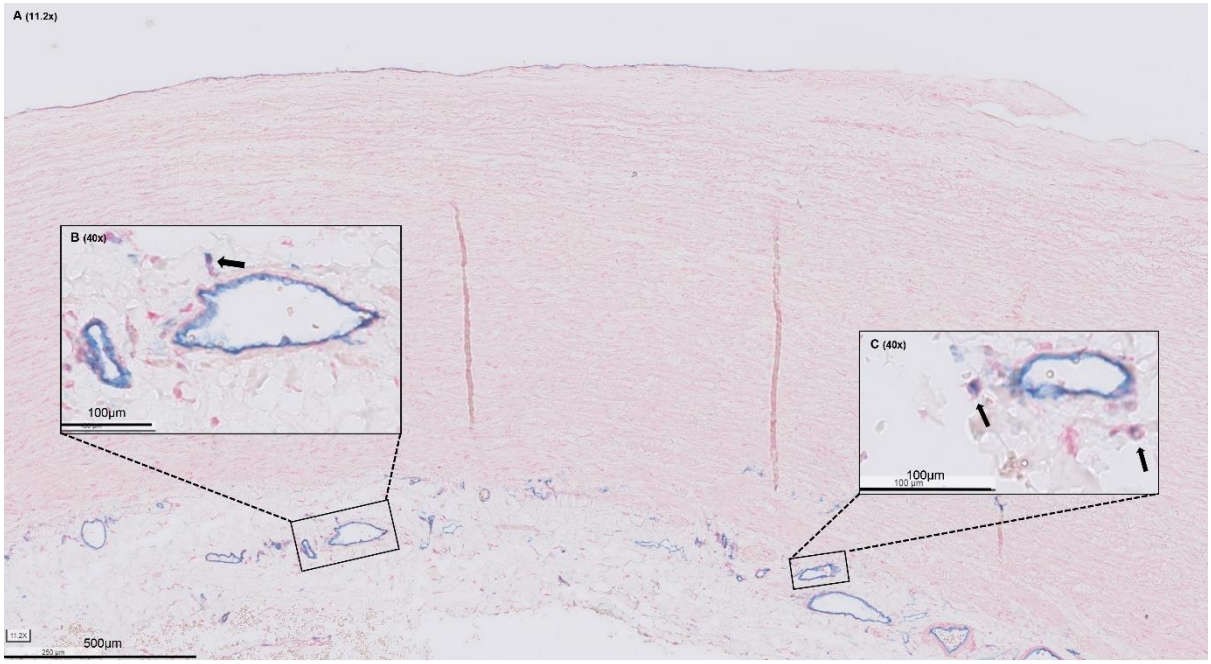

Figure S8.1: A. Double IHC staining of CD31 (in *blue*) and Vimentin (in *red*) on LFA. The inserts (**B/C**) show solitary double Vimentin^{+}/CD31^{+} cells in the vicinity of the vasa vasora (in purple; **arrows**).

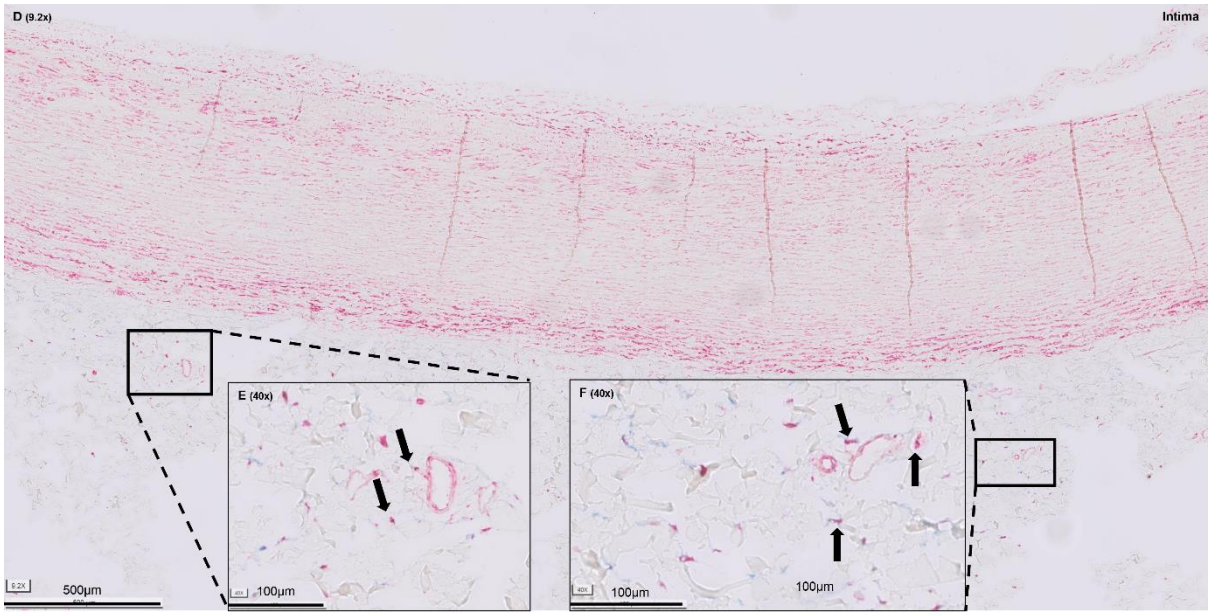

Figure S8.2: D. Double IHC staining of CD34 (in *blue*) and Vimentin (in *red*) on LFA. The inserts (**E/F**) show solitary double Vimentin^{+}/CD34^{+} cells in the vicinity of the vasa vasora (in purple; **arrows**).

Figure S9. Fibrocytes in luminal vascular repair sites.

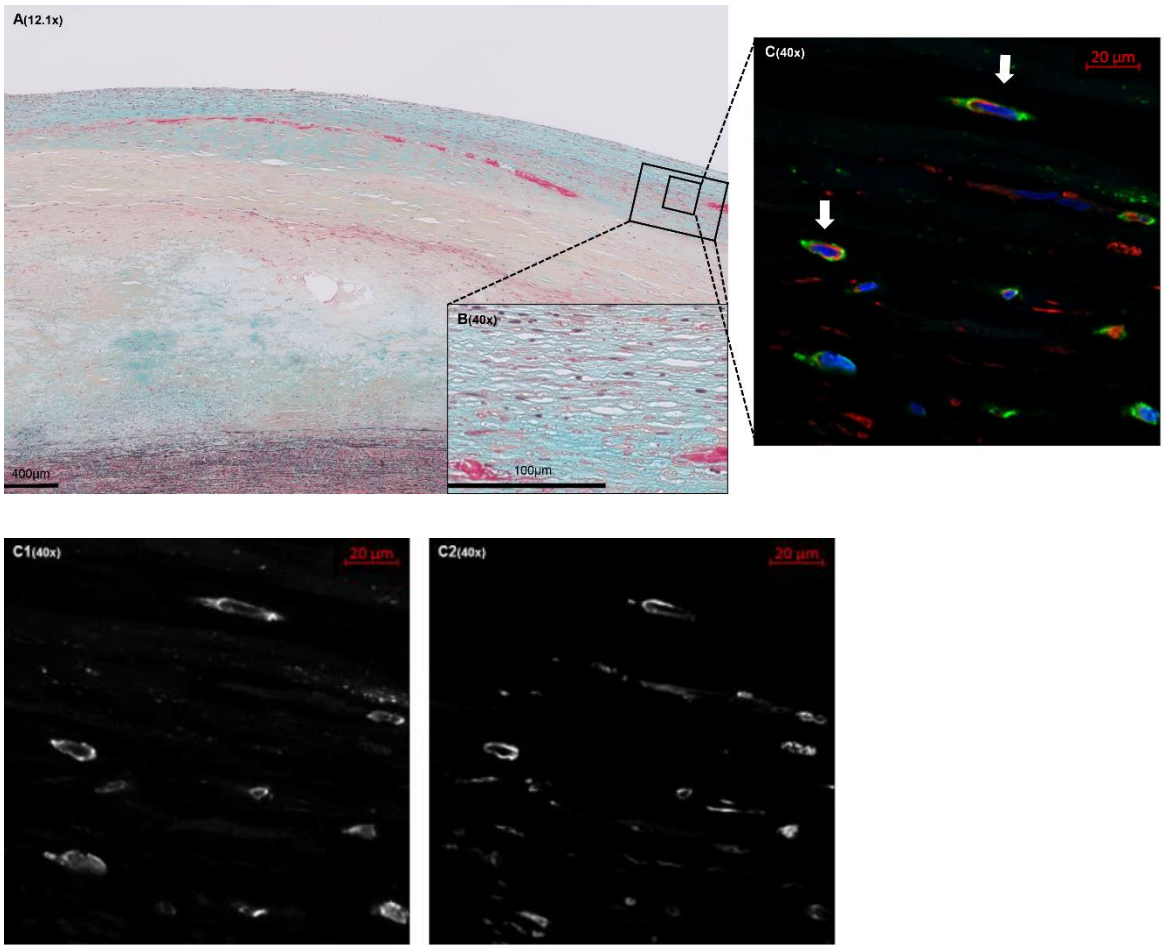

Figure S9.1: **A**. Healed Rupture (HR) stained by Movat pentachrome. Plaque consolidation (wound healing process) is characterized by a spindle-shaped mesenchymal-rich (**B;** nuclei in red) and proteoglycan-rich matrix (**B**; green-blue) cap covering the fibrotic remnants of the former cap (**A**; yellow region). **C**. Confocal images of spindle-shaped double Vimentin^{+} (in *green*; AF488)/ CD45^{+} (in *red*; AF647) in the proteoglycan-rich granulation tissue. **C1**. Shows single channel information for Vimentin and **C2** shows single channel information for CD45.

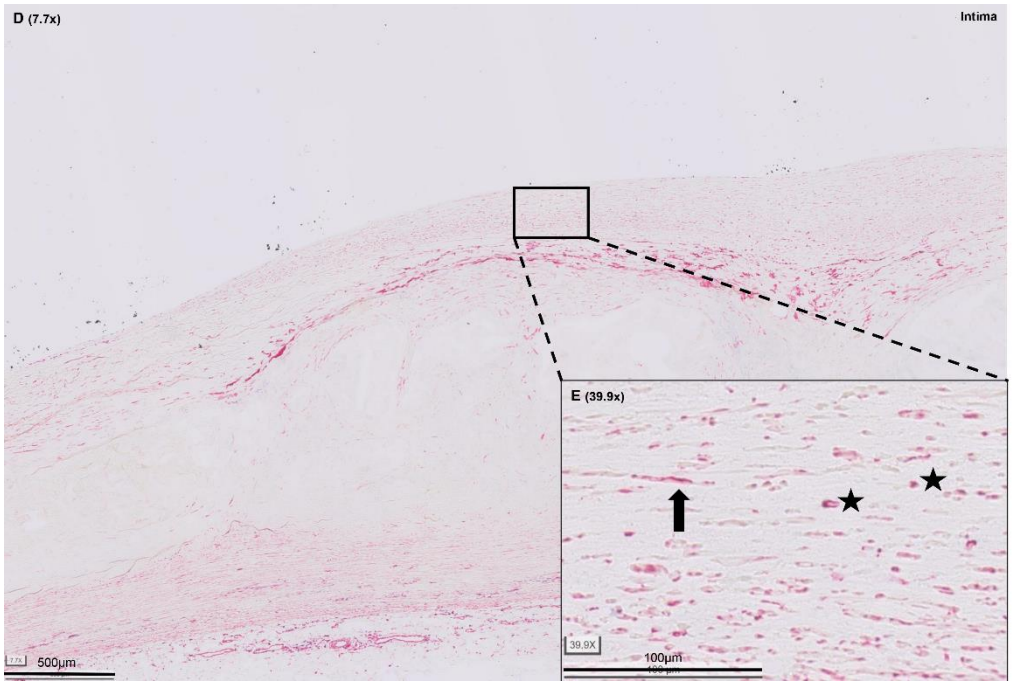

Figure S9.2: **D**. Late Fibroatheroma (LFA) double IHC stained for Vimentin (in *red*) and CD45 (in *blue*). **E**. In the cap of LFA, both spindle shaped double Vimentin$^+$/CD45$^+$ (arrow) cells and round-shaped double Vimentin$^+$/CD45$^+$ (stars) are present.

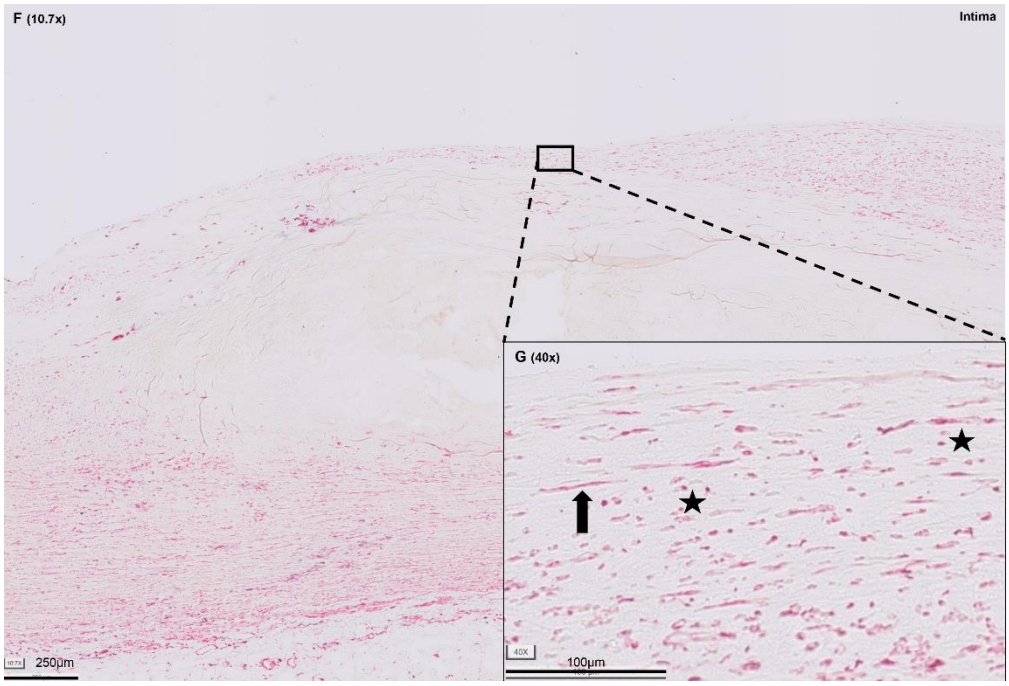

Figure S9.3: **F**. Fibrocalcific Plaque (FCP) double IHC stained for Vimentin (in *red*) and CD45 (in *blue*). **E**. In the neo-intima of FCP, both spindle shaped double Vimentin^{+}/CD45^{+} (arrow) cells and round-shaped double Vimentin^{+}/CD45^{+} (stars) are present.

Figure S10. Subset of elongated Smemb+ are synthetic.

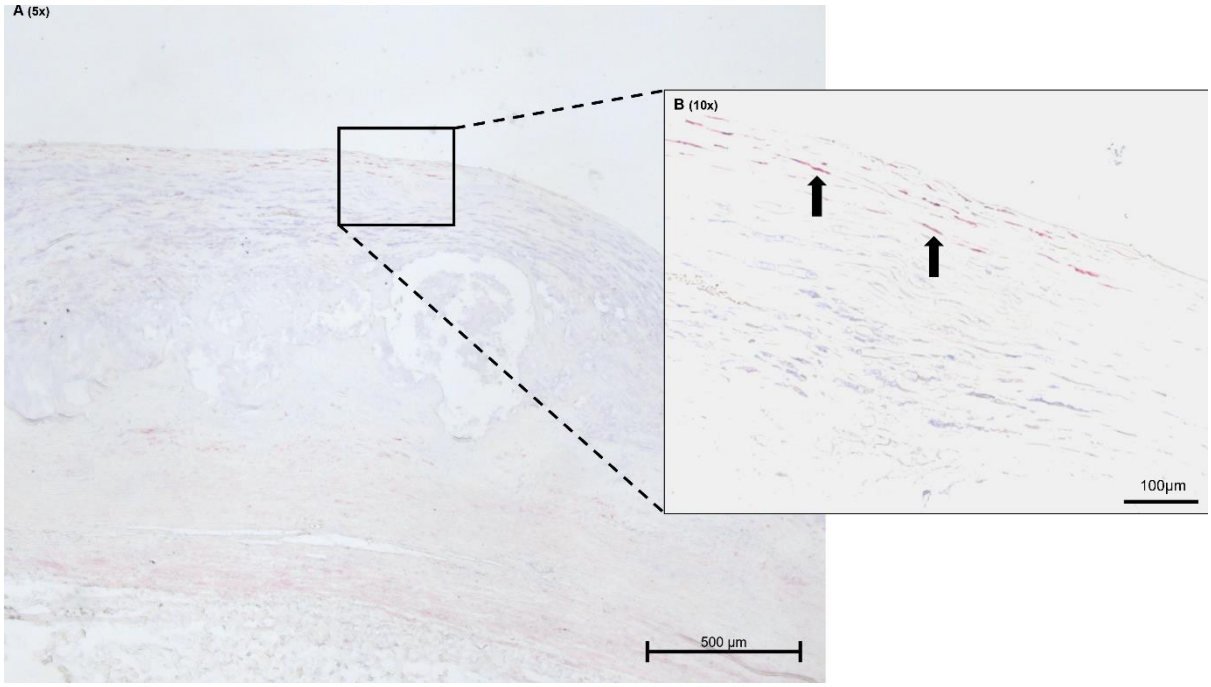

Figure S10: A. Late Fibroatheroma (LFA) section double IHC stained for Smemb (in *red*) and P4HB (in *blue*). Most Smemb+ elongated cells in the cap and shoulder region were found to also express the synthetic marker P4HB, but single Smemb+ elongated cells were also present in these regions (**B**; arrows).

Figure S11. Spatial distribution of h1-Calponin in progressive atherosclerosis.

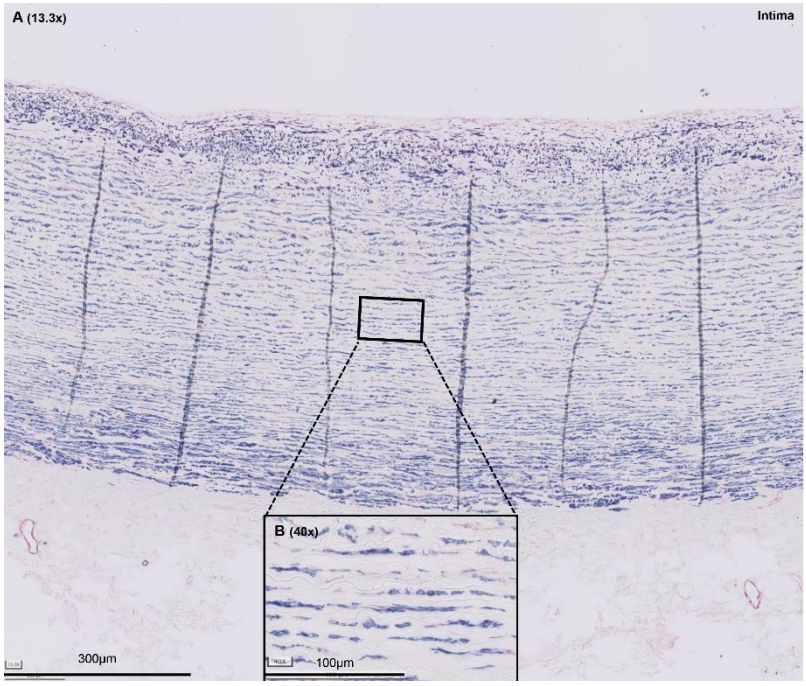

Figure S11.1: A. Adaptive Intimal Thickening (AIT) section double IHC stained for αSMA (in *red*) and h1-Calponin (in *blue*). In AIT, they show complete colocalization (**B**; in purple), except from the vasa vasora which are often single αSMA^{+} (**A**; in *red*).

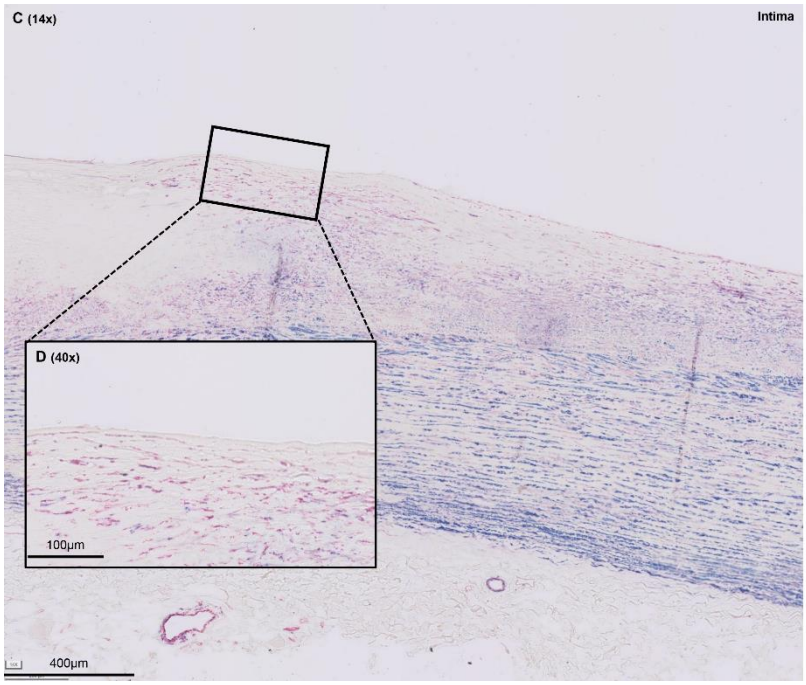

Figure S11.2: A. Late Fibroatheroma (LFA) section double IHC stained for αSMA (in *red*) and h1-Calponin (in *blue*). In LFA, there is a dissociation of the staining pattern for αSMA and h1-Calponin in the cap/shoulder region, reflected by single h1-Calponin^{-}/ αSMA^{+} cells (in *red*).

Figure S12. Tropomyosin, Telokin and Paxillin are not contractile cell specific.

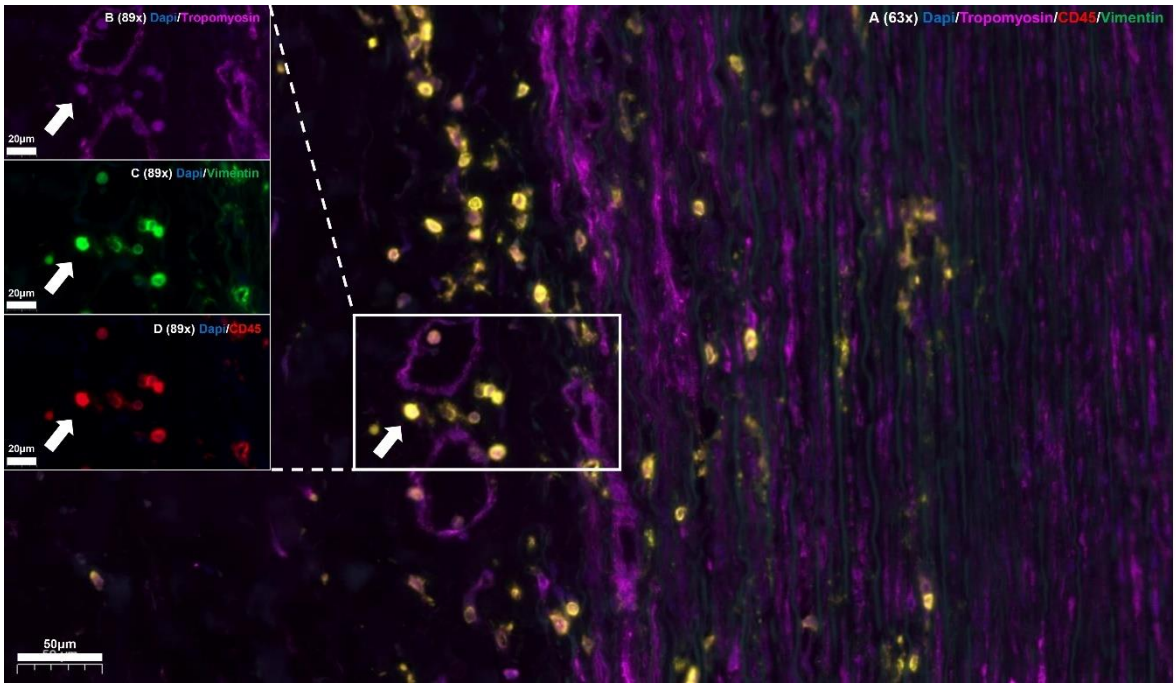

Figure S12.1: A. Triple staining of Tropomyosin (in *magenta*; AF647; Cy5-channel), Vimentin (in *green*; AF488; FITC-channel) and CD45 (in *red*; Vulcan Red; TRITC-channel) in the adventitia. The three left inserts show the single channel information for Tropomyosin (**B**), Vimentin (**C**) and CD45 (**D**), counterstained by Dapi (in *blue*). The vast majority of Tropomyosin+ cells were triple positive for Tropomyosin^{+}/Vimentin^{+}/CD45^{+}.

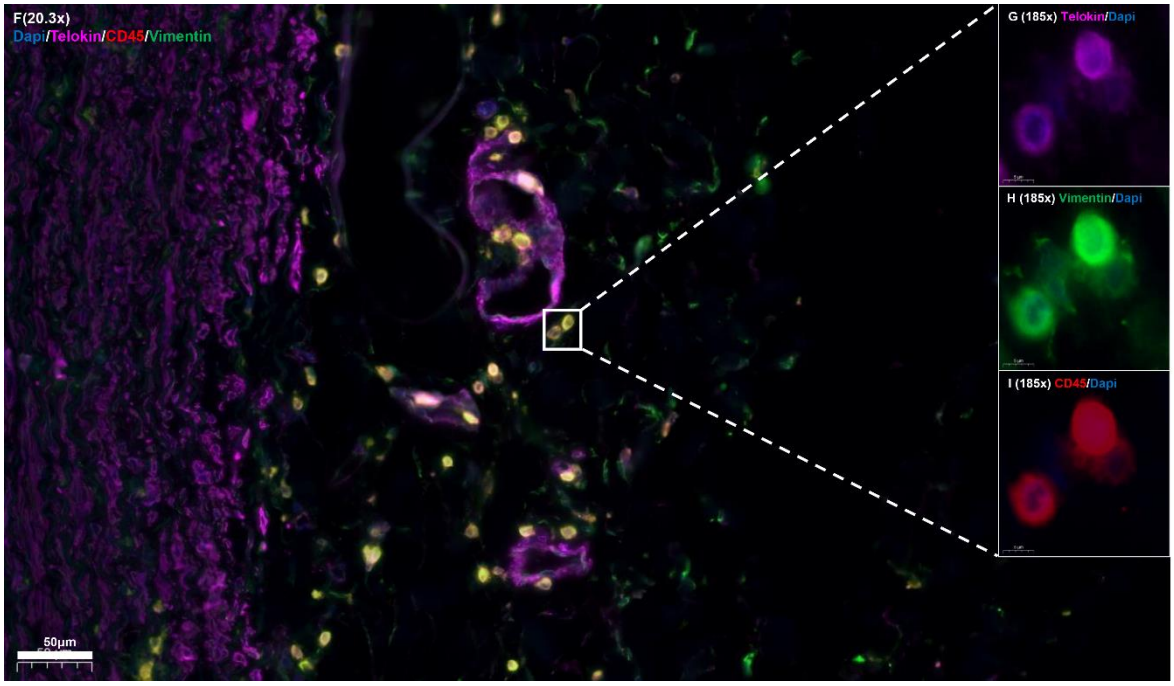

Figure S12.2: F. Triple staining of Telokin (in *magenta*; AF647; Cy5-channel), Vimentin (in *green*; AF488; FITC-channel) and CD45 (in *red*; Vulcan Red; TRITC-channel) in the adventitia. The three left inserts show the single channel information for Telokin (**G**), Vimentin (**H**) and CD45 (**I**), counterstained by Dapi (in *blue*). The vast majority of Telokin+ cells were triple positive for Telokin^{+}/Vimentin^{+}/CD45^{+}.

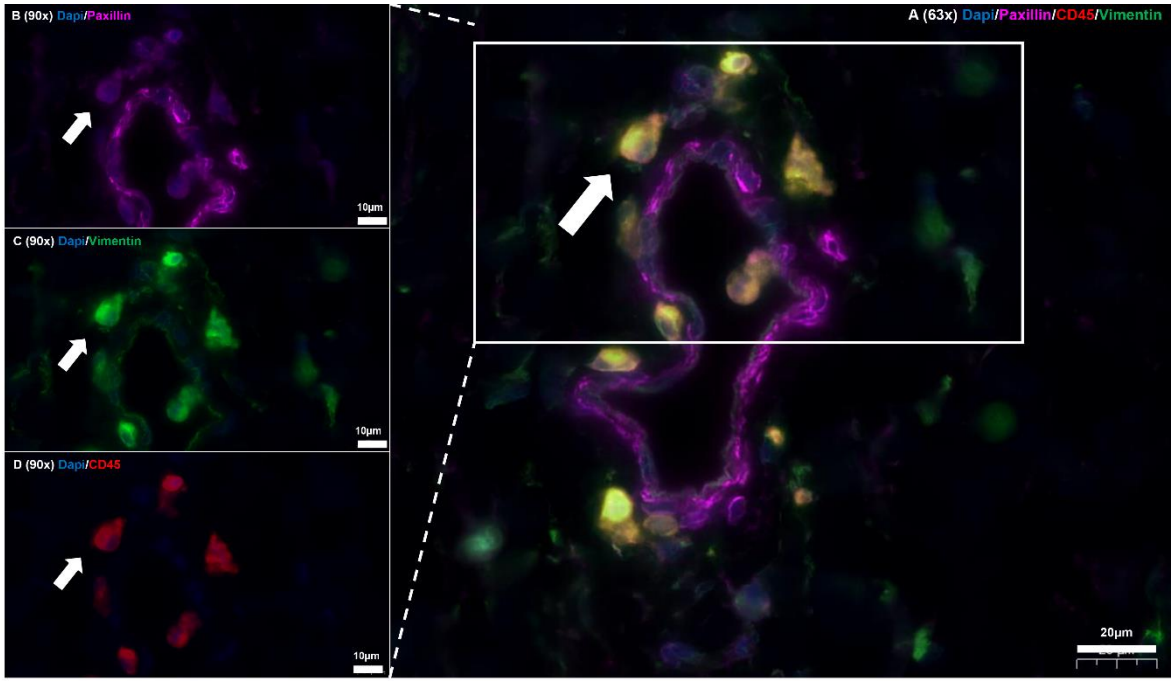

Fig S12.3: A. Triple staining of Paxillin (in *magenta*; AF647; Cy5-channel), Vimentin (in *green*; AF488; FITC-channel) and CD45 (in *red*; Vulcan Red; TRITC-channel) in the adventitia. The three left inserts show the single channel information for Paxillin (**B**), Vimentin (**C**) and CD45 (**D**), counterstained by Dapi (in *blue*). Although the vast majority of Paxillin$^+$ cells in the adventitia were triple positive for Paxillin$^+$/Vimentin$^+$/CD45$^+$, single Vimentin$^+$ cells were also present (**A**).

Figure S13. αSMA challenged as all-inclusive contractile marker.

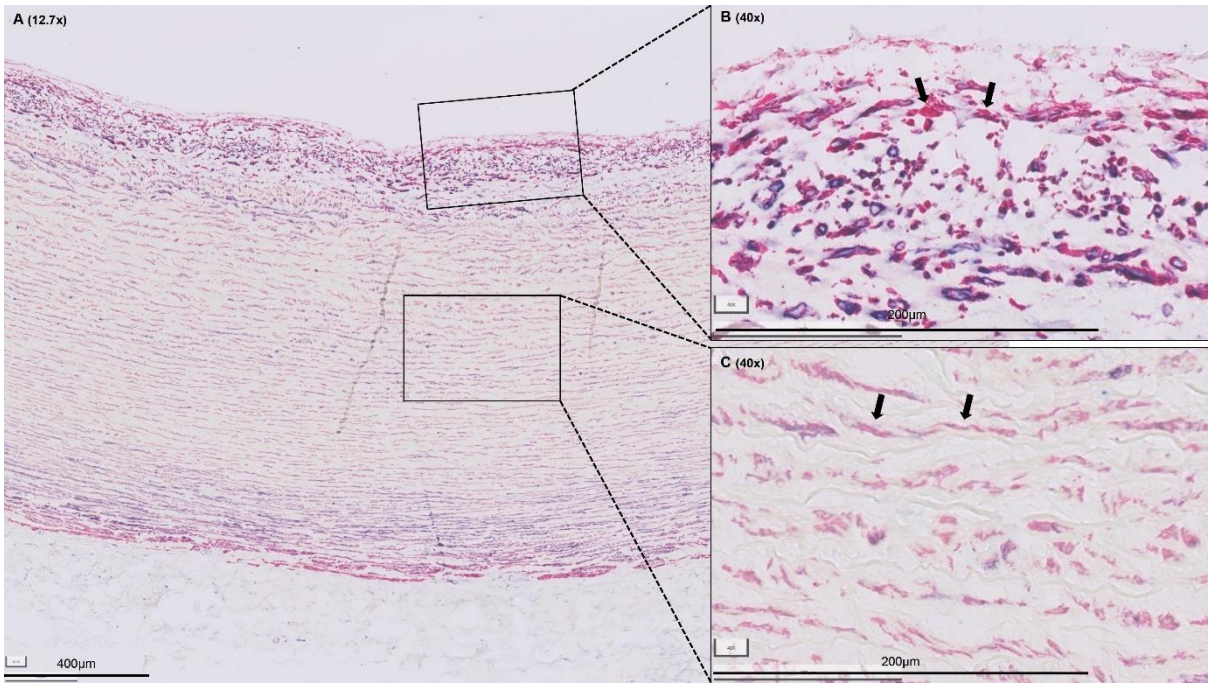

Figure S13.1: **A.** Adaptive Intimal Thickening (AIT) section double IHC stained for αSMA (in *red*) and Tropomyosin (in *blue*). In AIT, single αSMA^{+} cells (arrows in **B**) are present in the intima, as well as in the outer media. In the inner and medial media, all elongated cells are double αSMA^{+}/Tropomyosin^{+} *(in purple)*, but Tropomyosin is expressed in varying degrees (**C**. arrows: αSMA^{high}/Tropomyosin^{low}).

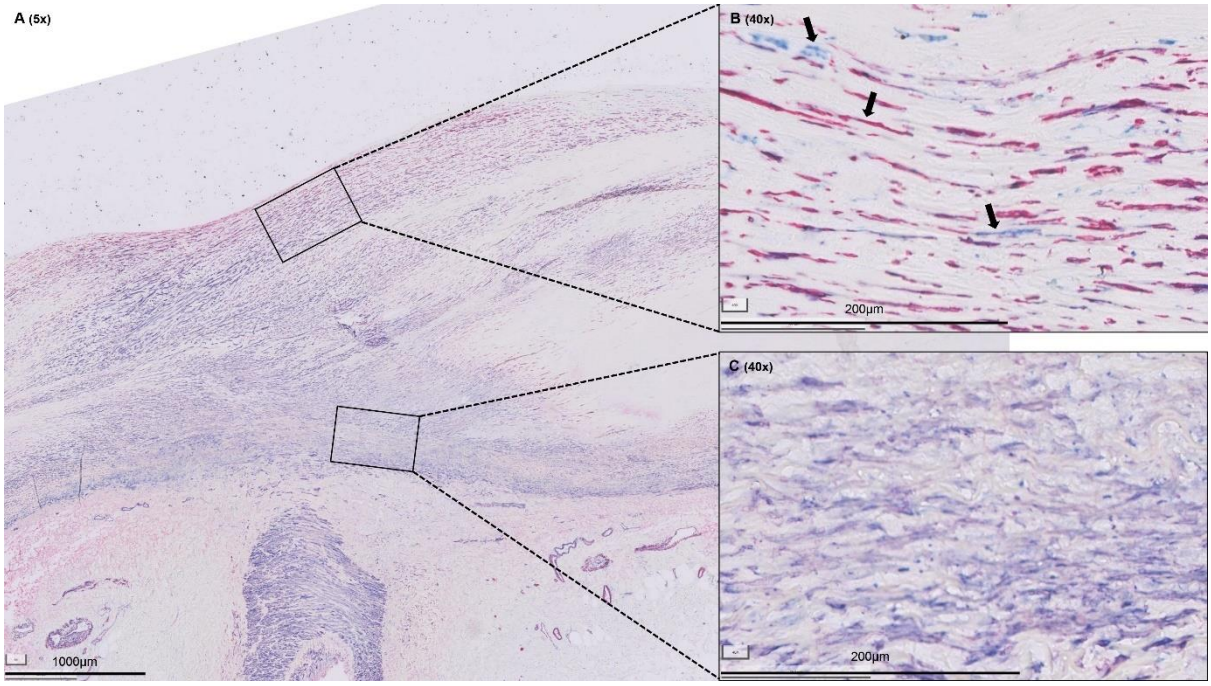

Figure S13.2: A. Late Fibroatheroma (LFA) section double IHC stained for αSMA (*red*) and Tropomyosin (*blue*). While in the media Tropomyosin and αSMA show complete overlap (**C**), in the cap and shoulder regions in LFA both single αSMA$^+$ cells and single Tropomyosin$^+$ cells are present (**B; arrows**).

Figure S14. Excluded synthetic and pro-inflammatory IHC markers.

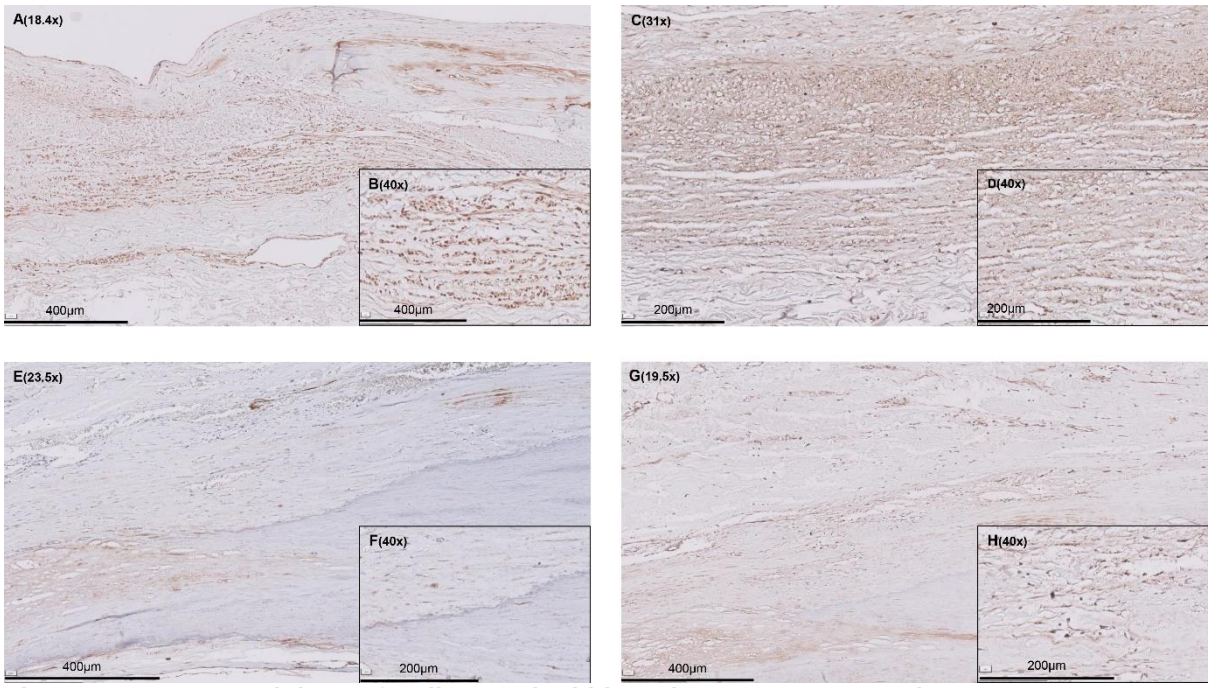

Figure S14.1: IHC Stainings of Collagen-I (Rabbit IgG), MBS502155, MyBioSource. In FCP tissue, significant non-specific staining was present, regardless of protein block usage and use of either a heat retrieval (**A**. Tris-EDTA, dilution 1:400) or an enzyme retrieval (**C**. Pepsin, dilution 1:400), similarly for AAA tissue (**E**. Tris-EDTA, dilution 1:400; **G**. Pepsin, dilution 1:400).

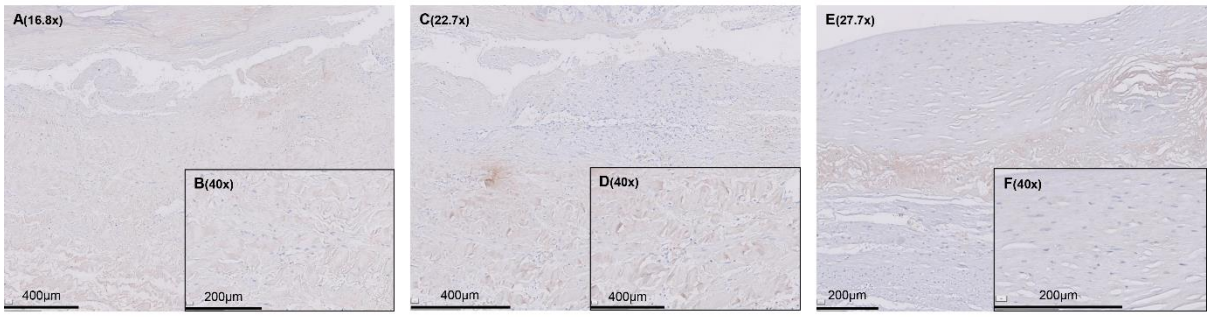

Figure S14.2: IHC Stainings of Collagen-I (Goat IgG), C7510-17K, USBIO. In AAA tissue, and even more outspoken in FCP tissue (**E**. Citrate, dilution 1:250), significant non-specific staining was present, regardless of protein block usage and use of either a heat retrieval (**A**. Citrate, dilution 1:250) or an enzyme retrieval (**C**. Pepsin, dilution 1:250).

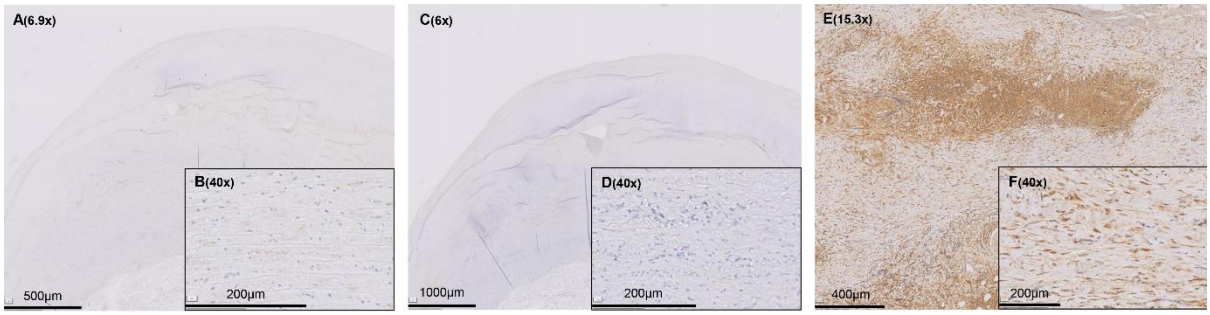

Figure S14.3: IHC Stainings of Pro-collagen-I (Rat IgG1), clone MAB1912, Millipore. In EFA tissue, regardless of antigen heat retrieval pH (**A**. Tris-EDTA, dilution 1:500; **B**. Citrate, dilution 1:500), there was little to no signal. However, in positive controls (**C**. AAA tissue, Tris-EDTA, dilution 1:500), a lot of non-specific staining was present, especially in lymphocyte infiltrates.

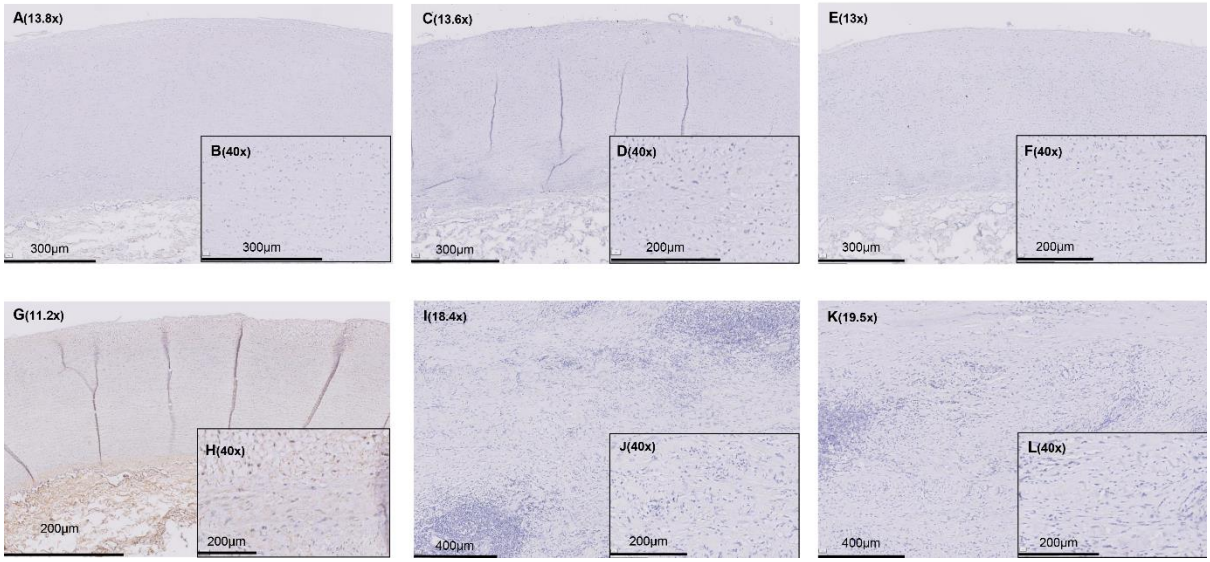

Figure S14.4: IHC Stainings of Pro-collagen-I (Mouse IgG1), clone PC8-7, Abnova. In EFA tissue, regardless of antigen heat retrieval pH (**A**. no retrieval, dilution 1:300; **C**. Tris-EDTA, dilution 1:300; **E**. Citrate, dilution 1:300), no protein expression was detected, confirmed by absence of staining in positive controls (**H**. AAA, no retrieval, dilution 1:300; **I**. AAA, Tris-EDTA, dilution 1:300). In contrast, in higher concentrations (**G**. dilution 1:100, EFA, no retrieval) there was significant background staining.

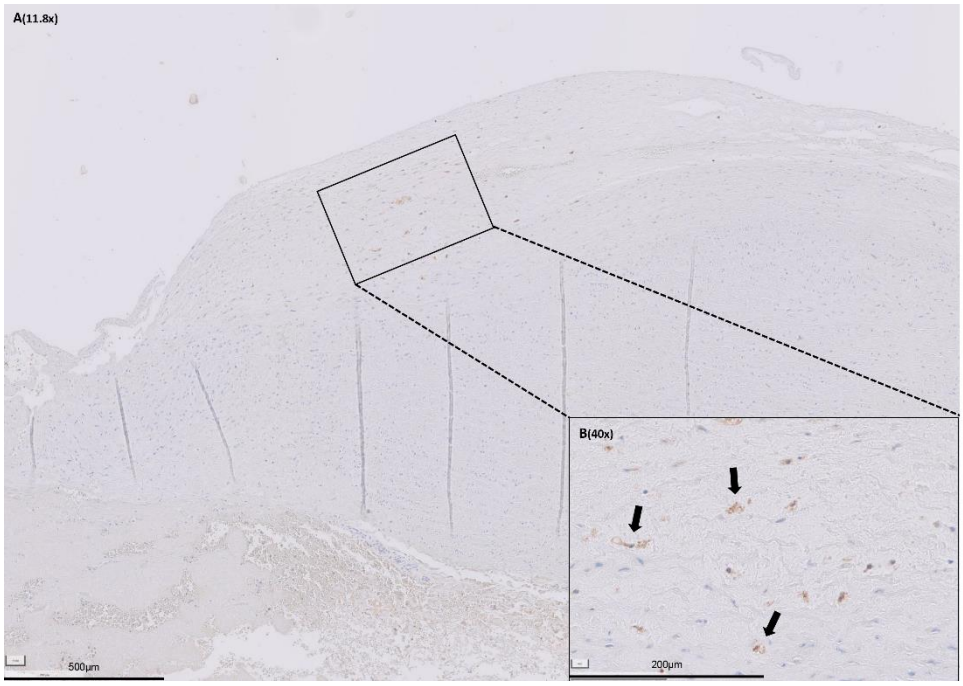

Figure S14.5: IHC Staining of Osteopontin (Goat IgG), AF1433, R&D Systems. A. (PIT (Pathological Intimal Thickening) tissue, Tris-EDTA, dilution 1:400). **B.** As Osteopontin is an ECM-protein (arrows), it is less convenient for cell phenotyping.

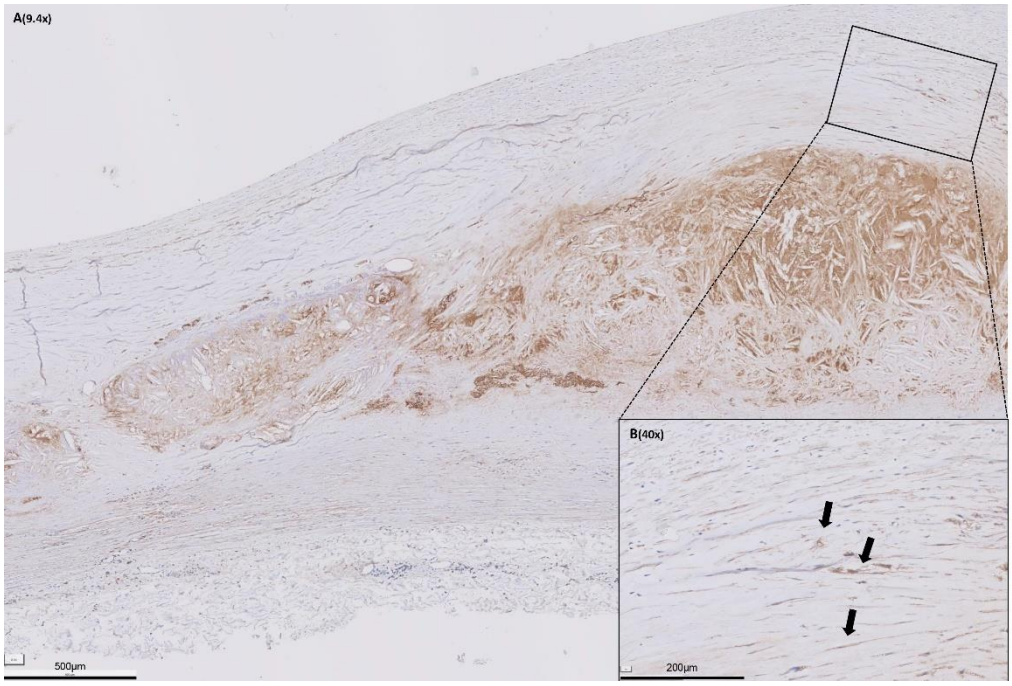

Figure S14.6: IHC Staining of Fibronectin (Mouse IgG1), clone FBN11, Thermofisher. A (LFA tissue, no retrieval, dilution 1:900)**. B.** As Fibronectin is an ECM-protein (arrows), it is less convenient for cell phenotyping.

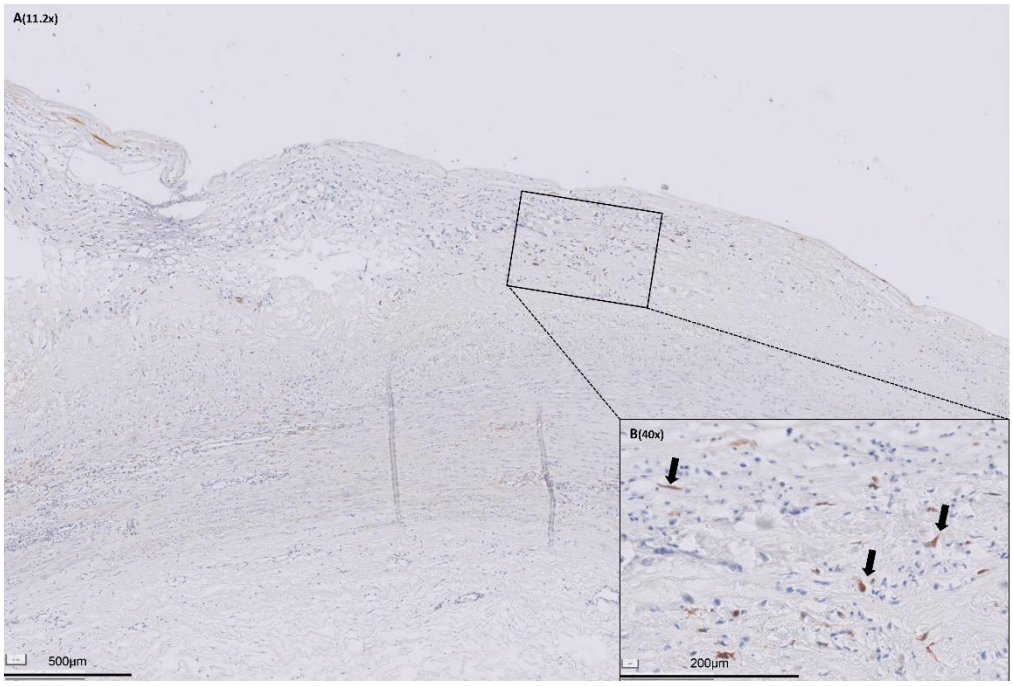

Figure S14.7: IHC staining of Laminin (Rabbit IgG), ab11575, Abcam. A. (Thin-cap Fibroatheroma tissue (advanced atherosclerosis), no retrieval, dilution 1:200)**. B.** As Laminin is an ECM-protein (arrows), it is less convenient for cell phenotyping.

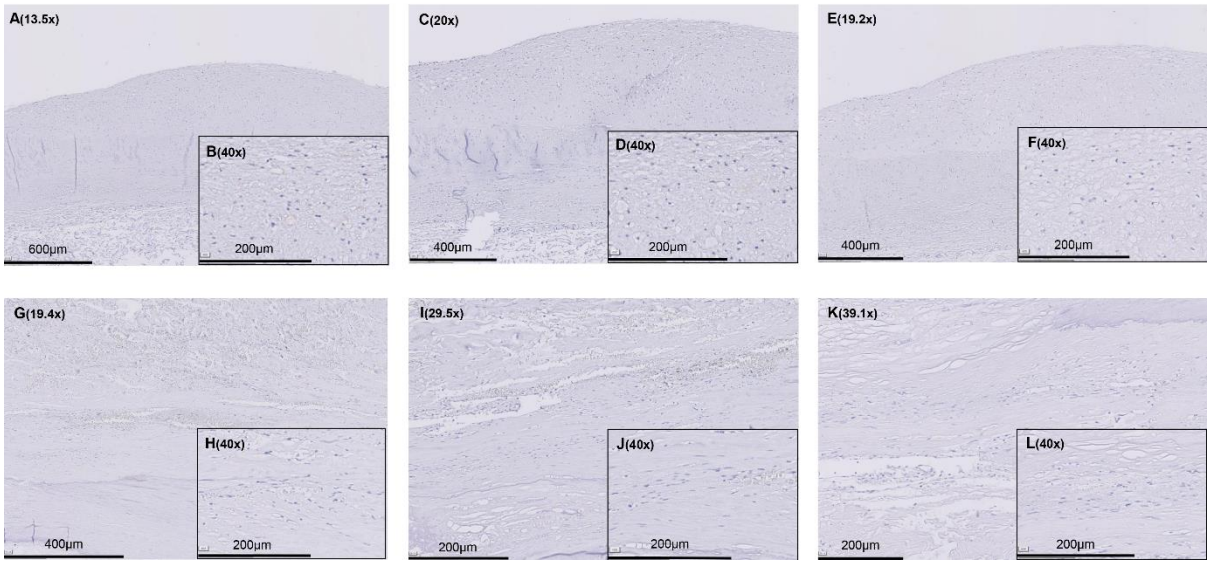

Figure S14.8: IHC staining of CRBP-1 (Rabbit IgG), ab11575, Abcam. In EFA (Early Fibroatheroma; advanced atherosclerosis) and AAA, no CRBP-1 signal was present, regardless of high primary antibody concentration and various antigen retrieval (**A**.EFA, Tris-EDTA, 1:30; **C**. EFA, Citrate, 1:30; **E**. EFA, Pepsin, 1:30; **G**. AAA, Tris-EDTA, 1:30; **I**. AAA, Citrate, 1:30; **K**. AAA, Pepsin, 1:30).

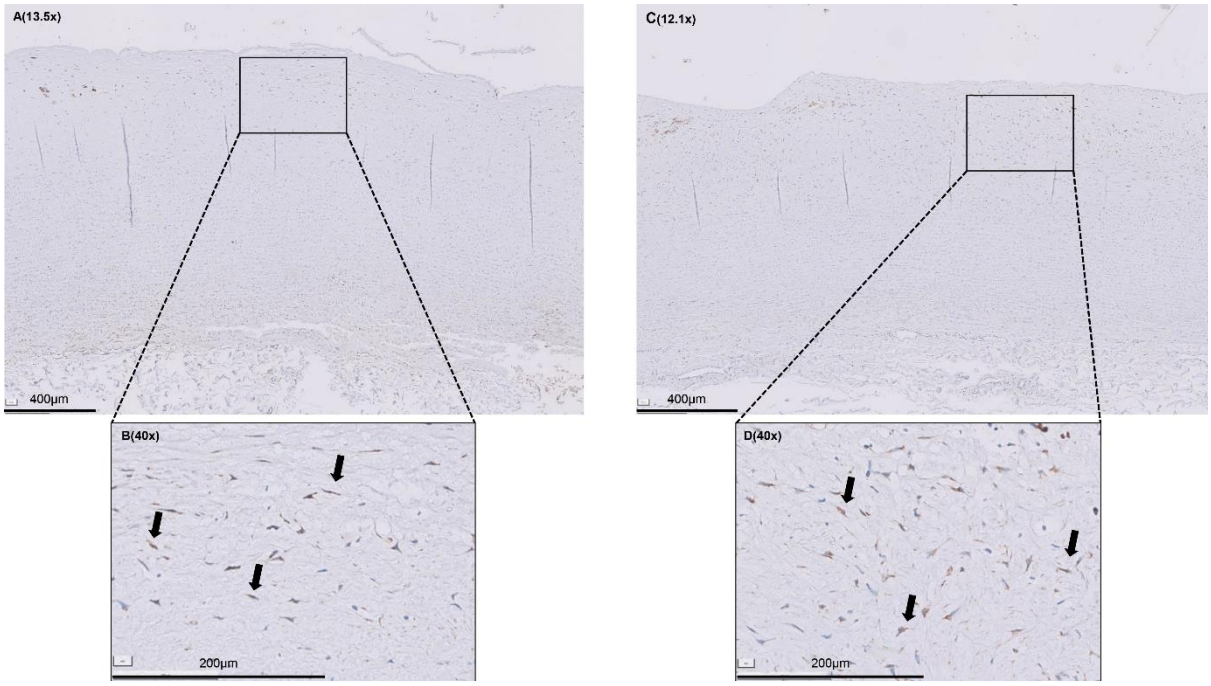

Figure S14.9: IHC stainings (n=1) of PDGFR-α (Rabbit IgG), ab61219, Abcam. Although PDGFR-α is expressed on the cell membrane, nuclear staining was observed (arrows in **B** (Citrate, dilution 1:400) and **D** (Tris-EDTA, dilution 1:400)). A small number of studies[326,327] has reported nuclear localization of the PDGFR-α, but those observations are based on IHC/IF, which makes it questionable whether it is really localized in the nucleus or whether it is background staining.

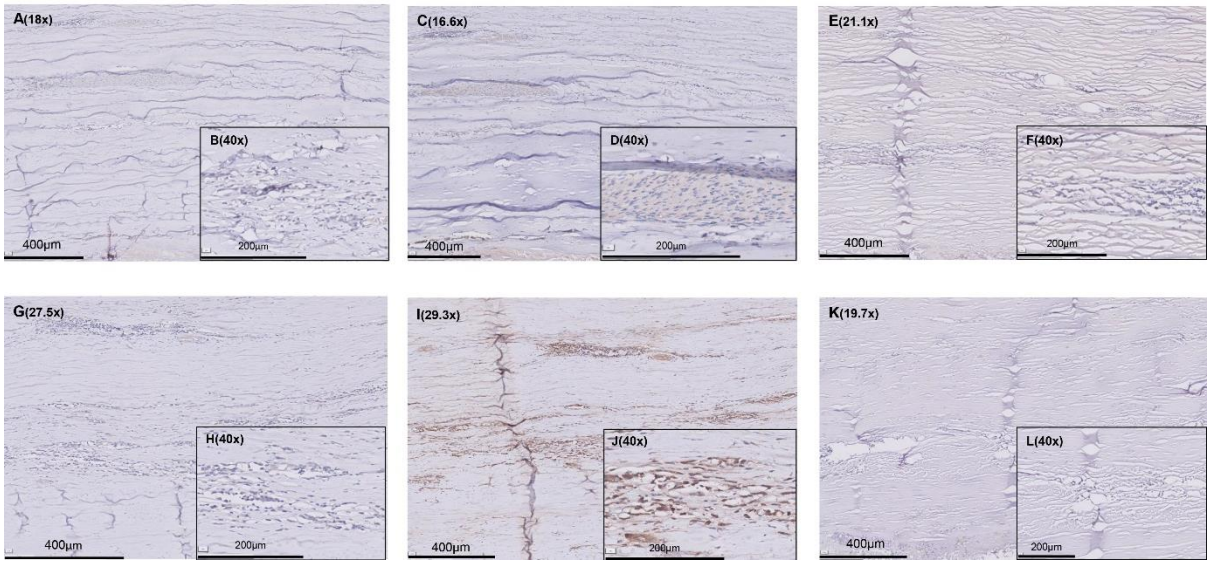

Figure S14.10: IHC Stainings of Phospho-NFκB p65 (Mouse IgG1), clone MCFA30, ThermoFisher. Although AAA is typically highly infiltrated by immune cells, there was weak staining of NFκB, regardless several antigen retrievals (**A**. Citrate, dilution 1:100; **C**. Tris-EDTA, dilution 1:100; **E**. Pepsin, dilution 1:100). In higher concentrations, more background staining was observed (**I**. Tris-EDTA, dilution 1:50). As NFκB is expressed intracellularly, the contribution of 0,1% Triton X-100 in PBS was also tested, although most nuclei are dissected in the 4 µ-sections (**G**. Citrate, Triton X-100, dilution 1:100; **K**. Pepsin, Triton X-100, dilution 1:100). However, more background (cytoplasmatic) staining was present if Triton X-100 was applied.

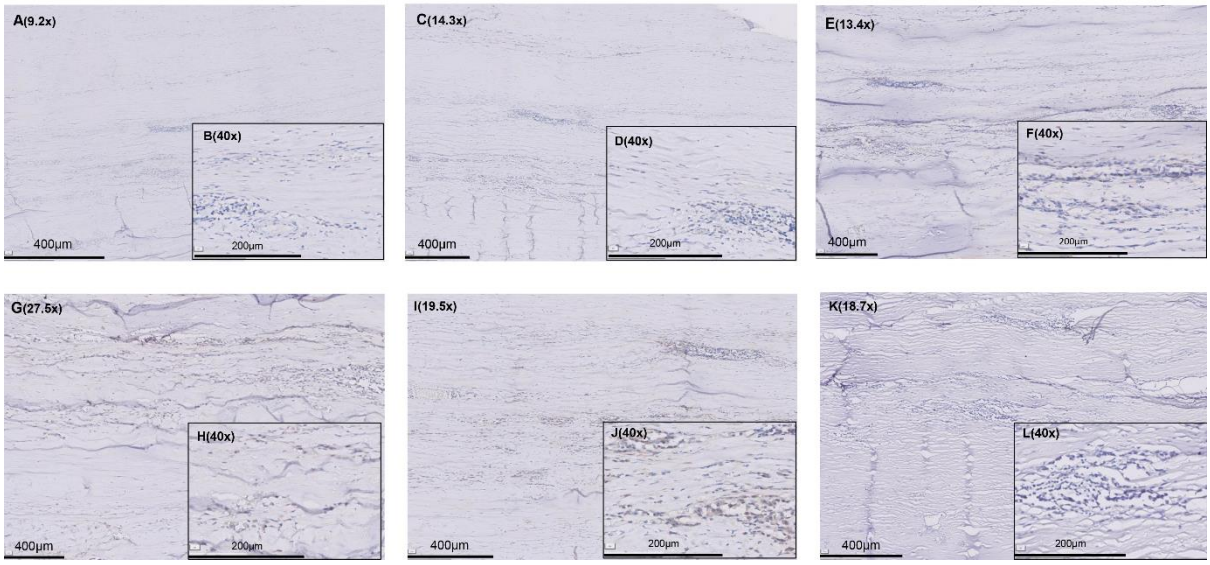

Figure S14.11: IHC Stainings of Phospho-NFκB 105 (Mouse IgG1), 178F3, Cell Signaling Technology.

Although AAA is typically highly infiltrated by immune cells, there was weak staining of NFκB, regardless several antigen retrievals (**A**. Tris-EDTA, dilution 1:100; **C**. Citrate, dilution 1:100; **E**. Pepsin, dilution 1:100). In higher concentrations, more background staining was observed (**K**. Tris-EDTA, dilution 1:50). As NFκB is expressed intracellularly, the contribution of 0,1% Triton X-100 in PBS was also tested, although most nuclei are dissected in the 4 µ-sections (**G**. Tris-EDTA, Triton X-100, dilution 1:100; **I**. Citrate, Triton X-100, dilution 1:100). However, more background (cytoplasmatic) staining was present if Triton X-100 was applied.

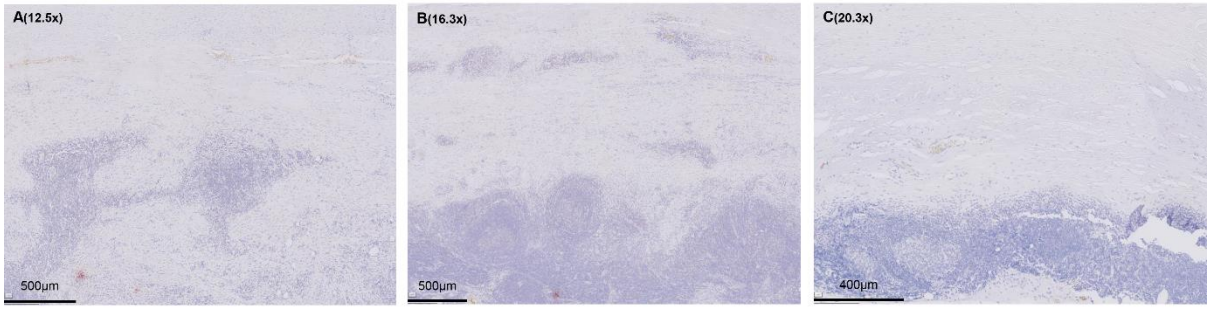

Figure S14.12: IHC Stainings of MCP-1 (Mouse IgG2b), 23002, R&D Systems.

Weak to no staining of MCP-1 in infiltrates of AAA tissue, regardless antigen retrieval (**A**. Tris-EDTA, dilution 1:100; **B**. Pepsin, dilution 1:100) and high primary antibody concentration (**C**. Tris-VEDTA, dilution 1:50).

Figure S15. Illustration of inflammatory cells in atherosclerosis.

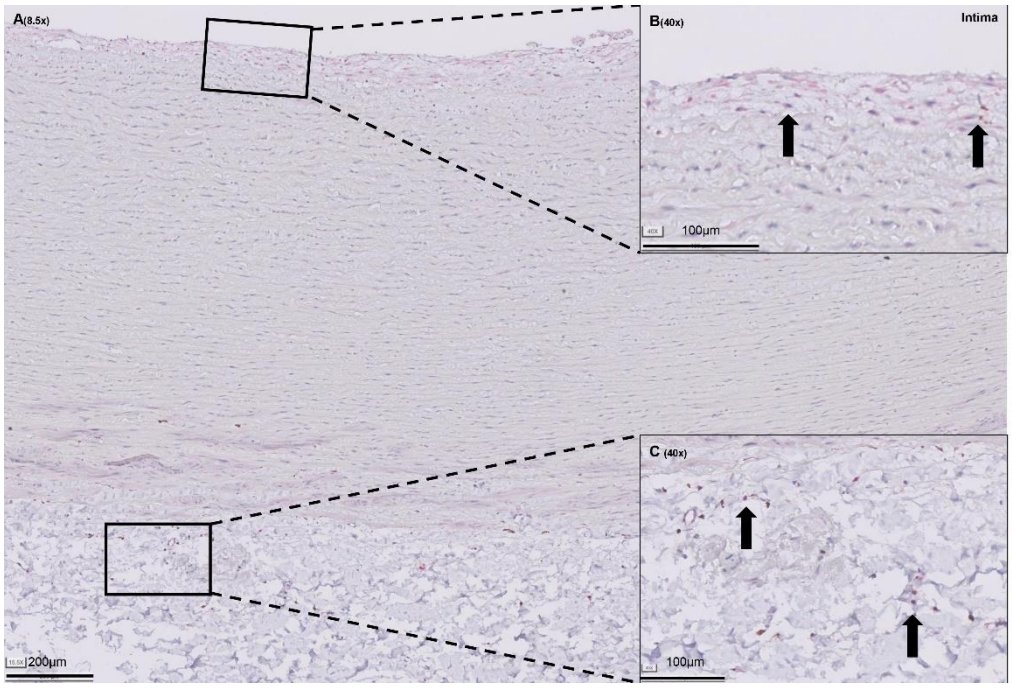

Figure S15.1: A. Double IHC staining for T-cells (CD4/CD8 co-staining; in *red*) and macrophages (CD68; in *brown*) in AIT reference sample (early atherosclerosis). **B.** Close up of T-cells (arrows) in the intima and **C**. close up of macrophages (arrows) in the adventitia.

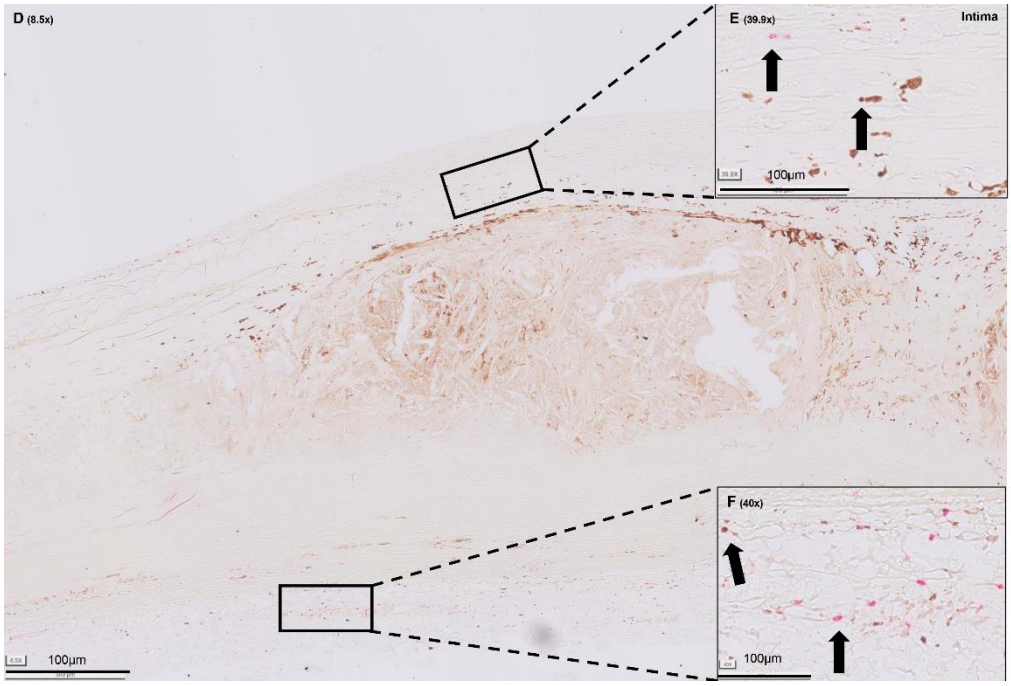

Figure S15.2: D. Double IHC staining for T-cells (CD4/CD8 co-staining; in *red*) and macrophages (CD68; in *brown*) in LFA reference sample (progressive atherosclerosis). **E.** Close up of T-cells (left arrow) and macrophages (right arrow) in cap area. **F**. Close up of macrophages (left arrow) and T-cells (right arrow) in adventitia.

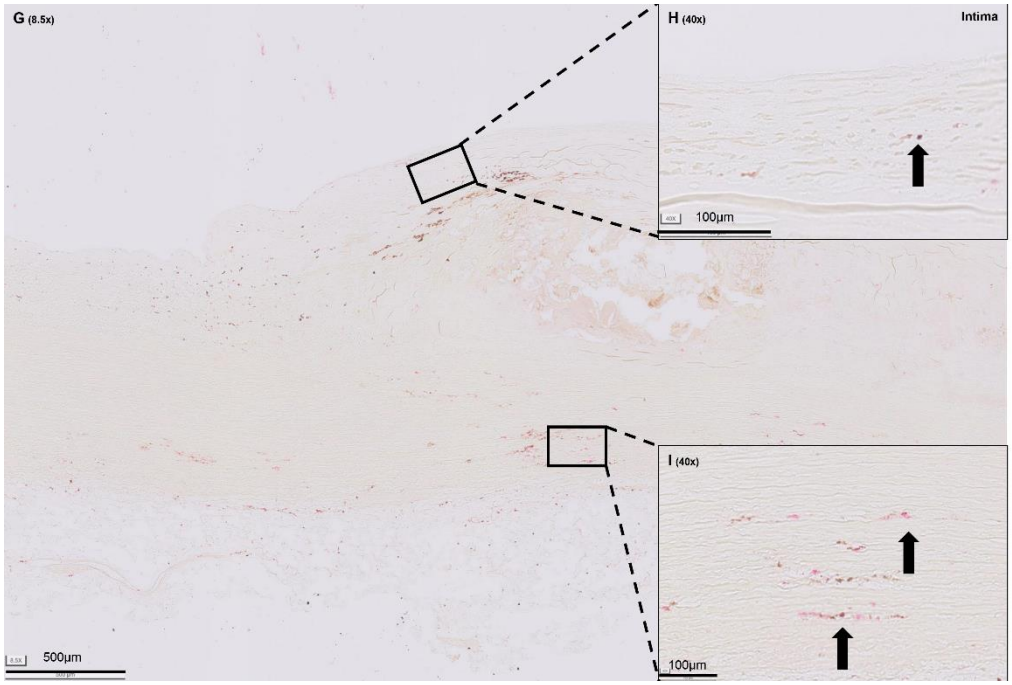

Figure S15.3: G. Double IHC staining for T-cells (CD4/CD8 co-staining; in *red*) and macrophages (CD68; in *brown*) in FCP reference sample (end-stage atherosclerosis). **H.** Close up of macrophages in the neo-intima. **I**. Close up of macrophages (left arrow) and T-cells (right arrow) in the adventitia.